


June 2018

# Design and Testing of a Passive Prosthetic Ankle Foot Optimized to Mimic an Able-Bodied Gait

Millicent Schlafly

University of South Florida, mschlafly@mail.usf.edu

Follow this and additional works at: <https://scholarcommons.usf.edu/etd>

 Part of the [Biomechanics Commons](#), [Biomedical Engineering and Bioengineering Commons](#), and the [Mechanical Engineering Commons](#)

## Scholar Commons Citation

Schlafly, Millicent, "Design and Testing of a Passive Prosthetic Ankle Foot Optimized to Mimic an Able-Bodied Gait" (2018).  
*Graduate Theses and Dissertations*.  
<https://scholarcommons.usf.edu/etd/7710>

This Thesis is brought to you for free and open access by the Graduate School at Scholar Commons. It has been accepted for inclusion in Graduate Theses and Dissertations by an authorized administrator of Scholar Commons. For more information, please contact [scholarcommons@usf.edu](mailto:scholarcommons@usf.edu).

Design and Testing of a Passive Prosthetic Ankle Foot Optimized to Mimic an Able-Bodied Gait

by

Millicent Schlafly

A thesis submitted in partial fulfillment  
of the requirements for the degree of  
Master of Science in Mechanical Engineering  
Department of Mechanical Engineering  
College of Engineering  
University of South Florida

Major Professor: Kyle Reed, Ph.D.  
Stephanie Carey, Ph.D.  
Seok Hun Kim, Ph.D.

Date of Approval:  
June 8, 2018

Keywords: Roll Over Shape, Ankle-Foot Prosthesis,  
Biomimetic Prosthetic Device

Copyright © 2018, Millicent Schlafly

## ACKNOWLEDGEMENTS

Firstly, I want to express my sincerest gratitude for Dr. Kyle Reed for guiding the direction of my research and meeting with me weekly since I began in his lab in the spring of 2016. This project would not have been possible without his knowledge and support. I also want to thank my committee, Dr. Seok Hun Kim and Dr. Stephanie Carey, for their continual guidance.

I want to acknowledge all of the friends I have made at the University of South Florida, members of REED Lab and otherwise, for providing much needed laughter and encouragement.

I am grateful for Annmarie Kavumkal's help conducting the experiment and all of the enthusiastic volunteers who participated in this study.

Finally, I want to thank my family for inspiring the creativity and discipline that made this thesis possible.

This material is based upon work supported by the National Science Foundation under Grant Number MRI-1229561.

## TABLE OF CONTENTS

LIST OF TABLES .....	iii
LIST OF FIGURES .....	iv
ABSTRACT .....	vii
CHAPTER 1: INTRODUCTION .....	1
1.1 Main Contributions .....	3
CHAPTER 2: BACKGROUND .....	4
2.1 Conventional and Dynamic Response Ankle-Foot Prostheses .....	4
2.2 Active Prostheses .....	5
2.3 Push-off vs. Range of Motion .....	6
2.4 Roll Over Shape .....	7
CHAPTER 3: BIOMIMETIC DESIGN OF THE COMPLIANT AND ARTICULATING PROSTHETIC ANKLE FOOT .....	9
3.1 Defining the “Ideal” Prosthetic Ankle .....	9
3.1.1 The Gait Cycle .....	10
3.1.2 Kinematics .....	10
3.1.3 Kinetics .....	11
3.1.4 Roll Over Shape .....	12
3.2 The Compliant And Articulating Prosthetic Ankle Foot .....	13
3.2.1 Description and Resemblance to Human Ankle .....	14
3.2.2 Other Advantages: Cheap, Customizable, and Sloped Walking .....	16
3.3 Mathematical Model .....	17
3.3.1 Kinematic Equations .....	18
3.3.2 Roll Over Shape .....	20
3.3.3 Optimization .....	21
3.3.3.1 Stiffness .....	21
3.3.3.2 The Effect of Changing Various Geometries .....	22
3.4 Final Experimental Designs .....	24
CHAPTER 4: METHODS .....	29
4.1 Computer Assisted Rehabilitation Environment .....	30
4.2 Prosthetic Simulator .....	31
4.3 Procedure .....	31
4.4 Data Analysis .....	35
CHAPTER 5: RESULTS .....	37
5.1 Ankle Angles .....	37



5.2 Ground Reaction Forces .....	39
5.2.1 Vertical Ground Reaction Forces.....	39
5.2.2 Sagittal Plane Ground Reaction Forces .....	40
5.2.3 Ground Reaction Forces Produced by CAPA Foot .....	41
5.3 Roll Over Shape .....	42
5.3.1 Comparison With Calculated.....	45
5.3.2 Validation of Roll Over Shape Based Design.....	48
5.4 Difficulty Level and Individual Preference .....	51
CHAPTER 6: DISCUSSION.....	55
6.1 Versions of the CAPA Foot .....	56
6.2 Customizable.....	57
6.3 Limitations .....	58
CHAPTER 7: CONCLUSIONS .....	59
REFERENCES.....	62
APPENDIX A: COPYRIGHT PERMISSIONS .....	68
APPENDIX B: TOE ANGLES.....	69
APPENDIX C: ANKLE ANGLES.....	71
APPENDIX D: SHANK ANGLES .....	73
APPENDIX E: VERTICAL GROUND REACTION FORCES .....	75
APPENDIX F: SAGITTAL PLANE GROUND REACTION FORCES.....	77
APPENDIX G: VERTICAL GROUND REACTION FORCES PRODUCED BY CAPA FOOT .....	79
APPENDIX H: INDIVIDUAL SUBJECT DIFFICULTY LEVEL RATING .....	81
APPENDIX I: STEP TIME .....	82

## LIST OF TABLES

Table 1	Fixed Geometric Parameters of CAPA Foot .....	19
Table 2	Ankle Loop Equations .....	20
Table 3	Arm Loop Equations .....	20
Table 4	Effective Rotational Stiffness Values of CAPA Foot at the End of the Moment Arm .....	22
Table 5	Summary of the Effect That Changing Individual Parameters Have on the Roll Over Shape Radius of Curvature (ROC) and Horizontal Center of Curvature (Xc) .....	24
Table 6	Experiment 2 Dorsiflexion Pretension (N) .....	26
Table 7	Experimental Trials 1.5 Minutes Each.....	29
Table 8	Age, Height, Weight, and Walking Speeds of Participants in Study.....	33
Table 9	Roll Over Shape of Best Fit Polynomial Median Radius of Curvature at Minimum, Median Forward Position at Minimum, Median Length of Shape in X-Direction.....	45
Table 10	Subject Individual Preference SACH Foot and Renegade® AT With vs. Without Weight.....	54
Table 11	Subject Individual Preference CAPA Foot Compliant vs. Stiff .....	54
Table H.1	Experiment 1 Individual Subject Difficulty Level Ratings .....	81
Table H.2	Experiment 2 Individual Subject Difficulty Level Ratings .....	81

## LIST OF FIGURES

Figure 1	Solid Articulating Cushioned Heel (SACH) foot .....	4
Figure 2	The Renegade® AT produced by Freedom Innovations .....	5
Figure 3	Right side angle ankles of able-bodied gait (left subplot) and individual wearing prosthetic simulator on the right leg with SACH foot (right subplot).....	11
Figure 4	Right side vertical ground reaction forces of able-bodied gait (left subplot) and individual wearing prosthetic simulator on the right leg with SACH foot (right subplot).....	12
Figure 5	Right side sagittal plane ground reaction forces of able-bodied gait (left subplot) and individual wearing prosthetic simulator with SACH foot (right subplot) on right foot.....	12
Figure 6	Right side roll over shapes of able-bodied gait (left subplot) and individual wearing prosthetic simulator with SACH foot (right subplot) on the right foot .....	14
Figure 7	A human ankle-foot compared to the CAPA foot to illustrate similarities [4].....	15
Figure 8	CAPA foot first version .....	16
Figure 9	Movement of the CAPA foot beginning with heel strike (top) and proceeding downward through stance phase to toe-off (bottom) for experiment 1 (A) and experiment 2 (B).....	17
Figure 10	Visual representation of vector loops on the CAPA foot during a step .....	19
Figure 11	The forces acting on the CAPA and the resulting center of pressure in the lab-based coordinate system (orange) and the shank-based coordinate system (green).....	21
Figure 12	Experiment 1 predicted roll over shapes of the compliant and stiff versions of the CAPA-foot-small-radius-long-moment-arm (left) and CAPA-foot-large-radius-short-moment-arm (right) compared to the able-bodied roll over shape found in section 3.1.4 .....	25
Figure 13	Experiment 2 CAPA-foot-small-radius-long-moment-arm (A) and CAPA-foot-large-radius-short-moment-arm (B).....	26
Figure 14	Top view of an exemplary CAPA foot prototype used for experiments 1 and 2 showing the arm mechanism used to increase the stiffness .....	28
Figure 15	Computer Assisted Rehabilitation ENvironment (CAREN) .....	30

Figure 16	Prosthetic simulator with the SACH foot and reflective markers .....	32
Figure 17	Toe angles (yellow) and heel angles (green) on an able-bodied leg (left) and the CAPA foot (right).....	36
Figure 18	Ankle angles for experiment 1 and 2.....	38
Figure 19	Vertical ground reaction forces for experiment 1 and 2.....	40
Figure 20	Sagittal plane ground reaction forces for experiment 1 and 2.....	41
Figure 21	Ground reaction forces produced by each CAPA foot during experiment 1 and experiment 2 using first method of representation .....	43
Figure 22	Sagittal plane component of ground reaction forces produced by each CAPA foot during experiment 1 and experiment 2 using second method of representation .....	44
Figure 23	Experiment 1 roll over shapes for subjects 1-5 .....	46
Figure 24	Experiment 2 roll over shapes for subjects 6-10 .....	47
Figure 25	Roll over shapes experimental versus calculated for all versions of the CAPA foot.....	49
Figure 26	Experimental roll over shapes compared to calculated roll over shapes using the same experimental data (green) and the experimental data of the opposite trial (magenta) .....	50
Figure 27	The difficulty level rating for each trial averaged among all subjects .....	53
Figure B.1	Experiment 1 Toe Angles Subjects 1-5.....	69
Figure B.2	Experiment 2 Toe Angles Subjects 6-10.....	70
Figure C.1	Experiment 1 Ankle Angles Subjects 1-5.....	71
Figure C.2	Experiment 2 Ankle Angles Subjects 6-10.....	72
Figure D.1	Experiment 1 Shank Angles Subjects 1-5.....	73
Figure D.2	Experiment 2 Shank Angles Subjects 6-10.....	74
Figure E.1	Experiment 1 Vertical Ground Reaction Forces Subjects 1-5 .....	75
Figure E.2	Experiment 2 Vertical Ground Reaction Forces Subjects 6-10. ....	76
Figure F.1	Experiment 1 Sagittal Plane Ground Reaction Forces Subjects 1-5 .....	77
Figure F.2	Experiment 2 Sagittal Plane Ground Reaction Forces Subjects 6-10 .....	78
Figure G.1	Vertical component of ground reaction forces produced by each CAPA foot during experiment 1 .....	79

Figure G.2 Vertical component of ground reaction forces produced by each CAPA foot during experiment 2 .....	80
Figure I.1 Average mode step time between subjects for trials with an ankle-foot prosthesis.....	82

## ABSTRACT

Currently there are nearly 2 million people living with limb loss in the United States [1]. Many of these individuals are either transtibial (below knee) or transfemoral (above knee) amputees and require an ankle-foot prosthesis for basic mobility. While there are an abundance of options available for individuals who require an ankle-foot prosthesis, these options fail to mimic an intact ankle when it comes to key evaluation criteria such as range of motion, push-off force, and roll over shape. The roll over shape is created by plotting the center of pressure during a step in a shank-based coordinate system. To address the need for a prosthesis that effectively replaces the ankle's contribution to an able-bodied gait, a biomimetic approach is taken in the design the Compliant & Articulating Prosthetic Ankle (CAPA) foot. The passive CAPA foot consists of four components connected by torsion springs representing the Phalanges, Metatarsal bones, Talus, and Calcaneus. Biomimetic functionality is exhibited by CAPA foot with regards to the roll over shape and a linear relationship between moment exerted and ankle angle, distinguishing the CAPA foot from other ankle-foot prostheses. A mathematical model of the CAPA foot is created to determine the roll over shape a specific CAPA foot geometry would produce and support eventual customization of the 3D printed components.

The mathematical model is used to optimize the design to two distinctly different roll over shapes, one with a rocker radius closer to that of the Talus bone and the other closer to the energetically advantageous value of 0.3 times leg length [2, 3]. Compliant and stiff versions of the two CAPA feet were compared to a conventional Solid Articulating Cushioned Heel (SACH) foot and a passive dynamic response foot (Renegade® AT produced by Freedom Innovations). Ten able bodied subjects walked on the Computer Assisted Rehabilitation Environment normally, and then with a transfemoral prosthetic

simulator. The study was separated into two experiments. For the second experiment (subjects 6-10), the versions of the CAPA foot had pretension in the dorsiflexion springs.

Overall the ankle angles and sagittal plane ground reaction forces of the CAPA foot better mimicked an intact ankle-foot than the existing passive ankle-foot prostheses. Added pretension increased the sagittal plane ground reaction forces and roll over shape radius of curvature and arc length. Nine out of ten participants preferred the CAPA foot and there was a statistical significant difference ( $F=14.2$ ,  $p<0.01$ ) between the difficulty level rating given for trials with the CAPA foot versus the existing ankle-foot prostheses. The mathematical model is found to be capable of accurately predicting experimental roll over shape trends and the concept of roll over shape based design is demonstrated. Successful aspects of the CAPA foot can be applied to other ankle-foot prosthesis. The CAPA foot could provide a passive, cheap, and personalizable ankle-foot prosthesis that improves mobility the quality of life for individual's lacking an intact ankle.

## CHAPTER 1: INTRODUCTION

In 1983 the Flex-Foot® dramatically changed the field of prosthetics by introducing a stiff plastic board that flexes during gait to provide energy return [5]. The stiff plastic board became the mainstay of successful ankle-foot prosthesis. However, our understanding of the human gait has improved immensely since the discovery of the roll over shape in 2000 [6]. For the design of the Compliant & Articulating Prosthetic Ankle (CAPA) foot, the author relies on an improved understanding of human gait to take a more biomimetic and radically different approach to prosthetic design. Improvements in ankle-foot prostheses can ultimately improve the quality of life for individuals living with limb loss. It is estimated that the number of individuals in the United States living with limb loss will increase to 3.6 million by year 2050, largely due to an increase in dysvascular conditions [1]. Many of these individuals will be either transtibial (below knee) or transfemoral (above knee) amputees and require an ankle-foot prosthesis for basic mobility.

The CAPA foot was inspired by the anatomy and functionality of a human ankle-foot in order to mimic the kinematics, kinetics, and roll over shape of an intact ankle. It provides full range of motion and no more, braking and push-off forces that increase linearly with the ankle angle, and can be controlled by the stiffness of replaceable torsion springs. Made possible by the linearity and simplicity of the design, a mathematical model is created to predict the roll over shape that any particular version of the CAPA foot would create. The mathematical model is used to optimize geometric parameters in the CAPA foot design to specific roll over shapes. The resulting components are 3D printed. The aspects of the design of the CAPA foot that distinguish it from other passive ankle-foot prostheses are the structure, linearity between angle and moment, and roll over shape based design.



The mathematical model is used to create two CAPA feet with distinctly different roll over shapes. The first has been optimized to exhibit an able-bodied roll over shape with a rocker radius closer to that of the Talus bone [7]. The second has been optimized to have roll over shape characteristics that have been shown to be indicative of a healthier roll over shape with a rocker radius closer to the energetically advantageous value of 0.3 times leg length [2, 3]. A study was conducted with ten able-bodied subjects wearing a prosthetic simulator in the Computer Assisted Rehabilitation Environment (CAREN) to compare these two feet to two existing prosthetic feet, a conventional Solid Articulating Cushioned Heel (SACH) foot and a passive dynamic response foot, the Renegade® AT produced by Freedom Innovations. The results from the experiment will determine the effectiveness of this approach to designing ankle-foot prostheses.

The ankle angles, ground reaction forces, and roll over shapes of the intact ankle-foot, SACH foot, Renegade® AT, and four versions of the CAPA foot (CAPA-foot-small-radius-compliant, CAPA-foot-small-radius-stiff, CAPA-foot-large-radius-compliant, and CAPA-foot-large-radius-stiff) were evaluated. Participants provided their individual preference, comments, and difficulty level ratings. The experimental data was used in combination with the mathematical model to provide the contribution of the CAPA foot to the ground reaction forces for each trial and to compare the calculated and experimental roll over shapes. The study was separated into two experiments. Subjects 6-10 used the version of the CAPA foot with added dorsiflexion pretension. The experiment 2 version of the CAPA foot provided more push-off forces and increased standing stability. The results and main contributions of this study are discussed.

This thesis consists of chapters for the Introduction, Background, Design, Methods, Results, Discussion, and Conclusion. The Chapter 2: Background outlines information relevant to understanding the content and significance of this thesis. Chapter 3: Design begins by defining the “ideal” ankle-foot prosthesis and proceeds to explain the mathematical model, the design process, and final designs of the CAPA foot. Chapter 4: Methods includes the experimental procedure and Chapter 5: Results explains the ankle angle,

ground reaction force, and roll over shape results. The results and implications are explained in Chapter 6: Discussion. The thesis concludes with Chapter 7: Conclusions.

### **1.1 Main Contributions**

The main contribution of this thesis is the design and testing of a novel ankle-foot prosthesis and corresponding mathematical model that

- applies the concept of roll over shape based design,
- passively provides a linear relationship between ankle angle and force,
- shows improvement over existing passive ankle-foot prosthesis for individual preference, difficulty level, and stability, and
- is easily customizable to the individual and speed.

## CHAPTER 2: BACKGROUND

Portions of this section were published in the ASME's 2017 International Mechanical Engineering Congress and Exposition (IMECE) [8]. Copyright permission is given in Appendix A.

### 2.1 Conventional and Dynamic Response Ankle-Foot Prostheses

The simplest type of ankle-foot prosthesis is the conventional non-articulating SACH (Solid Ankle Cushioned Heel) foot shown in Figure 1. The SACH foot is able to closely resemble the shape of an actual foot and provides the user with some cushioning during movement. However, it is unable to provide the range of motion and energy return of an intact ankle [9]. Regardless, many less active amputees prefer the SACH foot because of the greater control it gives the amputee [10].



Figure 1: Solid Articulating Cushioned Heel (SACH) foot.

Unlike the SACH foot, the dynamic response ankle-foot shown in Figure 2 stores energy during the beginning of the gait cycle and uses the stored energy to propel the foot forward [11]. Also called ESR for Energy Storing and Returning, the energy storage mechanism of the dynamic response ankle-foot is similar to the role of the Achilles tendon. During gait, the Achilles tendon is stretched and stores potential energy that is released during push-off [12]. The energy storage mechanism in dynamic response feet are

typically primarily weight activated. This means the prosthetic will store energy while the individual is standing unlike an able-bodied ankle. Despite this difference, the dynamic response ankle-foot provides some resistance to movement similar to that of an intact ankle [12].



Figure 2: The Renegade<sup>®</sup> AT produced by Freedom Innovations. It is a type of ESR foot.

## 2.2 Active Prostheses

Dynamic response feet can be further classified as either passive or active (microprocessors). Because the energy produced by the ankle joint during average walking speeds is almost completely self-sustaining with no net external energy loss, there is the potential for a purely mechanical mechanism such as the dynamic response ankle to generate the forward motion necessary for an able-bodied gait [13]. However, for speeds faster than normal walking, passive systems are not capable of fully emulating an intact ankle because a positive net external energy is produced by the ankle [13, 14]. The use of an active ankle-foot prosthesis for faster speeds may be necessary in the future, but current design limitations make this application less than ideal. An active ankle-foot prosthesis can be over twice as heavy as a conventional prosthesis, are expensive, and experience hardware and control issues adjusting to different speeds [15, 16]. Fundamentally, active prosthetic ankle-feet operate using preplanned kinematic trajectories as opposed to the impedance control mechanism of a human ankle [17]. Finally, while still operating as an ESR system, active ankle-foot prostheses are difficult to customize or match biomimetically in size and weight [18]. For

these reasons, this thesis focuses on designing a passive dynamic response ankle-foot prosthesis. However, the results could be used to inform active prosthetic design as well.

### **2.3 Push-off vs. Range of Motion**

The amount of energy stored in the prosthesis is dependent on the stiffness. Increasing the stiffness will increase the propulsion forces, however, it simultaneously decreases the range of motion (ROM) of the ankle [19, 20, 21]. The ankle joint has a ROM from about 45° plantar flexion to 20° dorsiflexion [22]. Forced to make a choice between propulsion forces and range of motion, many ankle-foot prostheses have only been designed for the ROM that is experienced during gait on an even surface, a value of no more than 30° [23]. While this may seem sufficient as the ROM of the ankle remains consistent with changes in speed [24], a study looking at individuals with limited ankle ROM due to a sprain showed that ankle ROM does impact gait symmetry in regards to step length and step time [25]. Additionally, ankle ROM is important for walking on sloped surfaces as it helps accommodate for movement about different equilibrium positions [26, 27].

While both the kinematics and kinetics of an intact ankle are important to its functionality, so far it has been impossible for a passive prosthetic ankle-foot to mimic both. There exists a discrepancy between design changes that improve the kinematics and kinetics. The effect of increasing stiffness is an example of this discrepancy [19, 20, 21]. In an able-bodied ankle, the relationship between angle and push-off moment is linear [13, 28]. However, most prostheses are built with a stiff plastic board that resembles a cantilever beam. A rudimentary knowledge of cantilever beams tells us that the linear relationship between deflection and force is restricted to small deflections and much less than the ankle angle experienced by an able-bodied individual. The stiffness of the foot also impacts the location of the ground reaction forces, and therefore, the rollover shape as discussed in section 2.4 [29]. Olesnavage and Winter noticed this effect and suggested the use of a rigid constraint to prevent the foot from over-deflecting [29].

Recent research in active prostheses has been able to demonstrate the effectiveness of applying a torque that is linear with ankle angle in single subject experiments in a lab environment. Caputo and Collins used a Universal Ankle-Foot Prosthesis Emulator that determined the desired torque by a piecewise linear function in 2014 [30]. A team at the Robotics and Multibody Mechanics Research Group at the Vrije Universiteit Brussel is making progress in mimicking both kinematics and kinetics in the development of the actuated prosthetic AMP-Foot. Although not explicitly stated, one of the major changes between the AMP-Foot 2.0 tested in 2014 [31] and the AMP-Foot 3.0 in 2016 [32] was a linear relationship between torque and ankle during initial contact to flat foot. The change resulted in a curve that better mimics an intact ankle as provided by Winter's data and an extra 5 Joules of energy storage [32]. It is interesting to note that the strategy used in the design of active prosthetics to achieve both push-off and range of motion in fast walking speeds is to effectively increase stiffness with ankle angle [15]. While this strategy has been applied to the design of a quasi-passive prosthetic ankle-foot that increases the stiffness with ankle angle using a cam-based transmission and an active sliding support beneath the leaf spring [33], the strategy cannot be used in a completely passive prosthesis because it requires positive work to be done by the prosthetic, nor should it be necessary for normal walking speeds [13].

## **2.4 Roll Over Shape**

Hansen developed a characteristic of gait called the roll over shape that incorporates both the kinematics and kinetics [6]. The roll over shape is created by plotting the center of pressure during a step in a shank-based coordinate system. Recent research, summarized by Hansen and Childress, has found that “roll-over shapes in able-bodied subjects do not change appreciably for conditions of level ground walking, including walking at different speeds, while carrying different amounts of weight, while wearing shoes of different heel heights, or when wearing shoes with different rocker radii” [34]. This suggests that able-bodied individuals will alter their ankle kinematics to preserve their roll-over shape. However, amputees do not have the adaptive control that an able-bodied individual has over their roll-over shape. Therefore, the de-

sign of the prosthetic predominantly controls the roll-over shape an amputee will produce. As a result, it has become a method to evaluate prosthetics [6, 35, 36, 37]. However, while the roll over shape demonstrates the relationship between kinematics and kinetics, it is not directly impacted by magnitude. Other evaluation methods are necessary to determine the late stance push-off [38].

## CHAPTER 3: BIOMIMETIC DESIGN OF THE COMPLIANT AND ARTICULATING PROSTHETIC ANKLE FOOT

This chapter outlines the process of designing an ankle-foot prosthesis that mimics the functionality of the human ankle in the sagittal plane during gait. To achieve this goal, it is first important to understand the role of the intact ankle during gait explained in section 3.1: Defining the “Ideal” Prosthetic Ankle. Next, the design of the CAPA foot is summarized in section 3.2. The mathematical model that describes the movement, forces, and the roll over shape the CAPA foot creates is explained in section 3.3. The mathematical model is used to optimize the design for experimentation. The final designs used for experimentation is presented in section 3.4.

### 3.1 Defining the “Ideal” Prosthetic Ankle

Human gait has evolved to maximize energy efficiency through adaptations such as beginning the gait cycle with heel strike [39]. The role of the ankle joint is crucial to healthy and efficient gait. As a result, individuals lacking an ankle consume over 20% more oxygen than able-bodied individuals [40]. The prospect of human augmentation has motivated prosthetic designs that sacrifice characteristics of the evolved able-bodied ankle for enhanced functionality in a specific area. However, for unilateral amputees in particular, any deviation in functionality from the able-bodied ankle causes gait asymmetry and requires extra effort by the amputee to compensate. By taking a more biomimetic approach to the prosthetic design, energy consumption required by amputees can be decreased and quality of life improved. Therefore, the ideal prosthetic can be defined in its ability to replace the able-bodied limb in size, shape, and most importantly, functionality. Prosthetic ankles can be evaluated by their ability to mimic the behavior of an intact ankle with regards to kinematics, kinetics, and roll over shape.



In order to mimic the functionality of the ankle during gait, it is necessary to identify the characteristics of an able-bodied gait that cannot be achieved without the ankle. Because the SACH foot provides very little ankle functionality, the author compares the gait produced by the SACH foot and an able-bodied gait to determine the role of the ankle joint during gait. Data was used from an experimental study conducted by the author looking at the effect that knee height has on the gait of a transfemoral amputee [41]. Five subjects were asked to walk at a self selected speed for two minutes and for at least one minute wearing the prosthetic simulator with the SACH foot shown in section 4.3 Figure 16. The collected data are discussed in Sections 3.1.2, 3.1.3, and 3.1.4 and shown in Figure 3, 4, 5 and 6.

### **3.1.1 The Gait Cycle**

The gait cycle is used to describe and graph behavior during a typical step. The gait cycle begins in stance phase by the heel initially striking the ground and exerting a braking force. The beginning 60% of the gait cycle is stance phase where the foot is in contact with the ground. As the step and stance phase proceeds, the foot becomes further dorsiflexed. In dorsiflexion the toes are pointed upward from the neutral position. As stance phase ends, the foot pushes off to propel the individual forward. During push-off the foot is in plantar flexion with the toes pointed downward. The gait cycle ends with swing phase to repeat again when the heel is returned to the frontmost position and strikes the ground. The sagittal plane divides the right and left hand sides of the body. Most of the analysis throughout this paper is performed in the sagittal plane.

### **3.1.2 Kinematics**

The kinematics of the ankle can be described by its angle during the gait cycle. The range of motion of the ankle during gait on an even surface is no more than  $30^\circ$  and remains consistent with changes in speed [23, 24]. The ankle angles shown in Figure 3 supports previous findings. However, the full range of motion of the ankle joint is from about  $45^\circ$  plantar flexion to  $20^\circ$  dorsiflexion [22]. In conclusion, the

“ideal” prosthetic ankle should have a range of motion of about 45° plantar flexion to 20° dorsiflexion but exhibit a range of motion of less than 30° during gait [22, 23].

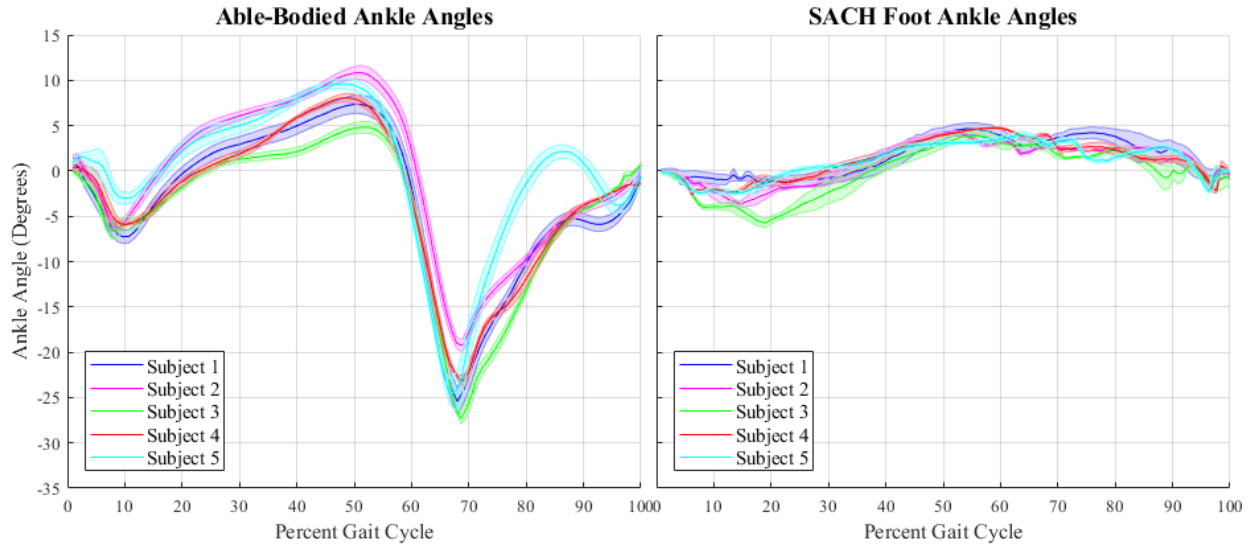


Figure 3: Right side angle ankles of able-bodied gait (left subplot) and individual wearing prosthetic simulator on the right leg with SACH foot (right subplot). These results are from an experimental study performed by the author on the effect of prosthetic knee height. Positive values indicate degrees dorsiflexion and negative values indicates degrees plantar flexion. The shaded areas represent half the standard deviation between steps.

### 3.1.3 Kinetics

Figures 4 and 5 show the ground reaction forces at each subject’s normal walking speed plotted against gait cycle in comparison with an individual wearing the prosthetic simulator with the SACH foot. The maximum vertical forces of the able-bodied individuals in Figure 4 exhibit two distinctive peaks that are not seen in the ground reaction forces for the SACH foot. The maximum push-off forces of the SACH foot in Figure 5 are much less than that produced by an able-bodied gait. Some subjects are able to compensate for the loss of the ankle’s contribution to push-off better than others. For example, Subject 4 has the lowest maximum able-bodied push-off force and the highest maximum SACH foot push-off force. In contrast, Subject 1 has the second highest maximum able-bodied push-off force and the lowest maximum SACH foot push-off force.

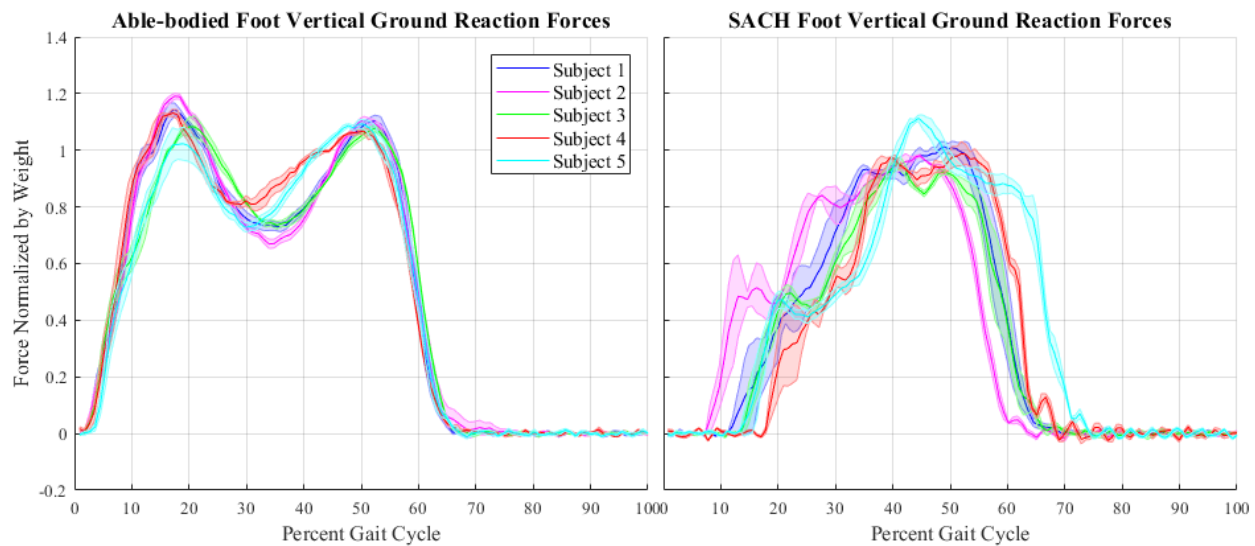


Figure 4: Right side vertical ground reaction forces of able-bodied gait (left subplot) and individual wearing prosthetic simulator on the right leg with SACH foot (right subplot). These results are from an experimental study performed by the author on the effect of prosthetic knee height. The forces are normalized by the weight of the subject. The shaded areas represent half the standard deviation between steps.

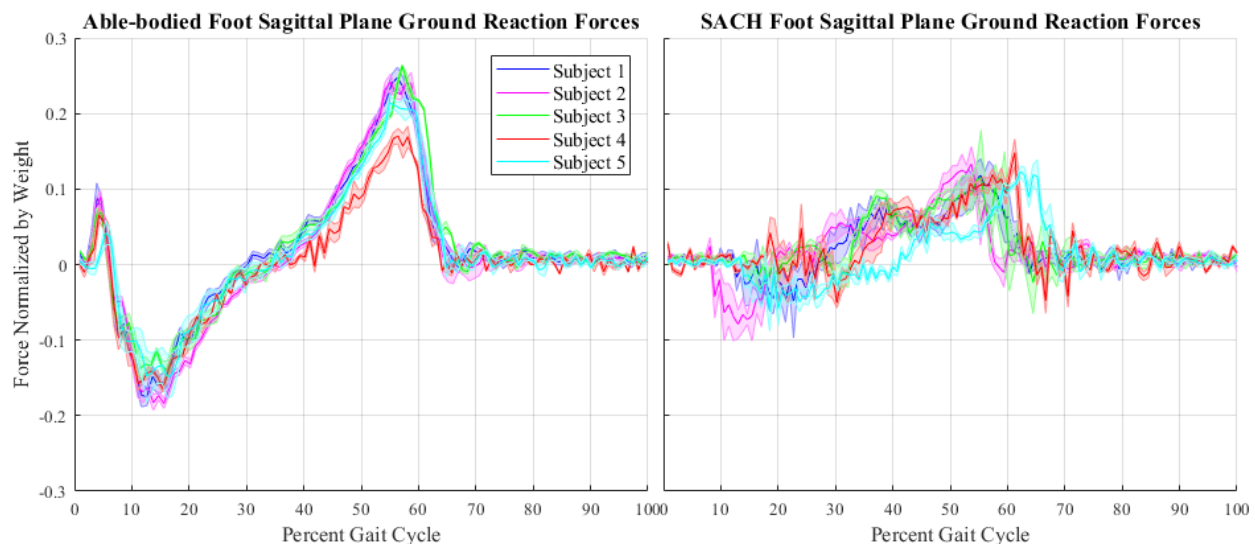


Figure 5: Right side sagittal plane ground reaction forces of able-bodied gait (left subplot) and individual wearing prosthetic simulator with SACH foot (right subplot) on right foot. These results are from an experimental study performed by the author on the effect of prosthetic knee height. The forces are normalized by the weight of the subject. The shaded areas represent half the standard deviation between steps.

### 3.1.4 Roll Over Shape

To establish the roll over shape of an able-bodied individual, the center of pressure is plotted in a shank-based coordinate system during stance phase in Figure 6. Stance phase is established when over 50%

percent of each subject's body weight is on the right platform. The inverted pendulum model approximation and a study of 16 subjects performed by Mitchell et al. shows that the ideal roll over shape radius is approximately 20% body height [42]. As all five subjects were between 177-187cm in height, literature would suggest the best fit radius to be 35.4-37.4cm. The roll over shape of the five able-bodied subjects shown in Figure 6 has a best fit radius of 38.8cm and is consistent with the study performed by Mitchell et al. [42].

By comparing the roll over shapes of physically impaired and able bodied individuals, characteristics such as a larger radius of curvature ( $R$ ) [43], a longer arc length [44, 43], and a longer roll over shape in the X-direction (EFL, Effective Foot Length) [45], have been determined to be preferable. Similarly, a positive x-coordinate center of curvature ( $X_c$ ) is an observable characteristic of able-bodied roll over shapes [42, 46, 47] and better prosthetics [43, 35, 37]. S. Miff et al. found that a  $X_c$  behind the ankle occurs during gait initiation, a  $X_c$  in front of the ankle occurs during gait termination, and the  $X_c$  is at a neutral position during steady state gait. The roll over shape of ankle-foot prostheses that lack adequate push-off prematurely curve upwards resulting in a smaller best fit radius, arc length, EFL, and center of curvature in the horizontal direction ( $X_c$ ) [46]. The center of curvature in the horizontal direction ( $X_c$ ) of the roll over shape of all five subjects shown in Figure 6 is positive as well with a value of 2.02cm, but smaller than the center of curvature for the SACH foot roll over shape (29.3cm).

While the roll over shape is usually modeled as a circular arc, it has also been modeled as a second order polynomial [48]. A second order polynomial was found to fit the roll over shape of the CAPA foot better and used to determine the radius of curvature,  $X_c$ , and forward length in the x-direction in section 5.3.

### **3.2 The Compliant And Articulating Prosthetic Ankle Foot**

The Compliant & Articulating Prosthetic Ankle (CAPA) foot was designed to emulate functionality of an intact ankle and exhibit the kinematics, kinetics, and roll over shape of an able-bodied gait described in section 3.1. The CAPA foot has a physical and functional resemblance to the intact ankle as described in sec-

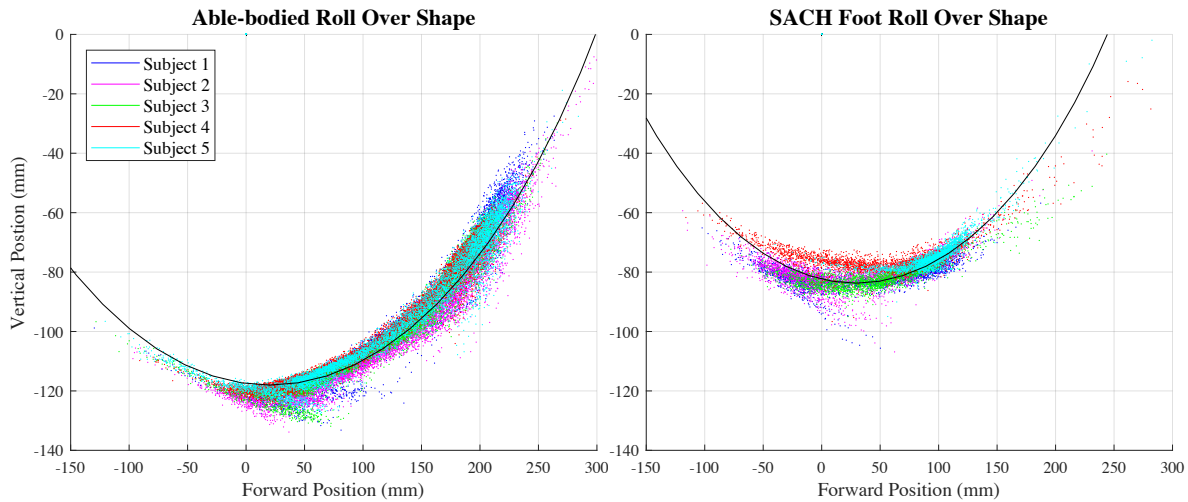


Figure 6: Right side roll over shapes of able-bodied gait (left subplot) and individual wearing prosthetic simulator with SACH foot (right subplot) on the right foot. The best fit circle is given by the black line with radius=388mm,  $X_c=20.2\text{mm}$ , and  $Y_c=270\text{mm}$  for able-bodied gait (left) and radius=318mm,  $X_c=29.3\text{mm}$ , and  $Y_c=234\text{mm}$  for SACH foot (right subplot). The ankle marker is located at coordinate (0,0) with the y-axis in line with the shank and the x-axis perpendicular to the shank. The forward position indicates the x-coordinate of the center of pressure in the shank based coordinate system. The vertical position indicates the y-coordinate of the center of pressure in the shank based coordinate system.

tion 3.2.1 and the other advantages such as cost, personalizable, and allowing for sloped walking described in section 3.2.2. Portions of this section were published in the ASME's 2017 International Mechanical Engineering Congress and Exposition (IMECE) [8]. Copyright permission is given in Appendix A.

### 3.2.1 Description and Resemblance to Human Ankle

The CAPA foot is assembled from four articulated components as shown in Figure 7 and Figure 8 for the Phalanges (1), Metatarsal bones (2), Ankle (3), and Calcaneus (4). The relative motion of these components allows for the CAPA foot to experience the full range of motion of the ankle joint in the sagittal plane. Platforms prevent excess flexion for greater stability. The ankle component, location 3 in Figure 8, has a rocker shape with a constant curvature. The rocker shape has been found to reduce the metabolic cost of step-to-step transitions in inverted pendulum models [49]. Literature has indicated a rocker radius of 0.3 times leg length is energetically advantageous [2, 3], however, the Talus bone can be approximated as having a constant curvature of 20-26.6mm in the sagittal place [7].

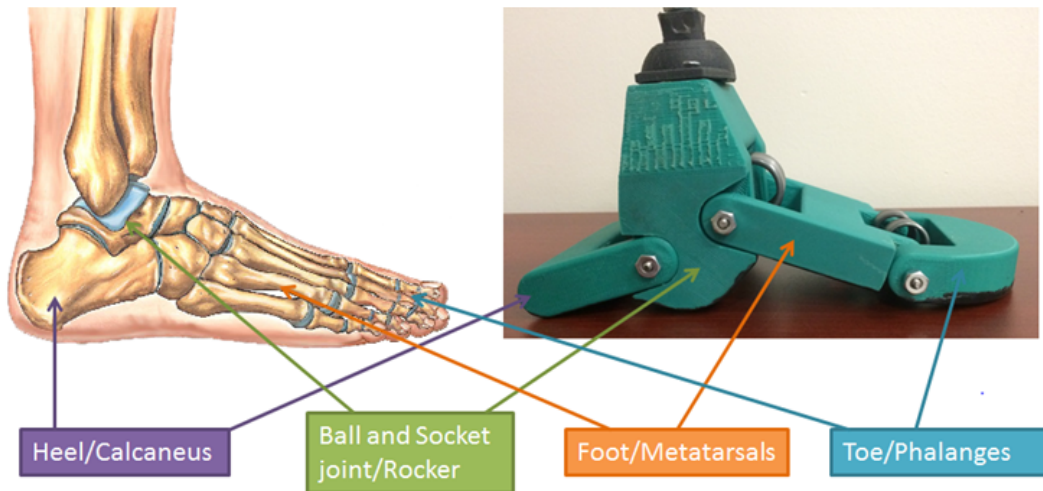


Figure 7: A human ankle-foot compared to the CAPA foot to illustrate similarities [4]

The CAPA foot would be classified as a type of dynamic response foot as it stores potential energy at the joints and releases that energy to assist in forward movement. Unlike the majority of current ankle-foot systems that only mimic the energy storage and return that occurs in the Achilles tendon for plantar flexion, the CAPA foot stores energy at each joint to mimic toe flexion at location 5 in Figure 8 and both plantar flexion and dorsiflexion at location 6. The energy is stored using torsion springs at locations 5 and 6 in Figure 8. The arms of the torsion springs are slid into holes designed into the 3D printed toe, foot, ankle, and heel components at locations 1-4 in Figure 8. During the unloading phase of an intact ankle, there is a linear increase in the moment exerted by the ankle [13]. This can be emulated by a torsion spring because the force exerted by a spring also follows a linear profile and the angular velocity of an ankle is constant about a point [50]. Rubber was painted onto the bottom of the CAPA foot for traction shown by location 8 in Figure 8.

Figure 9 shows the relative motion of the components of the CAPA foot in stance phase for experiment 1 (A) and experiment 2 (B). The difference between the experiment 1 and experiment 2 versions of the CAPA foot is added pretension between in the ankle and foot components in its neutral orientation during the gait cycle. The pretension makes the foot more stable while standing by making it harder for the

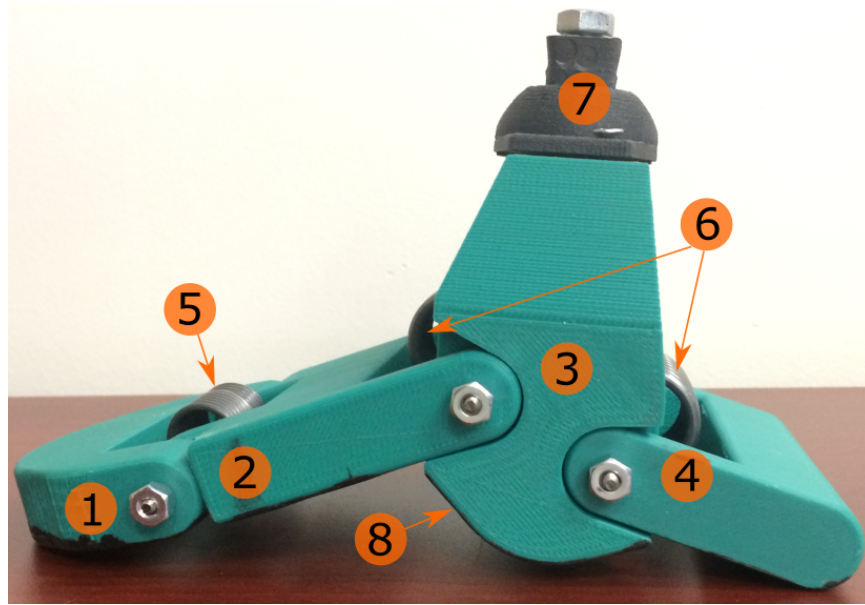


Figure 8: CAPA foot first version. ①-Toe/Phalanges ②-Foot/Metatarsals ③-Ankle ④-Heel/Calcaneus ⑤-Two 1.18 N-m 180° steel torsion springs ⑥-One 5.01N-m 120° steel torsion spring ⑦-Carbon-fiber and nylon composite pyramid ⑧-Rubber coating. This image was published in the ASME's 2017 International Mechanical Engineering Congress and Exposition (IMECE) [8]. Copyright permission is given in Appendix A.

individual to fall forward. Also, unlike the experiment 1 version of the CAPA foot, the experiment 2 version begins storing energy in the dorsiflexion springs at heel strike as opposed to when dorsiflexion begins.

### 3.2.2 Other Advantages: Cheap, Customizable, and Sloped Walking

Beyond the potential of the design to mimic an able-bodied gait, the application of 3D printing to the design allows for the CAPA foot to be easily and cheaply customized to better fit individuals of different sizes, natural gait patterns, and personal preferences. The design utilizes a rapidly advancing field and models can be later made from different materials that are lighter, more durable, and stronger [51]. The visual appeal of the CAPA foot can be optimized with 3D printing to avoid the uncanny valley and develop a prosthetic that has both a large degree of human likeness and familiarity [52, 53].

The springs can be easily replaced, allowing the same ankle-foot prosthesis to accommodate different applications or speeds. Each individual can adjust the stiffness to what would best reduce their metabolic cost of walking. Optimizing the stiffness is important to provide a balance between the greater propulsive forces provided by stiffer designs and the stabilization stiffer designs require [54]. Since the equivalent



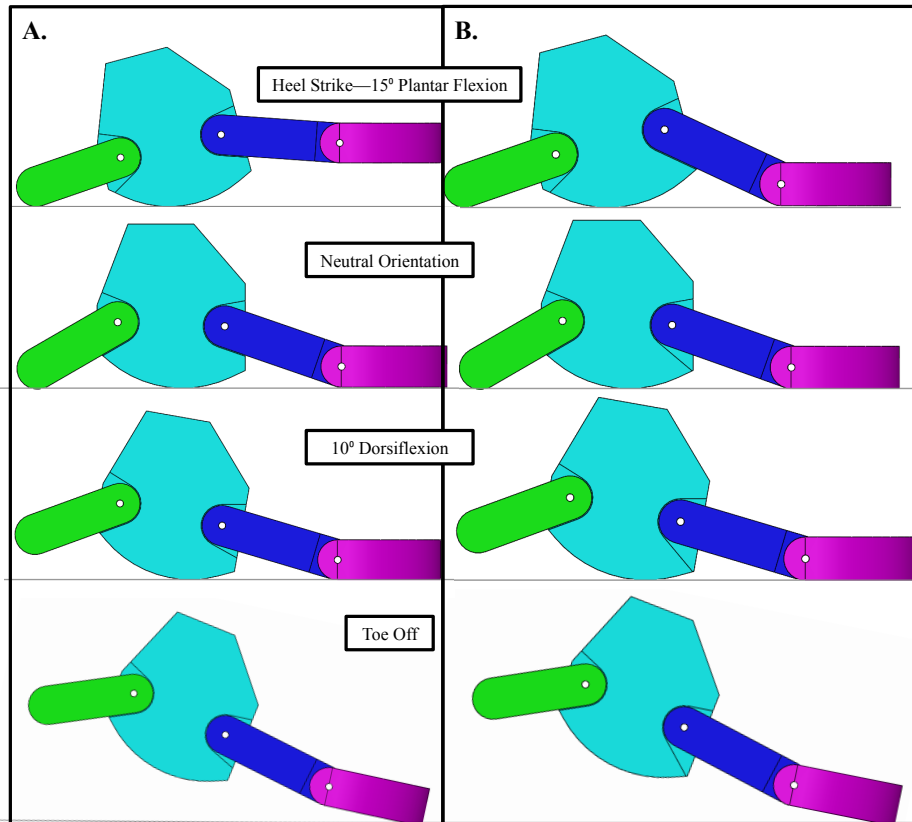


Figure 9: Movement of the CAPA foot beginning with heel strike (top) and proceeding downward through stance phase to toe-off (bottom) for experiment 1 (A) and experiment 2 (B).

stiffness of the foot during dorsiflexion is different than plantar flexion [28], the CAPA foot allows each of these stiffnesses to be personalized individually.

### 3.3 Mathematical Model

This section explains the mathematical model used to predict the roll over shape the CAPA foot will produce and optimize the design. For the purpose of better understanding the model, it is helpful to think of the CAPA foot as a rocker with two arms and a toe in the 2-dimensional sagittal plane. The first step to calculating the roll over shape is to develop equations for the kinematics of the foot during a step. Using the rotational velocity of the shank and the geometry of the foot at its neutral position, a series of kinematic equations were developed to solve for the relative positions of all components during stance phase. When the components are rotated, potential energy is stored in the springs. This creates a resultant force at the



point of contact between the arm and the ground. The force distribution is used to find the center of pressure during the step and then plot the roll over shape.

During the beginning of the gait cycle, the foot is in plantar flexion and the heel component is rotated upward. For the first version of the CAPA foot, only the heel and rocker components are in contact with the ground during plantar flexion. For the second version, the foot component is in contact with the ground as well. Once the shank angle passes the vertical position, the CAPA foot dorsiflexes and only the foot and the rocker is in contact with the ground. The arm geometry is the only difference between the kinematic equations governing the rotation upward of the heel arm versus the foot arm. Therefore, the same kinematic equations can be used. When solving for the ground reaction forces and force distribution, the stiffness of the joint is also adjusted according to the spring constant. The contribution of the toe is disregarded in this model.

### 3.3.1 Kinematic Equations

Points on the rocker and heel arm component can be connected by two loops of vectors as shown in Figure 10. Many of these points and vectors can be considered fixed and part of either rigid body 1 or 2 circled in orange. Rigid body 2 will rotate about the ankle marker with the rotation velocity of the shank labeled  $\dot{\theta}$  resulting in Equation 1. Rigid body 1 will rotate about the Rotational Center in Figure 10. Since the ground is level, the points of contact between ground and both the arm and the rocker are constrained in the y-direction. Geometrically fixed vector lengths and points are shown in black and unknown vector lengths and angles are shown in blue. The fixed lengths and angles are shown in Table 1 with the angles defined from the positive x-axis.

$$\dot{\theta} = \dot{\theta}_1 = \dot{\theta}_5 \quad (1)$$

At every position of the CAPA foot, each of the two vector loops shown in Figure 10 must make one full circle meaning that each vector sum must equal to 0 as given by the first line Tables 2 and 3. This equation is expanded to solve for the relative positions and the velocities in the following rows of both tables.

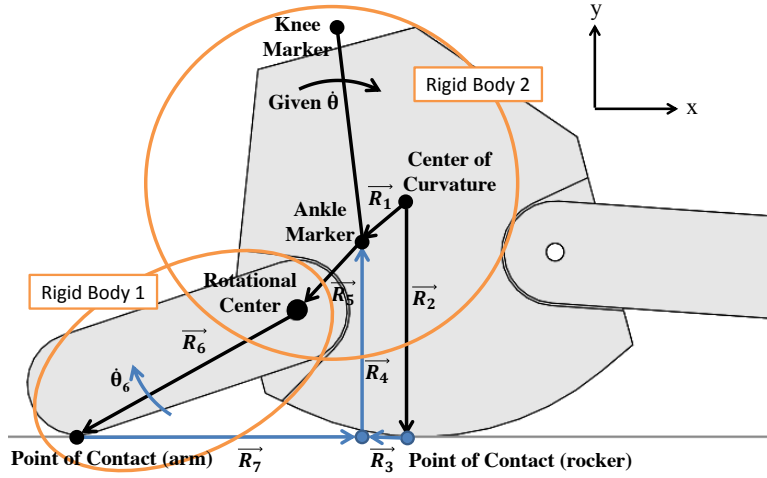


Figure 10: Visual representation of vector loops on the CAPA foot during a step. Geometrically fixed vectors lengths and points are shown in black and unknown vector lengths and angles are shown in blue. The angles defined from the positive x-axis. Rigid body 1 and 2 circled in orange represent the heel and ankle component respectively.

Table 1: Fixed Geometric Parameters of CAPA Foot

$r_1 =$	Distance from the center of curvature of the rocker to the ankle marker
$r_2 =$	Radius of the rocker
$r_5 =$	Distance from the ankle marker to the arm center of rotation
$r_6 =$	Distance from the arm center of rotation to the point of contact with the ground
$\theta_2 =$	$-90^\circ$
$\theta_4 =$	$90^\circ$
$\theta_3 =$	0, 180
$\theta_7 =$	0, 180

By applying the fixed geometries listed shown in Table 1 and Equation 1, the equations from Table 2 reduce to Equations 2 and 3 and the equations from Table 3 reduce to Equations 4 and 5.

$$\dot{r}_3 = \frac{-r_1 \dot{\theta} \sin(\theta_1)}{\cos(\theta_3)} \quad (2)$$

$$\dot{r}_4 = r_1 \dot{\theta} \cos(\theta_1) \quad (3)$$

$$\dot{\theta}_6 = \frac{r_5 \dot{\theta} \cos(\theta_5) + \dot{r}_4}{-r_6 \sin(\theta_6)} \quad (4)$$

$$\dot{r}_7 = \frac{r_5 \dot{\theta} \sin(\theta_5) + r_6 \dot{\theta}_6 \sin(\theta_6)}{\cos(\theta_7)} \quad (5)$$

Given the lengths of the vectors when the foot is in the neutral orientation, the vector velocities can be used to solve for all remaining positions of the vectors. The same parameters are used in the ankle loop equations

Table 2: Ankle Loop Equations

Vector Sum	$\vec{R}_1 = \vec{R}_2 + \vec{R}_3 + \vec{R}_4$
Position	$r_1 e^{i\theta_1} = r_1 e^{i\theta_1} + \bar{r}_3 e^{i\theta_3} + \bar{r}_4 e^{i\theta_4}$
X-Direction	$r_1 \cos(\theta_1) = r_2 \cos(\theta_2) + r_3 \cos(\theta_3) + r_4 \cos(\theta_4)$
Y-Direction	$r_1 \sin(\theta_1) = r_2 \sin(\theta_2) + r_3 \sin(\theta_3) + r_4 \sin(\theta_4)$
Velocity	$r_1 i \dot{\theta}_1 e^{i\theta_1} = 0 + \dot{r}_3 e^{i\theta_3} + \dot{r}_4 e^{i\theta_4}$
X-Direction	$-r_1 \dot{\theta}_1 \sin(\theta_1) = \dot{r}_3 \cos(\theta_3) + \dot{r}_4 \cos(\theta_4)$
Y-Direction	$r_1 \dot{\theta}_1 \cos(\theta_1) = \dot{r}_3 \sin(\theta_3) + \dot{r}_4 \sin(\theta_4)$

Table 3: Arm Loop Equations

Vector Sum	$0 = \vec{R}_4 + \vec{R}_5 + \vec{R}_6 + \vec{R}_7$
Position	$\bar{r}_4 e^{i\theta_4} + r_5 e^{i\theta_5} + r_6 e^{i\theta_6} + \bar{r}_7 e^{i\theta_7} = 0$
X-Direction	$r_4 \cos(\theta_4) + r_5 \cos(\theta_5) + r_6 \cos(\theta_6) + r_7 \cos(\theta_7) = 0$
Y-Direction	$r_4 \sin(\theta_4) + r_5 \sin(\theta_5) + r_6 \sin(\theta_6) + r_7 \sin(\theta_7) = 0$
Velocity	$\dot{r}_4 e^{i\theta_4} + r_5 i \dot{\theta}_5 e^{i\theta_5} + r_6 i \dot{\theta}_6 e^{i\theta_6} + \dot{r}_7 e^{i\theta_7} = 0$
X-Direction	$\dot{r}_4 \cos(\theta_4) - r_5 \dot{\theta}_5 \sin(\theta_5) - r_6 \dot{\theta}_6 \sin(\theta_6) + \dot{r}_7 \cos(\theta_7) = 0$
Y-Direction	$\dot{r}_4 \sin(\theta_4) + r_5 \dot{\theta}_5 \cos(\theta_5) + r_6 \dot{\theta}_6 \cos(\theta_6) + \dot{r}_7 \sin(\theta_7) = 0$

given in Table 3 and Equations 4 and 5 to describe the movement of the rocker throughout the entire step. However, different values for  $r_5$ ,  $r_6$ , and  $\theta_7$  are used depending on the arm in contact with the ground. For example, when the shank passes the vertical position, the heel arm is not in contact with the ground anymore and there will be no resultant force between the heel arm and the ground. When the value of  $r_3$  equals zero and the center of curvature crosses the ankle marker, the value of  $\theta_3$  switches between 0 and 180 degrees.

### 3.3.2 Roll Over Shape

When either of the arms are bent upward, the springs are compressed at an angle equal to the difference between  $\theta_6$  and its initial value. The resultant force ( $F_{arm}$ ) given by Equation 6 will push against the ground at the point of contact between the arm and the ground. The remaining forces ( $F_{rocker}$ ) will occur at the point of contact between the rocker and the ground. To find  $F_{rocker}$ ,  $F_{arm}$  is subtracted from the total experimental ground reaction forces ( $F_{total}$ ) shown in Equation 7. The difference between the x direction location of the center of pressure and the ankle marker is given by Equation 8. Figure 11 shows forces acting on the foot and the COP in both the lab-based coordinate system and the shank-based coordinate system. These points are plotted to create the roll over shape.

$$F_{arm} = K * (\dot{\theta}_6 - \dot{\theta}) \text{ where } K = \text{Spring constant} \quad (6)$$

$$F_{rocker} = F_{total} - F_{arm} \text{ where } F_{total} \text{ is collected experimentally} \quad (7)$$

$$X_{lab} - X_{ankle} = \frac{-1}{F_{total}} * [(F_{rocker}r_3\cos(\theta_3)) + (F_{arm}r_7\cos(\theta_7))_{heel} + (F_{arm}r_7\cos(\theta_7))_{foot}] \quad (8)$$

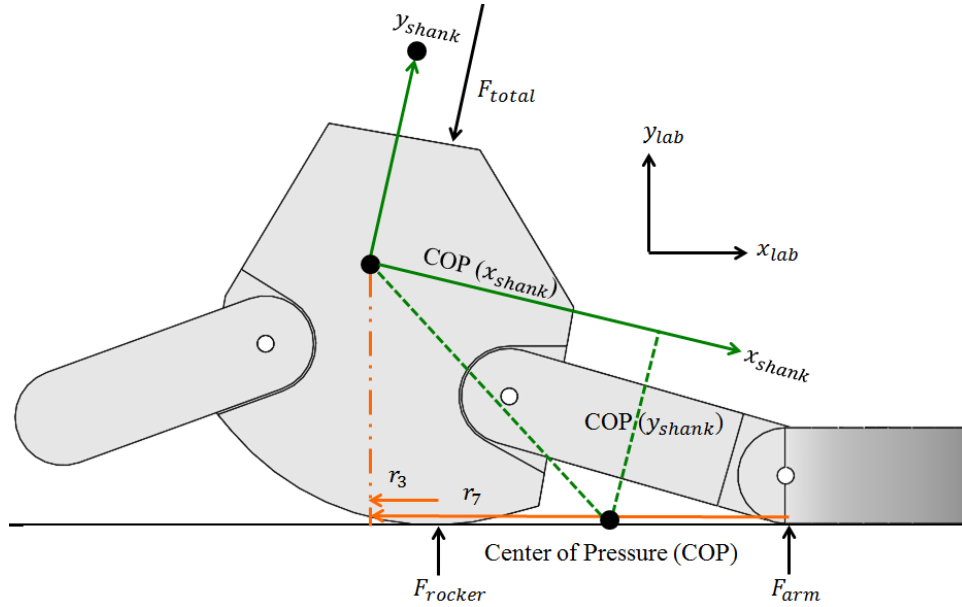


Figure 11: The forces acting on the CAPA and the resulting center of pressure in the lab-based coordinate system (orange) and the shank-based coordinate system (green)

### 3.3.3 Optimization

The mathematical model can be used to optimize the component geometries and stiffness of the design that will produce the desired ground reaction forces and roll over shapes.

#### 3.3.3.1 Stiffness

The role of the springs in the CAPA foot design is to mimic the energy storage and return function of the ankle tendons and provide the required push-off force for forward motion. If the spring constant is too small, the foot will not be able to produce the required push-off force to facilitate forward motion. On the other hand, a spring constant that is too large requires the amputee to compensate for the extra forces and affects stability. As a result, several studies have attempted to quantify the contribution of the ankle joint in terms of a spring constant. The quasi-stiffness of the human ankle can be evaluated by measuring the slope of

the ankle angle versus ankle moment graph. Data collected by Hansen found an equivalent quasi-stiffness during dorsiflexion of approximately  $5.7 \frac{N-m}{kg-rad}$  [13] and Shamaei found an equivalent stiffness values of  $3.38 \frac{N-m}{kg-rad}$  during dorsiflexion and  $2.09 \frac{N-m}{kg-rad}$  during plantar flexion at self selected walking speeds [28]. Rouse makes a point to distinguish these equivalent stiffness values as measurements of quasi-stiffness as opposed to stiffness because the measurements only describe the equivalent stiffness values when the ankle is acting as a passive system [55]. Rouse conducts his own study using a Perturberator Robot to measure an average stiffness of  $1 \frac{N-m}{kg-rad}$  at the beginning of stance phase and  $4.6 \frac{N-m}{kg-rad}$  at the end of stance phase [56].

Even though ankle stiffness changes with weight and speed [28], for this particular study, the same stiffness values were used for every participant regardless of weight and speed. An alternative way of determining the joint stiffness required by the CAPA foot is to look at the discrepancy between the gait of an able-bodied individual and the gait of the same individual wearing the SACH foot that provides very little push-off. Figure 5 shows the discrepancy to be approximately 10% the individual's body weight. The average participant in the study weighed 72.22kg so the CAPA foot must reach 70.8N of force at 10 degrees dorsiflexion. The rotational stiffness of  $7.08 \frac{N}{deg}$  and practical constraints were used to guide the effective rotational stiffness values given in Table 4. For experiment 2, the same rotational stiffness values were used with an additional dorsiflexion pretension of 26.3N, 52.6N, 33.6N, and 67.2N as shown in Table 6.

Table 4: Effective Rotational Stiffness Values of CAPA Foot at the End of the Moment Arm

	Plantar flexion( $\frac{N}{deg}$ )	Dorsiflexion( $\frac{N}{deg}$ )
CAPA Small Radius Long Moment Arm Compliant	1.9	1.8
CAPA Small Radius Long Moment Arm Stiff	3.8	3.5
CAPA Large Radius Short Moment Arm Compliant	1.9	2.2
CAPA Large Radius Short Moment Arm Stiff	3.8	4.5

### 3.3.3.2 The Effect of Changing Various Geometries

After determining the spring constant, the geometries of the CAPA foot can be chosen to produce the desired roll over shape. Shank angle and force data from one subject is used with the mathematical model to evaluate the effect of changing various geometries on the CAPA foot. Since the roll over shape is

determined by the foot as opposed to the individual wearing the foot, it is theorized that the resulting shape and trends will remain the same with a different subject's gait data. These roll over shapes would change if the springs are replaced. However, it was observed that the effect of increasing the stiffness at either the heel or toe is to lengthen the roll over shape rather than changing some of the more nuanced characteristics of the roll over shape.

It was observed that increasing the distance between the ankle marker and the center of curvature of the rocker ( $r_1$ ) by using a larger radius will cause the point of contact between the rocker and the ground to move more during the step. This will result in a flatter and longer roll over shape, qualities that previous studies have found desirable [44, 43, 45]. In order to achieve a larger radius within the dimensions of a normal foot, the center of curvature and point of contact when the foot is in the neutral position must be moved in front of the ankle marker in the horizontal direction. The resulting roll over shape will also have a center of curvature with a forward shift.

Another change that can be made to the CAPA foot is increasing the length of the arm piece by increasing the length of  $r_6$ . This change will increase the distance of the point of contact between the arm and the ground ( $x_{arm}$ ) and the ankle marker causing the center of pressure to move further forward and the roll over shape to lengthen. However, lengthening the arm simultaneously lengthens the moment arm and decreases the ground reaction force between the arm and the ground creating the opposite effect to the resulting roll over shape. As long as the arm is long enough to reach the forward-most center of pressure position on the roll over shape, these effects will essentially cancel each other out. An alternative is to increase both the length of the arm and the stiffness. In general, larger stiffnesses at either the heel or the foot provide more ground reaction forces and lengthen the roll over shape. The observed results of changing the various parameters in the mathematical model are summarized in Table 5.

Table 5: Summary of the Effect That Changing Individual Parameters Have on the Roll Over Shape Radius of Curvature (ROC) and Horizontal Center of Curvature ( $X_c$ )

Parameter	Geometric Equivalent	Effect on roll over shape
$\vec{R}_1(r_1, \theta_1)$	Vector from the center of curvature of the rocker to the ankle marker	Larger $r_1$ – ROC increases, $\theta_1 = 270^\circ$ – largest ROC, $\theta_1 = 180^\circ$ – largest $X_c$
Heel $\vec{R}_5(r_5, \theta_5)$	Vector from the ankle marker to the heel arm center of rotation	No major effect
Heel $\vec{R}_6(r_6, \theta_6)$	Vector from the heel arm center of rotation to the point of contact with the ground	Larger $r_6$ – smaller ROC and $X_c$ , $\theta_6$ – No effect
Foot $\vec{R}_5(r_5, \theta_5)$	Vector from the ankle marker to the foot arm center of rotation	Larger $r_5$ – ROC increases and $X_c$ decreases, As $\theta_5$ approached $180^\circ$ , $X_c$ increases and ROC decreases
Foot $\vec{R}_6(r_6, \theta_6)$	Vector from the foot arm center of rotation to the point of contact with the ground	Larger $r_6$ – smaller ROC and $X_c$ , $\theta_6$ – No effect

### 3.4 Final Experimental Designs

The mathematical model was used to create two models of the CAPA foot that would result in the roll over shapes shown in Figure 12. Shank angle and force plate data was used from one subject wearing a previous version of the CAPA foot with the prosthetic simulator. Geometric parameters were chosen iteratively using the trends observed in section 3.3.3.2 to optimize the design to the two roll over shapes. The first roll over shape to the left in Figure 12 was optimized to be as close as possible to that of the able-bodied roll over shape found in section 3.1.4. This resulted in CAPA foot design radius of 30mm and longer moment arm. The radius of the small radius CAPA foot is relatively close to the radii of the talus bone (between 20 and 26.6 mm) [7].

The geometric parameters for the second roll over shape were created to maximize the radius of curvature and effective foot length. Both characteristics have been found to be indicative of a healthier gait as explained in section 3.1.4. This resulted the in a CAPA foot with a radius of 85mm, the largest radius reasonably possible in the space provided. For each model of the CAPA foot, a compliant and stiff version was tested with the rotational stiffness values given in Table 4. Figure 12 shows the effect that the change in stiffness is expected to have on the roll over shape.

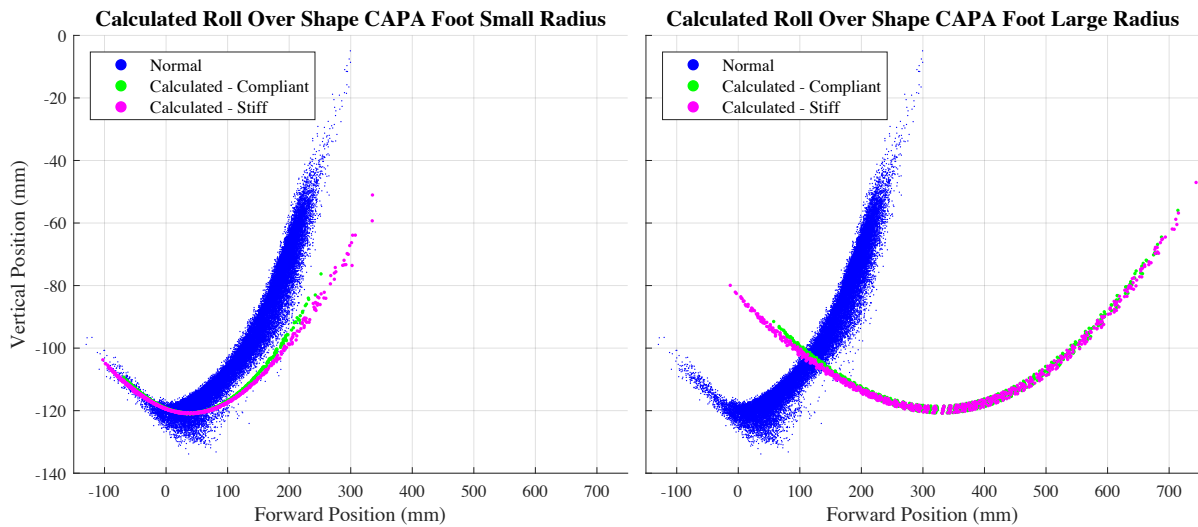


Figure 12: Experiment 1 predicted roll over shapes of the compliant and stiff versions of the CAPA-foot-small-radius-long-moment-arm (left) and CAPA-foot-large-radius-short-moment-arm (right) compared to the able-bodied roll over shape found in section 3.1.4. The prediction was made using the mathematical model.

The experimental procedure was another consideration in the final designs. All CAPA feet used in experimental testing had a neutral length of 22cm, approximately equal to the length of the SACH foot (22cm) and Renegade<sup>®</sup> AT (23cm) used for comparison. For all experimental testing and roll over shapes shown in Figure 12, the same exact heel component, toe component, toe stiffness, and ankle marker positioning relative to the back of the foot were used for every trial. The center of the universal connector was 70mm from the back of the foot for both the small radius and large radius ankle component. The ankle marker is positioned to be in line with the center of the universal connector. These design choices were made in order to focus on the effect that changing the joint stiffnesses and geometries of the ankle and foot components may have on the resultant gait.

This study was separated into two experiments. The only difference between the two experiments is the angle of the platform circled in orange in Figure 13. For experiment 2, the platform was angled further downward by 15 degrees. This design change means that there is a pretension in the springs between the ankle and foot components when the foot is in its neutral orientation equal to values shown in Table 6. It also means that when the CAPA foot begins dorsiflexion in experiment 2, there is already energy stored at



the joint. Figure 13 shows the resting side profile of the final geometries during experiment 2. When an individual puts weight on the foot during experiment 2, the front arm will bend upward and the ankle rocker will touch the ground. For experiment 1, the platform circled in orange is 15 degrees higher and the ankle rocker will rest on the ground without weight. Figure 9 in section 3.2.1 shows an animation of both designs during stance phase.

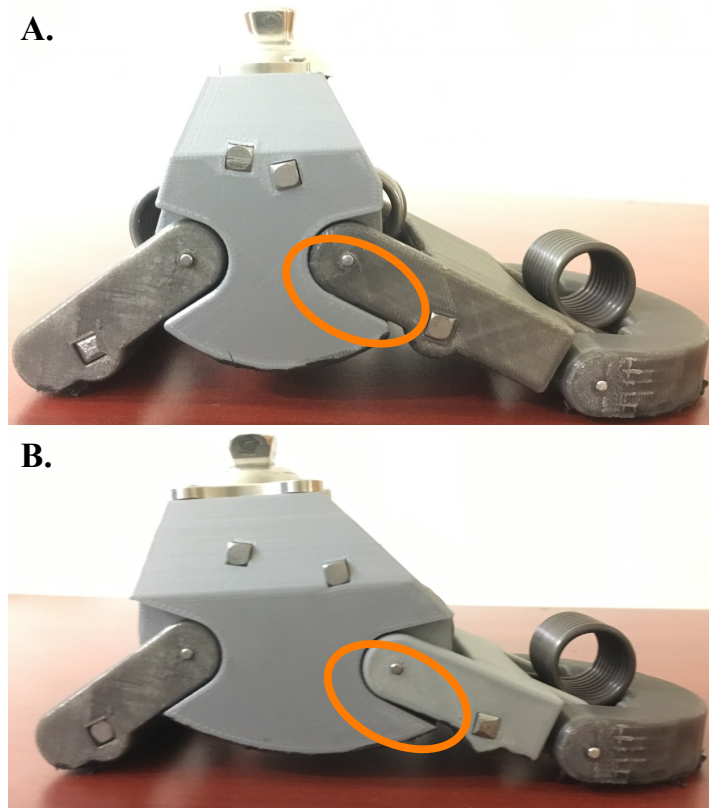


Figure 13: Experiment 2 CAPA-foot-small-radius-long-moment-arm (A) and CAPA-foot-large-radius-short-moment-arm (B). The platform circled in orange is angled 15 degrees upward in experiment 1.

Table 6: Experiment 2 Dorsiflexion Pretension (N)

CAPA Small Radius Long Moment Arm Compliant	26.3
CAPA Small Radius Long Moment Arm Stiff	52.6
CAPA Large Radius Short Moment Arm Compliant	33.6
CAPA Large Radius Short Moment Arm Stiff	67.2

Final designs were 3D printed using PLA (Polylactic Acid) filament with 100% infill. During printing, the parts were oriented with the faces shown in Figure 14 facing up. The universal connector was connected to the ankle component by drilled holes. The toe and heel components remain intact throughout all training sessions and experiments. The foot broke three times during the course of experimentation. During the first, the subject fell and the screws connecting the universal connector and the CAPA-foot-small-radius ankle component snapped. The second time occurred during a fall as well and the short moment arm foot component on the CAPA-foot-large-radius broke. The last time occurred when the entire foot was dropped. The short moment arm foot component on the CAPA-foot-large-radius broke. New ankle components were printed between experiment 1 and 2.

It was desirable to have a larger rotational stiffness than could be achieved in the space given using commercially available springs. While it is possible to get these springs custom made, for the purposes of making one foot, it is expensive and provides less flexibility than could be achieved by connecting springs in series. An arm of springs shown in Figure 13 was created to effectively increase the spring constant at the joints. The four components are indicated by locations 1-4 in Figure 13. Location 5 in Figure 13 labels the universal adapter. Three 1/8" steel rotary shafts at location 10 in Figure 13 connect the components. The 1/8" steel rotary shafts that connect the heel and foot components to the ankle component pass through the center of all of the springs. The arms of the springs rest on four 1/4" steel square bars such as at location 6 in Figure 13. Because the large forces exerted by the springs can cause the 1/8" shafts to deflect, the shafts are held in place by pieces of Delrin® at Location 9 in Figure 13. The Delrin® was laser cut to connect the circular shafts with the stronger square shafts and still allow for rotation at the joints. Each shaft was 12 inches in length.

The weight of the CAPA-foot-small-radius and CAPA-foot-large-radius with the arm of springs was the 1631.4g and 1780.8g respectively. This is much heavier than the SACH foot (415g). and Renegade® AT (471g). However, the majority of the weight is due to the arm of steel shafts and springs. This arm

can be replaced by two single stiffer springs, one at the joint between the heel and ankle and the other at the joint between the ankle and foot. Without the arm of springs, the four 2D printed components and the universal adapter only weighted 737.7g and 887.1g respectively. This weight could be further reduced with the use of more advanced 3D printing techniques. The CAPA foot was wider than the SACH foot (75mm) and Renegade<sup>®</sup> AT (75mm) with a total width of 103mm.

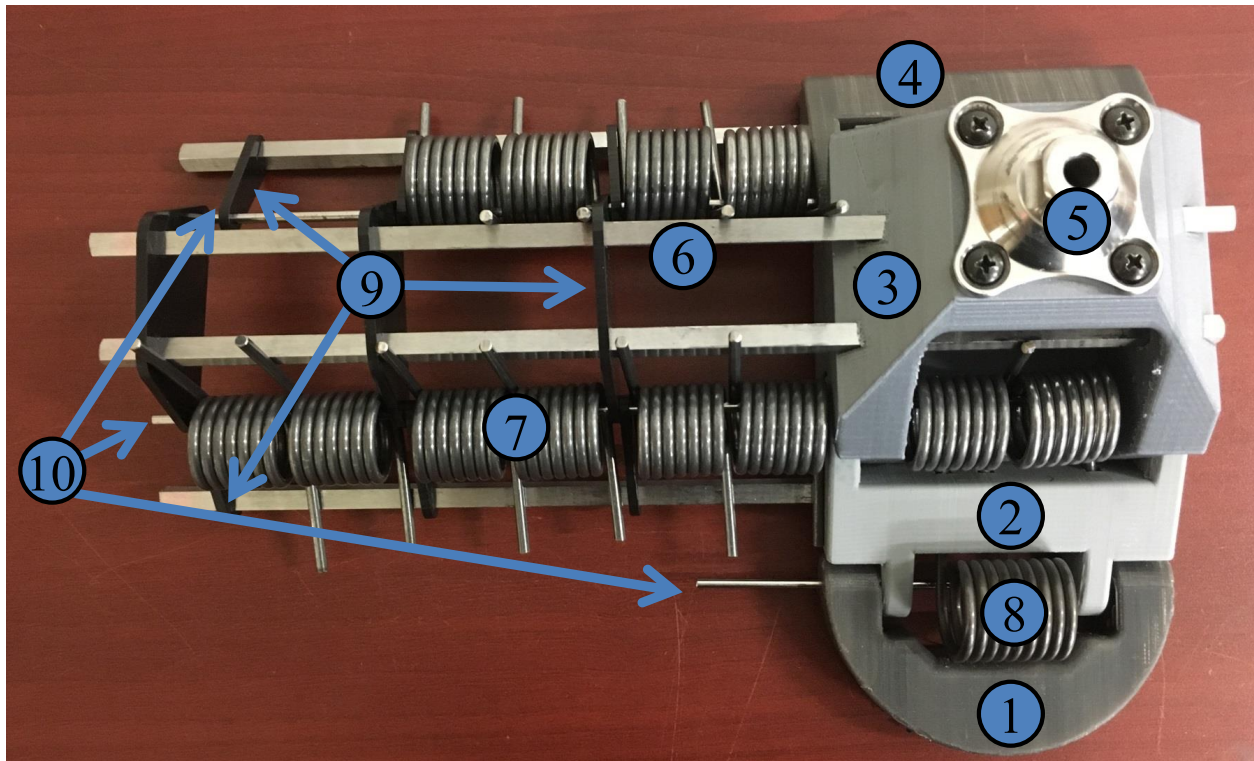


Figure 14: Top view of an exemplary CAPA foot prototype used for experiments 1 and 2 showing the arm mechanism used to increase the stiffness. ①-Toe ②-Foot ③-Ankle ④-Heel ⑤-Universal Connector ⑥-4 1/4" Hardened 4140 Alloy Steel Square Bars ⑦-5.01N-m 120° Steel Torsion Springs ⑧-4.84N-m 180° Steel Torsion Springs ⑨-Delrin<sup>®</sup> connectors ⑩-1/8" Steel Rotary Shafts.

## CHAPTER 4: METHODS

This study was aimed at comparing the the different versions of the CAPA foot explained in section 3.4 to each other and to existing ankle-foot prostheses. The existing prostheses used were the SACH foot and a type of ESR foot, the Renegade<sup>®</sup> AT produced by Freedom Innovations shown in section 2.1 Figures 1 and 2. On the Computer Assisted Rehabilitation Environment (explained in section 4.1), ten able-bodied individuals walked normally and then with a transfemoral prosthetic simulator (explained in section 4.2) for a series of 8 trials shown in Table 7. For each subject, the order of the four different feet (SACH foot, Renegade<sup>®</sup> AT, CAPA-Foot-Small-Radius-Long-Moment-Arm, and CAPA-Foot-Large-Radius-Short-Moment-Arm) was randomized. If the ankle-foot was either the SACH foot or the Renegade<sup>®</sup> AT, the order of the versions with no weight and with a weight was randomized. If the ankle-foot was the CAPA foot, the order of the compliant and stiff versions was randomized.

Table 7: Experimental Trials 1.5 Minutes Each

Perturbation	Total Weight of Prosthetic and Shank
1. SACH foot	415.0g
2. SACH foot with weight	1850.1g
3. Renegade <sup>®</sup> AT	419.3g
4. Renegade <sup>®</sup> AT with weight	1854.4g
5. CAPA Small Radius Long Moment Arm Compliant	1631.4g
6. CAPA Small Radius Long Moment Arm Stiff	1631.4g
7. CAPA Large Radius Short Moment Arm Compliant	1780.8g
8. CAPA Large Radius Short Moment Arm Stiff	1780.8g

One of the most obvious differences between the two existing prostheses and the CAPA foot is the weight of the ankle-foot. Despite this, the weight of the CAPA foot prototypes used in experimentation is not necessarily representative of the weight of a final version of the CAPA foot. For this reason, each of the existing prostheses was tested with and without an ankle weight added to the shank of the prosthetic leg so that the total weight approximately equals that of the CAPA foot as shown in Table 7. Performing these

additional trials helped control the effect that the difference in weight may have on the gait of an amputee, and it also allows for the effect that weight has on the gait of a transfemoral amputee to be evaluated. It should be noted that, while the total weight of the existing prostheses with a weight is approximately equal to that of the CAPA foot, the location of the added weight on the existing prostheses was around the ankle/lower shank and at a more proximal position to the knee than the CAPA foot. In other words, the center of mass of the CAPA foot is at a more distal location and closer to the ground in comparison to the center of mass of the existing prostheses with a weight. This difference in location could impact the results, particularly during swing phase.

The study was separated into two experiments. Subjects 1-5 participated in the first experiment and subjects 6-10 participated in the second experiment. The only difference between the two experiments was the orientation of one of the platforms on the CAPA foot explained in section 3.4. The second experiment was performed in order to evaluate if added pretension improved the design.

#### **4.1 Computer Assisted Rehabilitation Environment**



Figure 15: Computer Assisted Rehabilitation ENvironment (CAREN)

The Computer Assisted Rehabilitation ENvironment (CAREN) shown in Figure 15 is equipped with 180° projection screens, a six degree of freedom motion base, split-belt treadmill with force plates, video cameras, and 10 motion capture cameras. It is human rated and has numerous safety features and procedures including a harness, multiple stop buttons, handrails, and sensors that stop the treadmill if the individual goes too far to the front or back of the platform. During each trial, positions from 18 reflective markers, ground reaction forces, and center of pressure data were gathered at a rate of 100Hz.

#### **4.2 Prosthetic Simulator**

Testing was performed using able-bodied subjects wearing a transfemoral prosthetic simulator on their right leg. The simulator was assembled using part of an iWalk<sup>©</sup>, a polycentric prosthetic knee, and an ankle-foot prosthesis as shown in Figure 16. Figure 16 also shows the marker placement on the simulator. Because the knee used is polycentric with two rotational centers, markers were placed above and below the knee. The height the Renegade<sup>®</sup> AT and arm of springs on the CAPA foot made it difficult to place the ankle marker at its correct anatomical position. Instead, the ankle marker was placed at the prosthetic component that connects the universal connector on the ankle-foot to the shank on the prosthetic simulator. Components between the prosthetic knee and the ankle-foot prosthesis were switched out in order to keep the height of the prosthesis the same.

The gait of transfemoral amputees and individuals wearing an above the knee prosthetic simulator have similar kinematic and kinetic joint mechanics [57], and, as a result, has been used as a tool to study the gait of a transfemoral amputee [58, 41, 59, 60, 61]. Using a simulator allowed the gait produced by each ankle-foot prosthesis to be analyzed without putting an amputee through undue stress.

#### **4.3 Procedure**

Ten able-bodied subjects volunteered their time to participate in this study. The participants were recruited through flyers and two emails sent to the entire engineering student body at the University of South





Figure 16: Prosthetic simulator with the SACH foot and reflective markers.

Florida. The study and flyer were approved by the Institutional Review Board at the University of South Florida. All subjects read and signed consent forms before taking part in the experiment.

The study consisted of two sessions. For the first session, lasting approximately 1 hour, the individual was fitted and trained over ground with the prosthetic simulator. The first session began by the author explaining the study, the Computer Assisted Rehabilitation Environment (CAREN), and the task required by the able-bodied volunteer. Questions were answered and the author explained how to walk on the prosthetic simulator. Each subject began the training session wearing the SACH foot with no weight. For the duration of the training session, each subject tried either the experiment 1 CAPA-foot-large-radius-stiff or the experiment 1 CAPA-foot-small-radius-stiff, the Renegade<sup>®</sup> AT produced by Freedom Innovations, and at least one of the existing prosthetics with a weight. The degree to which the ankle-foot was “turned out,”

Table 8: Age, Height, Weight, and Walking Speeds of Participants in Study. Subjects 1-5 participated in experiment 1 and used CAPA feet without pretension and subjects 6-10 participated in experiment 2 and used CAPA feet with pretension.

Subject	Age	Height	Weight	Normal Walking Speed	Simulator Walking Speed
1	20	5'11"	164lb	1.4m/s	0.5m/s
2	22	5'10"	151lb	1.3m/s	0.7m/s
3	22	5'10"	147lb	1.2m/s	0.8m/s
4	25	5'9"	174lb	1.4m/s	0.5m/s
5	23	6'1"	174lb	1.5m/s	0.8m/s
6	25	6'2"	146lb	1.7m/s	0.7m/s
7	25	5'9"	170lb	1.1m/s	0.75m/s
8	18	6'2"	193lb	1.4m/s	0.75m/s
9	22	5'10"	147lb	1.2m/s	0.8m/s
10	19	5'9"	134lb	1.3m/s	0.88m/s

the rotational angle of the ankle-foot in relation to the knee, was left up to individual preference between approximately 0° and 15°. This is because many individuals walk with their toes angled slightly outward. The SACH foot was oriented in a slightly dorsiflexed position for all trials. The height of the prostheses was determined for each subject by measuring the individual's intact knee height and watching each individual walk with the prostheses. The height remained the same throughout the experiment. The minimum knee height for participation in the study was determined by that required to walk with the Renegade® AT. If the height of the prosthetic simulator was too tall, a second session was not scheduled and the subject was excluded from the study.

The experiment was conducted during the second session, lasting between 2.25 and 3 hours. During the beginning of the second experimental session, basic information was gathered about the subject such as age, height, weight, and knee height summarized in Table 8. Inadvertently, all subjects were male. A 10m walk test was performed to get each individual's normal walking speed. Each individual began by walking normally in the CAREN system for a period of 2 minutes with eighteen reflective markers. The eighteen reflective markers were placed at the base of the second toe, heel, ankle joint, point of knee rotation, tibia, femur, point of hip rotation, and the anterior and posterior iliac on both the right and left sides of the body. Then, the prosthetic simulator with the first ankle-foot prosthesis was strapped on to the subject's right



leg and the reflective markers moved to the prosthetic leg. The subject was allowed to practice walking with the prosthetic simulator on a treadmill in the CAREN system until they felt comfortable beginning the experiment. After trying a couple of speeds, each subject self-selected the prosthetic simulator walking speed. The same speed was used for all trials.

Each individual walked on the four feet and the eight total configurations listed in Table 7 for periods of 1.5 minutes each. The order was randomized using the method explained in the beginning of Chapter 4. If the individual had difficulty adapting to a new ankle-foot, they were allowed time to practice on the CAREN system before the trial began. The practice trials were kept to a minimum to prevent fatigue. Walking with the prosthetic simulator can be physically difficult and require muscles to be used differently than normal walking. Subjects reported soreness in the foot and hip of the leg not wearing the prosthetic simulator as well as discomfort behind the knee of the leg wearing the prosthetic simulator. While the simulator ankle-foot configurations were changed, the subjects were given a chance to rest and walk around if needed. Water was provided.

Subjects were instructed to only hold onto the safety bars on either side of their body if it was necessary. During a trial, if the subject was unable to maintain a steady gait without falling or touching the handrails repeatedly, the trial was repeated. Throughout the 10 subjects, none of the individual trials were repeated more than once. After each trial, a student who was not involved in the design of the CAPA foot asked each subject to rate the difficulty level of that particular trial on a scale from 1 (easiest) to 5 (hardest). She recorded the response and any comments given about the trial. At the end of the experiment, she asked each subject “Which foot would you prefer to walk on? Why?” “Would you prefer to walk [on the SACH foot and Renegade® AT] with or without a weight,” and “Would you prefer more of less springs [on the CAPA foot]?” Responses recorded and the subject was asked for any final comments.

#### 4.4 Data Analysis

After data collection, analysis was performed to extract the ankle angles, ground reaction forces, and the roll over shape during a typical step for each subject and perturbation. Steps were distinguished by finding the times at which the position of the heel marker was in its frontmost position. The mode step time was used to define the typical step. For each subject and trial, up to 15 steps, with step times closest to the mode step time within an allowable frame error of  $\pm 50$ ms were chosen. Afterward, each trial was then translated horizontally to that beginning of the gait cycle was occurred at heel strike indicated by positive vertical ground reaction forces.

The ankle angles for each step was computed using the positions of the knee marker beneath the prosthetic knee, ankle, heel, and toe marker. The position of the ankle marker was moved down the shank so that the average distance to the ground during stance phase equals that of the subject's normal walking trial. The ankle angles were represented by first computing the toe angle and the heel angle shown in Figure 17. The angle of zero degrees for every step occurs when the foot is in the neutral position and the shank is vertical. During able-bodied walking, the toe and heel are coupled and result in very similar graphs. However, the heel flexion and toe flexion on the CAPA foot are not coupled. For this reason, the heel angles were used to represent the ankle angles during heel strike plantar flexion until the shank reaches the vertical position and the toe angles were used for the rest of gait cycle. The ground reaction forces were divided by the weight of the subject.

The same procedural analysis was performed with marker position data that had been post-processed using Nexus software and the original marker position and force data that had been collected by D-flow. Each step was scaled to 180 frames using spline interpolation. In comparison, the number of frames in a typical step ranged from 100 to 162 for across all trials. For each frame, outliers defined as values outside 1.5 times the interquartile range were excluded and the mean value, standard deviation, and number of included steps were recorded. These values were used to plot the typical step and standard error for each subject and trial as

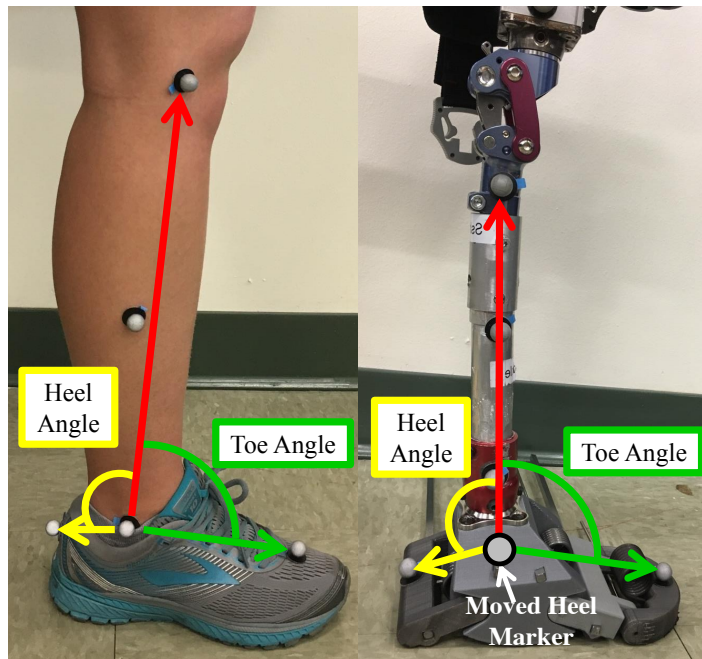


Figure 17: Toe angles (yellow) and heel angles (green) on an able-bodied leg (left) and the CAPA foot (right). The shank vector from the ankle marker to the knee marker is shown in red. The toe angle is the angle between the vector from the ankle marker to the toe marker and the shank vector. The heel angle is the angle between the vector from the ankle marker to the heel marker and the shank vector.

shown in Appendix . Mean and standard error were computed for each trial across all subjects and displayed in the results.

Finally, the position of the ankle marker, position of the center of pressure, and shank angle of the typical step was determined using the method above and used to compute the position of the center of pressure in a shank-based coordinate system. These points were plotted when the vertical ground reaction forces were greater than 0.25 the weight of the subject to find the typical roll over shape for each subject and trial.

## CHAPTER 5: RESULTS

This chapter summarizes the results from both experiments. The ankle angles, ground reaction forces, and roll over shapes across all subjects and trials of the prostheses are compared to baseline that occurs on the right side during each individual's able-bodied gait. The figures are color coded according to the prosthesis worn by the subject. The different perturbations with that particular prosthetic, for example with weight versus no weight or compliant versus stiff, are graphed with different lines in the same color. This chapter also summarizes the difficulty level ratings given by the subjects, the accuracy of the mathematical model, and validates the concept of roll over shape based design.

### 5.1 Ankle Angles

When the toe and heel are coupled, such as in trials with the intact ankle-foot (baseline) and the SACH foot, the toe and heel ankles are related and only the toe angles can be used to represent the ankle angles. However, the heel and foot arms of the CAPA foot are uncoupled so the toe and heel angles capture different aspects of the CAPA foot movement. The upward rotation of the heel arm during heel strike plantar flexion is captured by the heel angles and the upward rotation of the foot arm is captured by the toe angles. For this reason, the ankle angles were determined by using the heel angles before the shank reached its vertical position and the toe angles afterwards. This was done for all trials except for the Renegade® AT. The Renegade® AT is decoupled as well with a board that will flex during heel strike. However, since the plantar flexion was minimal and there was no good position to place a heel marker that would encompass that angle, only the toe angles for the Renegade® AT are presented. The toe angles for each subject are shown in Appendix B and the ankle angles in Appendix C.

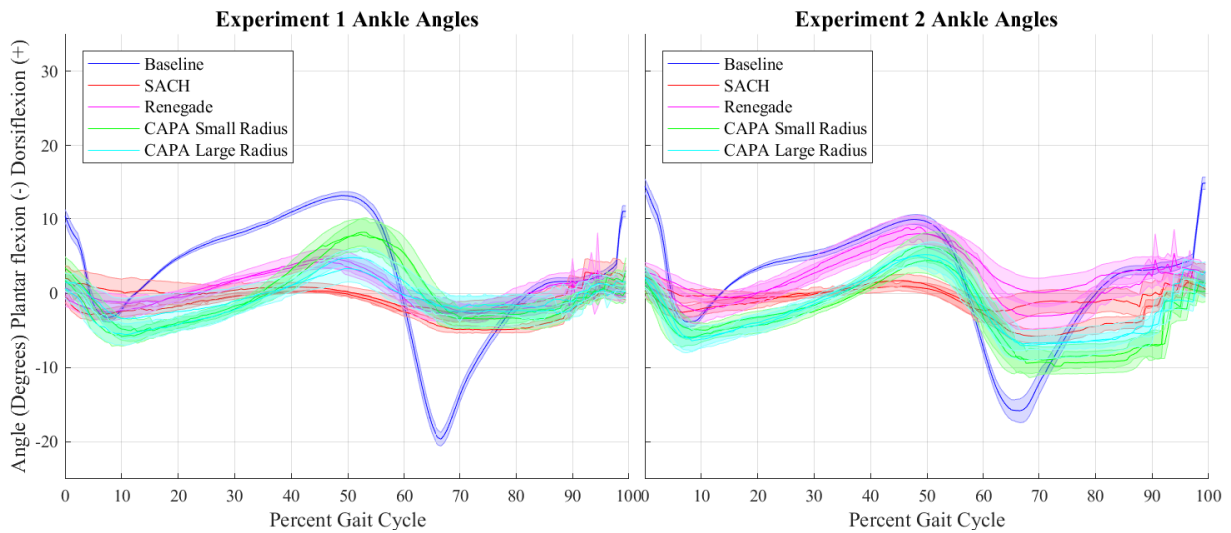


Figure 18: Ankle angles for experiment 1 and 2. The shaded error bars represent half the standard error between steps and subjects. Subject 1 SACH foot with weight and CAPA-foot-large-radius-stiff; subject 4 CAPA-foot-large-radius-compliant; subject 5 SACH foot with weight and CAPA-foot-large-radius-stiff; subject 7 Renegade with weight CAPA-foot-small-radius-stiff and CAPA-foot-large-radius; and subject 10 SACH foot without weight were removed because of difficulties post-processing the data. Individual subject figures for ankle angles are in Appendix C and toe angles are in Appendix B.

Figure 18 shows that all versions of the CAPA foot bend further in both dorsiflexion and plantar flexion than the SACH foot and look more like the ankle angles of the intact ankle-foot (baseline). For the majority of the gait cycle, the experiment 1 and experiment 2 CAPA feet ankle angles look similar. However, during toe off the experiment 2 CAPA feet are further plantar flexed and more similar to the intact ankle (baseline). This was expected because, unlike the experiment 1 CAPA feet, the resting position of the experiment 2 CAPA feet are in the plantar flexed position. Across both experiments, the CAPA-foot-small-radius bends further in dorsiflexion than the CAPA-foot-large-radius.

While the CAPA foot has a larger range of motion than the Renegade<sup>®</sup> AT in both experiments, the Renegade<sup>®</sup> AT during experiment 2 exhibits greater dorsiflexion, a stark contrast against the experiment 1 results. This is unusual because the same ankle-foot was used during both experiments. Because the experiment 2 Renegade<sup>®</sup> AT has a larger standard error bar, the results could have been increased by just a couple usual trials.

The ankle angles in Figures 18 have been graphed such that the shank is in its vertical orientation at zero degrees. When the individuals are wearing the prosthetic simulator with any version of the CAPA foot and the SACH foot, it takes approximately 35% of the gait cycle for the shank to reach neutral orientation and cross the x-axis. This is confirmed by the shank angles in Appendix D. The individuals with the CAPA feet or the SACH foot then reach maximum dorsiflexion in the next 15-20% of the gait cycle for push-off to occur. In comparison, the able-bodied individuals took less than 15% the gait cycle for their shank to reach the neutral orientation. As a result, the ankle angles for the CAPA feet may not have had time to reach maximum dorsiflexion. The prosthetic shank with the Renegade<sup>®</sup> AT reaches the vertical position sooner than either the SACH foot or the CAPA feet and later than intact ankle-foot (baseline), possibly allowing more time for dorsiflexion.

## **5.2 Ground Reaction Forces**

This section shows the normalized ground reaction forces collected by the force plates on the CAREN system for each prosthetic ankle-foot. It is first important to understand the difference between the forces produced by the ankle-foot itself and that being measured by the force plates. The force measured by the force plates is a net summation of the forces produced by the ankle-foot prosthesis and the forces produced by the human subject in reaction to the prosthesis. The mathematical model is used with the experimental shank angle to model the forces produced by the foot itself during every trial.

### **5.2.1 Vertical Ground Reaction Forces**

The vertical ground reaction forces for experiments 1 and 2 normalized by subject weight are shown in Figure 19. The intact ankle (baseline) exhibits a clear double bump while all of the ankle-foot prostheses do not. In the individual subject graphs in Appendix E, the force graphs were less smooth, especially between 20% and 50% gait cycle. There was often a peak at heel strike that was not exhibited with the intact ankle (baseline). Almost all of the subjects hit the ground particularly hard at heel strike to force the knee

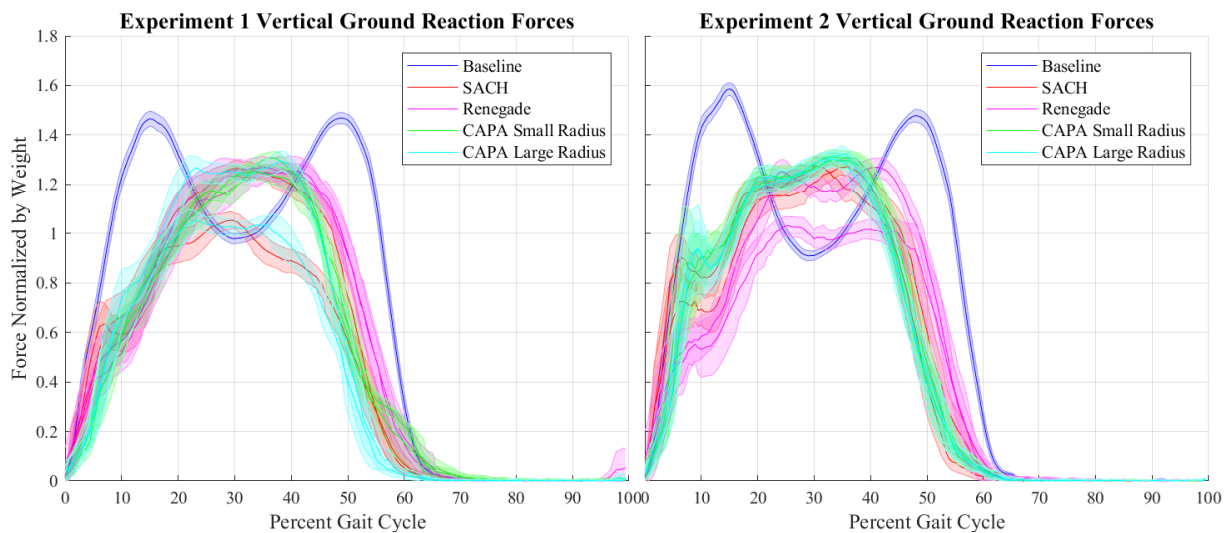


Figure 19: Vertical ground reaction forces for experiment 1 and 2. The shaded error bars represent half the standard error between steps and subjects. Subject 1 SACH foot with weight and CAPA-foot-large-radius-stiff and subject 7 Renegade with weight were removed because of difficulties post-processing the data. Individual subject figures are in Appendix E.

in its locked position before loading the leg. Therefore, the presence of the initial peak may be a result of either the polycentric knee or the prosthetic simulator itself and not a reflection on any of the particular feet.

### 5.2.2 Sagittal Plane Ground Reaction Forces

Ground reaction forces also occur in the sagittal plane. At the beginning of the gait cycle during braking, a negative force occurs. At the end of stance phase, a positive force provides the work necessary to propel the foot and proceed with forward motion. Figure 20 shows that none of the sagittal plane ground reaction forces of any of the prostheses match that of the intact ankle-foot (baseline). All versions of the CAPA foot exhibit greater push-off forces than either the SACH foot or the Renegade<sup>®</sup> AT. All versions of the experiment 2 CAPA foot exhibited greater braking forces. It was found that the Renegade<sup>®</sup> AT often exhibited a double peak profile instead of providing a braking force. The profile of the SACH foot was similar to the CAPA foot and the intact ankle-foot (baseline), but smaller in magnitude.

The experiment 2 versions of the CAPA foot with pretension exhibited greater sagittal plane ground reaction forces than the experiment 1 versions of the CAPA foot without pretension. Dorsiflexion energy is absorbed by the CAPA foot with pretension during braking, resulting in greater braking forces and greater

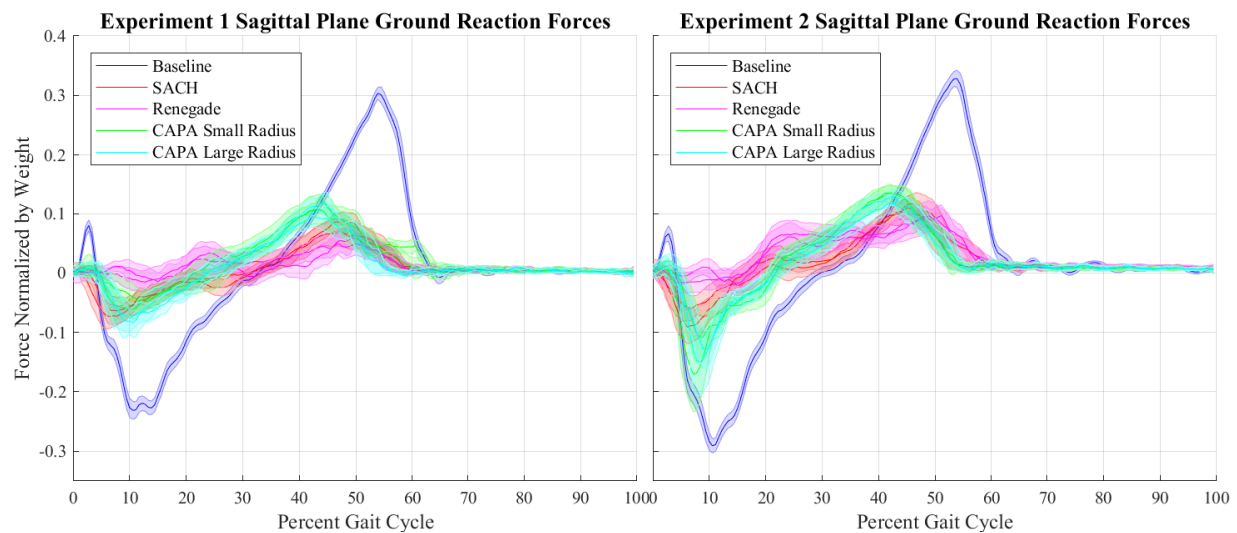


Figure 20: Sagittal plane ground reaction forces for experiment 1 and 2. The shaded error bars represent half the standard error between steps and subjects. Subject 1 SACH foot with weight and CAPA-foot-large-radius-stiff, and subject 7 CAPA-foot-small-radius-stiff were removed because of difficulties post-processing the data. Individual subject figures are in Appendix F.

forces during the release of the energy in push-off. Changes to just the rotational stiffness made little difference in the resulting push-off forces. However, the experiment 2 CAPA feet with pretension provided greater sagittal plane forces.

### 5.2.3 Ground Reaction Forces Produced by CAPA Foot

The experimental shank angle and ankle position data can be used with the mathematical model to determine the forces generated by the CAPA foot during the trial. While the magnitude and location of the forces is produced by the CAPA foot predicted directly by the mathematical model, the direction of the produced forces is less clear. For this reason the forces produced by the CAPA foot are represented in two ways. The first representation in Figure 21 assumes all of the force exerted by the heel arm contributes to braking in the sagittal plane and all of the force exerted by the foot arm contributes to push-off in the sagittal plane. Figure 21 is useful in understanding the magnitude of the forces produced by each CAPA foot throughout stance.

The second representation separates the magnitude of the total force generated by the CAPA foot into a sagittal plane component in Figure 22 and a vertical component in Appendix G. It is assumed that



the direction of the force will occur perpendicular to the arm of the torsion spring approximated by the arm angle ( $\theta_6$ ). The direction of the rocker force will likely adjust to balance the free body diagram of the CAPA foot in Figure 11. Figure 21 is useful in understanding how the forces produced by the CAPA foot contribute to the sagittal plane and vertical ground reaction forces individually.

In both Figure 21 and 22, negative values indicate plantar flexion braking forces and positive values indicate dorsiflexion push-off forces. The profile of the forces produced by the CAPA foot looks like the profile of an intact ankle-foot (baseline), but smaller in magnitude. For comparison to the sagittal plane forces in Figure 20, 70.8N is 10% of the body weight of the average subject. The mathematical model is only valid during stance phase so the forces are only shown when the vertical ground reaction forces are over 25% of the individual's body weight. The forces produced by the foot during experiment 2 are much greater than experiment 1 because of the added pretension. The forces exerted by the CAPA foot varied by subject and stiffness. Despite the CAPA-foot-small-radius having a smaller rotational stiffness because it has a longer moment arm as shown in Table 4, the push-off forces produced by the CAPA-foot-small-radius and CAPA-foot-large-radius were similar because the CAPA-foot-small-radius bended further in dorsiflexion as shown by Figure 18.

Subject 1 SACH foot with weight and CAPA-foot-large-radius-stiff; subject 6 CAPA-foot-small-radius-stiff; subject 7 Renegade with weight and CAPA-foot-small-radius-stiff; and subject 9 CAPA-foot-small-radius-stiff were removed from Figures 21 and 22.

### **5.3 Roll Over Shape**

One roll over shape for each trial was plotted using the typical shank angles, center of pressure positions, and ankle positions throughout stance phase when the vertical ground reaction forces were greater than 0.25 body weight in Figures 23 and 24. A best fit second order polynomial was found for each roll over shape. The important characteristics like the mean radius of curvature following the method used by Hansen [48], the forward position of the polynomial minimum given, and the forward length of the shape in

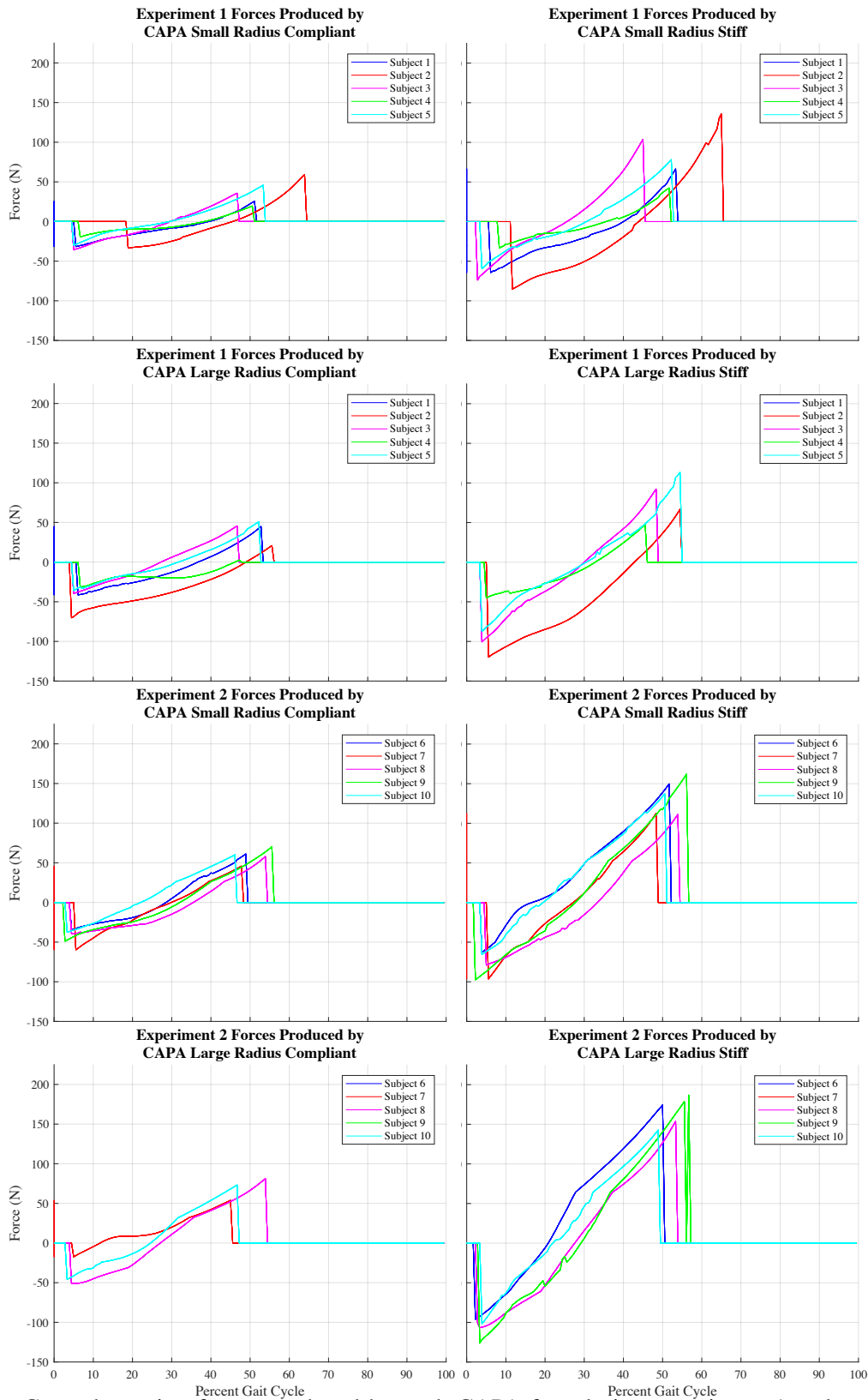


Figure 21: Ground reaction forces produced by each CAPA foot during experiment 1 and experiment 2 using first method of representation. Because the model is only valid during stance phase, the model is cut off when the vertical forces are less than 25% body weight.

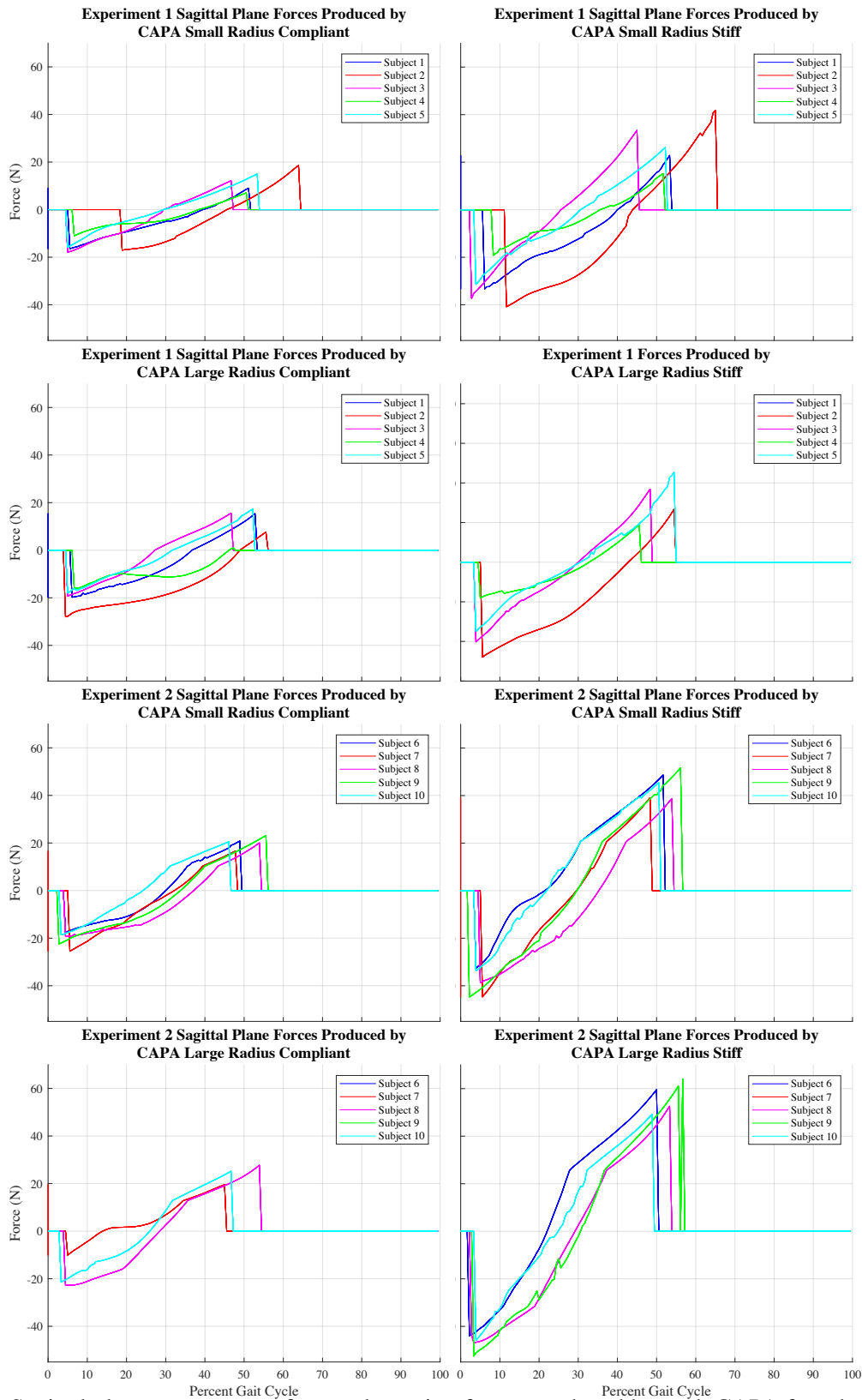


Figure 22: Sagittal plane component of ground reaction forces produced by each CAPA foot during experiment 1 and experiment 2 using second method of representation. Because the model is only valid during stance phase, the model is cut off when the vertical forces are less than 25% body weight.

the x-direction (maximum-minimum) were found for each shape and the median value is given in Table 9. The vertical position of the shape along the y-axis is mainly determined by the placement of the ankle marker and is of less importance.

The shape of the intact roll over shape in experiments 1 and 2 was consistent with the findings during the design stage in section 3.1.4. The radius of curvatures and forward length of the CAPA feet were less than the intact ankle-feet, but in general increased with added pretension and stiffness in Table 9. The radius of curvatures of the SACH foot and Renegade® AT were larger than the intact ankle-foot (baseline). It can be seen in Figures 23 and 24 that while the roll over shapes of the SACH foot and the Renegade® AT often had a longer arc length than the CAPA feet, the existing prosthesis were often the orientated differently than intact ankle-foot (baseline).

Table 9: Roll Over Shape of Best Fit Polynomial Median Radius of Curvature at Minimum, Median Forward Position at Minimum, Median Length of Shape in X-Direction

	Radius of Curvature	Forward Position	X-Direction Length
Intact Ankle-Foot	478	-0.16	334
SACH Foot	509	-0.54	276
SACH Foot With Weight	554	-0.17	310
Renegade® AT	1218	0.64	278
Renegade® AT With Weight	755	0.44	382
Experiment 1 CAPA Small Radius Compliant	200	-0.16	165
Experiment 1 CAPA Small Radius Stiff	268	-0.09	180
Experiment 1 CAPA Large Radius Compliant	249	-0.25	180
Experiment 1 CAPA Large Radius Stiff	253	-0.22	210
Experiment 2 CAPA Small Radius Compliant	247	-0.28	256
Experiment 2 CAPA Small Radius Stiff	236	-0.15	289
Experiment 2 CAPA Large Radius Compliant	236	-0.28	261
Experiment 2 CAPA Large Radius Stiff	386	-0.23	244

### 5.3.1 Comparison With Calculated

The experimental shank angle data is used to calculate the predicted position of the center of pressure using the method explained in section 3.3. The calculated and experimental positions of the center of pressure in a shank-based coordinate system are plotted for each CAPA foot in Figure 25. The roll over shape travels from the left to the right during the step. The points are connected sequentially with a line.

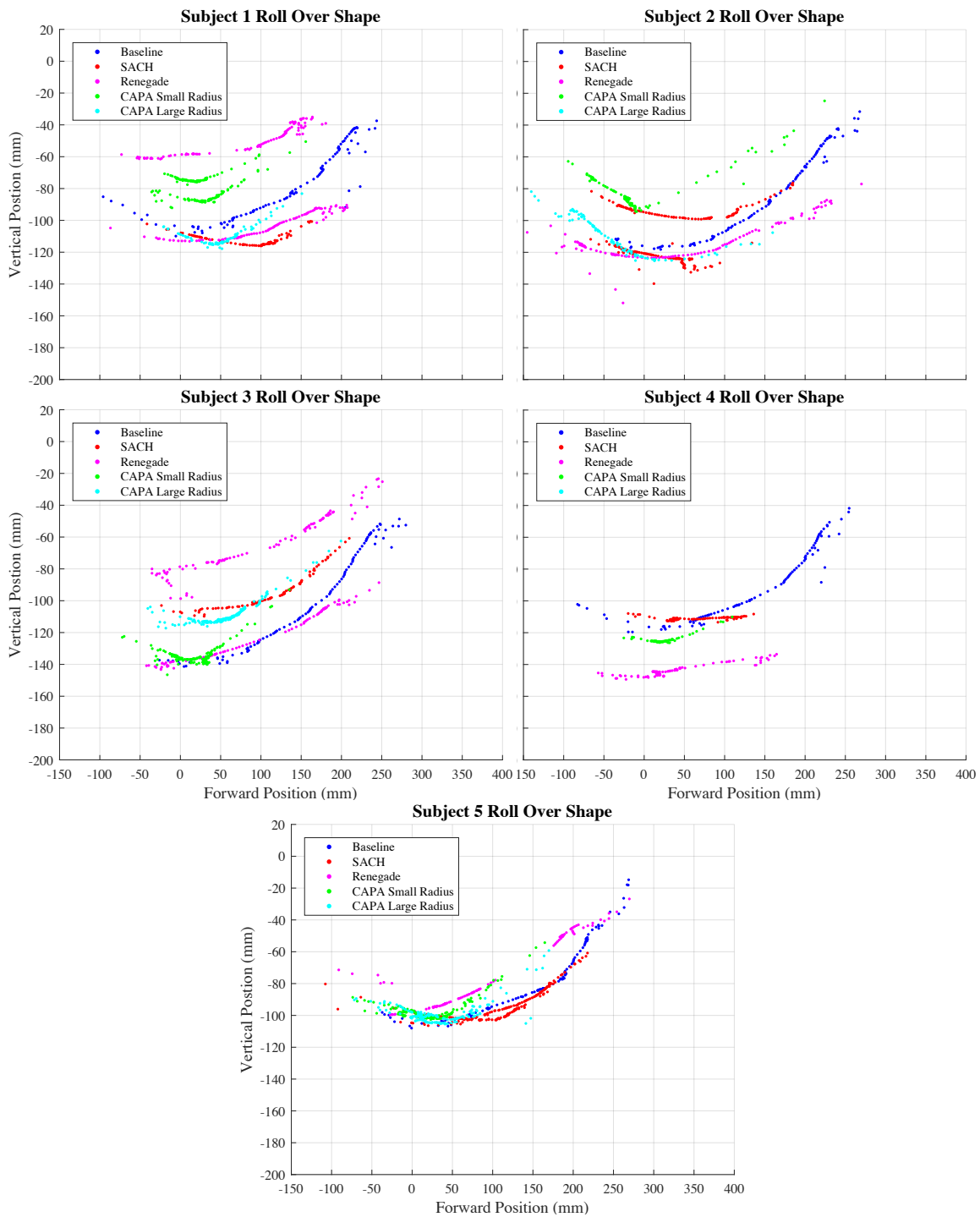


Figure 23: Experiment 1 roll over shapes for subjects 1-5. Subject 1 SACH foot with weight and CAPA-foot-large-radius-stiff; subject 2 SACH foot with weight, CAPA-foot-small-radius-compliant, and CAPA-foot-large-radius-stiff; subject 3 SACH foot no weight; subject 4 SACH foot with weight, Renegade with weight, CAPA-foot-small-radius-compliant, and CAPA-foot-large-radius; and subject 5 Renegade without weight were excluded from analysis. The ankle marker is located at coordinate (0,0) with the y-axis in line with the shank and the x-axis perpendicular to the shank. The forward position indicates the x-coordinate of the center of pressure in the shank based coordinate system. The vertical position indicates the y-coordinate of the center of pressure in the shank based coordinate system. The position of the center of pressure was only plotted when vertical ground reaction forces were greater than 0.25 the individual's body weight.

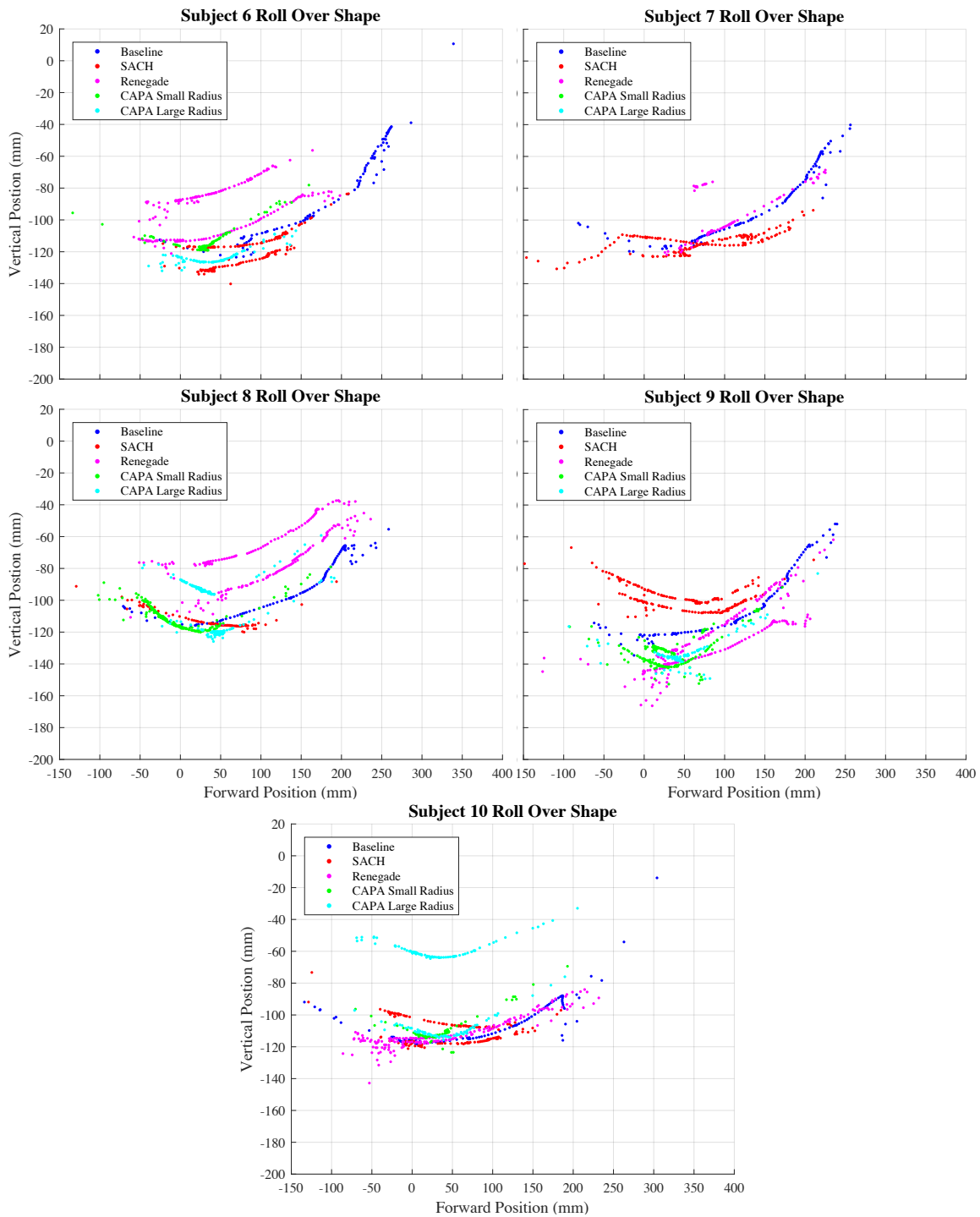


Figure 24: Experiment 2 roll over shapes for subjects 6-10. Subject 6 CAPA foot compliant; subject 7 all CAPA foot trials; subject 8 SACH foot with weight; subject 9 CAPA-foot-large-radius-compliant, and subject 10 CAPA-foot-small-radius-stiff were excluded from analysis. The ankle marker is located at coordinate (0,0) with the y-axis in line with the shank and the x-axis perpendicular to the shank. The forward position indicates the x-coordinate of the center of pressure in the shank based coordinate system. The vertical position indicates the y-coordinate of the center of pressure in the shank based coordinate system. The position of the center of pressure was only plotted when vertical ground reaction forces were greater than 0.25 the individual's body weight.

The experimental position of the ankle marker was used during the transformation to a shank-based coordinate system so that the calculated shape matched the corresponding experimental shape better in the vertical direction. The experimental position of the ankle marker was not used to calculate the center of pressure.

Figure 25 shows some consistency among the roll over shapes produced by each foot with all subjects. However, these roll over shapes do not match the length predicted during the design stage. The main difference between the shape calculated in the design stage and the shapes calculated in Figure 25 is the shank angle data. As discovered by looking at the ankle angles in Figure 18, the individuals wearing the prosthetic simulator are spending more time in plantar flexion for heel strike before the shank reaches its vertical position than was predicted. This could have prevented the individual from completing the roll over shape, resulting in a final shape that is cut short.

### **5.3.2 Validation of Roll Over Shape Based Design**

The mathematical model of the roll over shape was created to implement a process of roll over shape based design. The process is based on the theory that the roll over shape is dependent on the ankle-foot prosthesis as opposed to the subject wearing the prosthesis. To test the validity of the theory, the experimental data from one CAPA foot trial can be used with foot geometry of a different version of the CAPA foot. Subjects 3, 5, 6, and 8 were chosen because all four exhibited typical roll over shapes for both the CAPA-foot-small-radius-stiff and the CAPA-foot-large-radius-stiff. The calculated roll over shape was found using the experimental shank angle, geometry of the CAPA foot in the neutral orientation, and force plate data of the correct subject and trial shown in green. Then, for each subject, the experimental data of the CAPA-foot-small-radius was matched with the geometry of the CAPA-foot-large-radius and shown in magenta. Likewise, the experimental data of the CAPA-foot-large-radius was matched with the geometry of the CAPA-foot-small-radius. The calculated distance to the ground was used to plot the center of pressure points in a shank-based coordinate system.

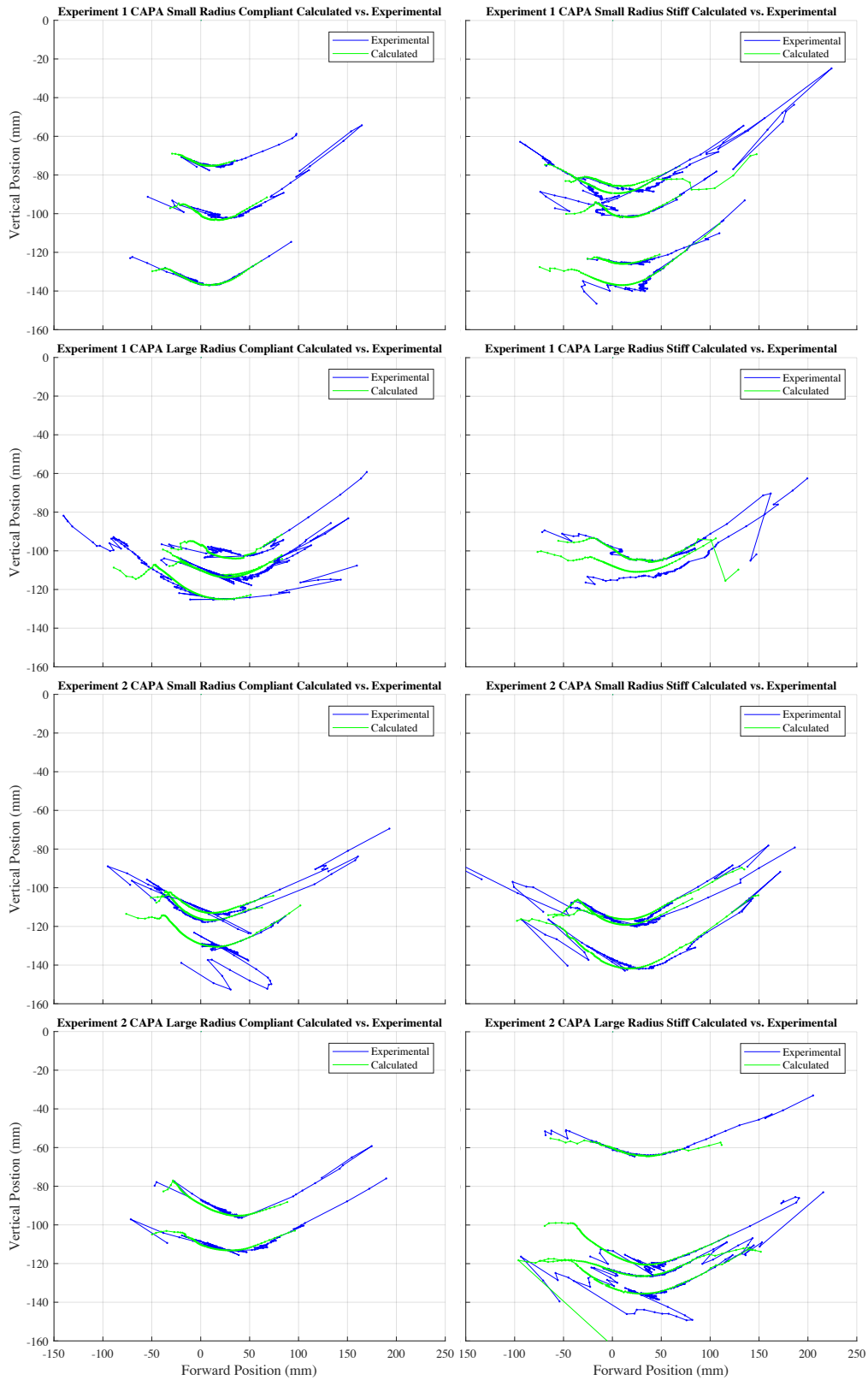


Figure 25: Roll over shapes experimental versus calculated for all versions of the CAPA foot. The captions of Figures 23 and 24 can be referenced for further details on the methods used to plot the experimental roll over shape.



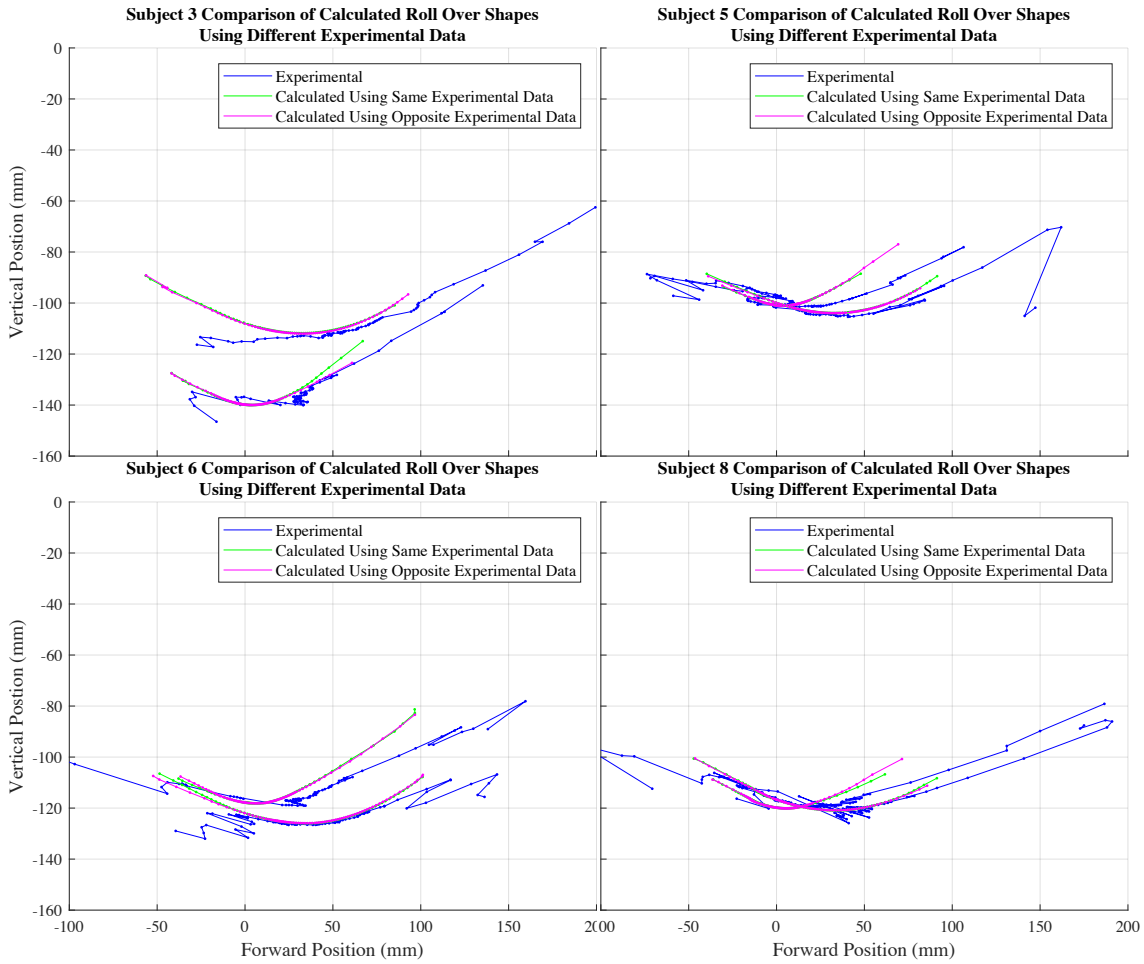


Figure 26: Experimental roll over shapes compared to calculated roll over shapes using the same experimental data (green) and the experimental data of the opposite trial (magenta). CAPA-foot-large-radius shapes are shifted further forward.

The resulting calculated shapes of both foot geometries were translated in the vertical direction so that the shapes coincide with the experimental shape. Shapes of the same foot geometry for each subject were translated by the same amount.

The magenta roll over shapes in Figure 26 using the experimental data from a different trial almost cover the green roll over shapes using the correct experimental data. It shows that experimental data could be used to predict the roll over shape of a completely different foot. When the CAPA-foot-large-radius is used with CAPA-foot-small-radius experimental data, the resulting shape is shifted further forward and the curvature increased so that the calculated shape corresponds more closely to the CAPA-foot-large-radius experimental roll over shape than the CAPA-foot-small-radius experimental roll over shape. The difference between the roll over shapes produced by the CAPA-foot-small-radius and the CAPA-foot-large-radius are the same as found during the design stage in Figure 12. The green and magenta shapes match closely for every foot, indicating that the roll over shape is dependent on the foot geometry instead of the specific trial's experimental data.

#### **5.4 Difficulty Level and Individual Preference**

Characteristics of a prosthesis such as stability are difficult to quantify. Individual preference matters as well. For this reason, after each trial, the subject was asked to rate the difficulty level on a scale from 1 (easiest) to 5 (hardest) and give comments. At the end of the experiment, the subject was asked more questions about their personal preference.

In response to the question “Which foot would you prefer to walk on? Why?,” nine out of ten participants said they would prefer to walk on the CAPA foot. In experiment 1, subject 1 preferred the small radius compliant version and subjects 2, 3, 4, and 5 preferred the large radius version. In experiment 2, subjects 7 and 8 preferred the CAPA foot but did not notice a difference between the radii and subject 9 and 10 preferred the large radius version. Subjects 1, 2, 4, 5, and 9 indicated that the major reason for choosing the CAPA foot was a concern with wobbling, balancing, stability, or the width of the foot. Additionally,

subject 2 liked the CAPA-foot-large-radius because there was less rocking than the CAPA-foot-small-radius and subject 3 liked the CAPA-foot-large-radius because it felt stiffer and was able to bend more than the CAPA-foot-small-radius. Subject 5 was able to “look straight ahead without worrying about the foot” and subject 9 said that when using the CAPA-foot-large-radius, he felt that he “wasn’t going to fall no matter where the foot was placed,” called the foot “dependable,” and commented on the swing/lag time. Subject 8 said the CAPA foot was more “natural.” In comparison, subjects 5 and 8 described the Renegade® AT as “springy.” Subject 5 commented that the Renegade® AT made his hips hurt.

Subject 6 preferred the SACH foot, indicating a different preference than the other nine subjects. During the CAPA foot and the Renegade® AT trials, he was having difficulty clearing the toe on the treadmill. Subject 6 also said that he did not like the weight of the CAPA foot and felt like the arm of shafts and springs was impacting his gait. If these issues were addressed, he said he would prefer the CAPA foot.

The overwhelming preference the subject had for the CAPA foot was also shown by the difficulty level ratings given at the end of each trial on a scale from 1 (easiest) to 5 (hardest) shown in Figure 27. There was a statistically significant difference between the rated difficulty level of the CAPA foot trials and the existing prostheses ( $F=14.2$ ,  $p<0.01$ ). The Renegade® AT with and without a weight (ESRNW and ESRW) was found to be the most difficult for the participants. These results are unusual as the Renegade® AT was designed for active users. Subjects 5 and 9 reacted more positively to the Renegade® AT during session 1 than the experimental session 2.

CAPA-foot-large-radius-stiff The next question asked was “Would you prefer to walk [on the SACH foot and Renegade® AT] with or without a weight.” Preferences were split between with a weight and without a weight. For subjects 2, 6, and 9, it also depended on the foot. Subjects 1, 3, 4, 5, 7, 8, 9, and 10 indicated that a major consideration was either the swing time, the lag time, or used adjectives describing the locking of the knee like “clicking” or “snapping.” The preferences for each individual is given in Table 10. The average mode step time for each trial in Appendix I shows that adding a weight to

### Average Difficulty Level Rating

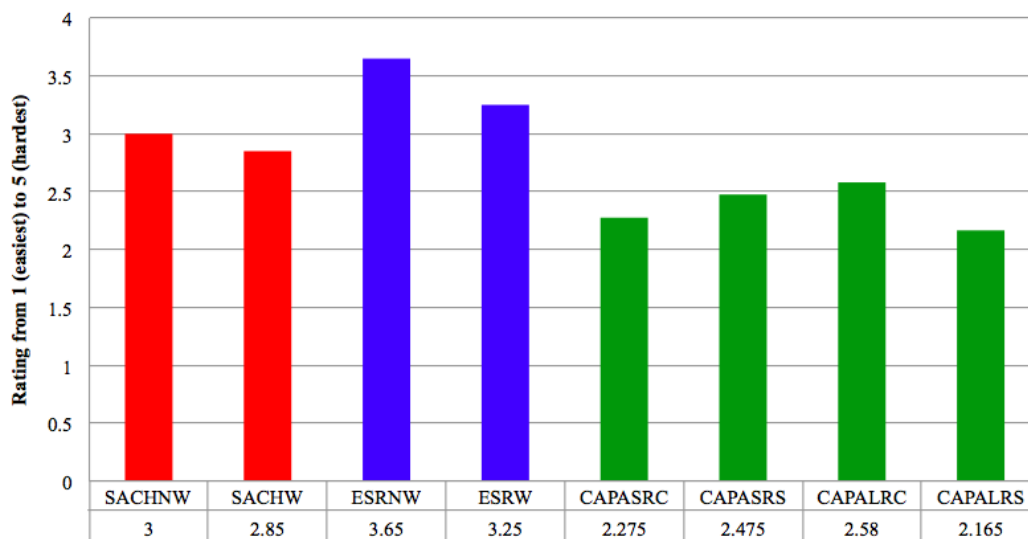


Figure 27: The difficulty level rating for each trial averaged among all subjects. The rating was given immediately following the experimental trial. The bars represent SACH Foot No Weight (SACHNW), SACH Foot With Weight (SACHW), Renegade<sup>®</sup> AT No Weight (ESRNW), Renegade<sup>®</sup> AT With Weight (ESRW), CAPA-foot-small-radius-compliant (CAPASRC), CAPA-foot-small-radius-stiff (CAPASRS), CAPA-foot-large-radius-compliant (CAPALRC), and CAPA-foot-large-radius-stiff (CAPALRS)

the prosthesis increases the step time. Adding a weight to the ankle of an able-bodied subject produces a similar effect [62]. The CAPA foot has the largest step time because the mass was located at a more distal position.

Subjects 4, 5, and 6 used the word “natural” to describe walking with a weight. Subject 5 used said he was more “confident” with the weight and subject 8 said he felt more control without the weight. Subject 5 also commented regarding the presence of a lag during the CAPA foot trials. Subject 9 preferred the weight, however, he thought less weight would be ideal and commented that the weight made it harder to raise the foot. Subject 10 liked the weight on the CAPA foot, but thought the weight hindered with the SACH foot and Renegade<sup>®</sup> AT. Regardless, every subject had a preference. While it might seem as if the wording of the question could have forced subjects to make a decision, subjects 2, 6, and 9 were comfortable stating a different preference for each of the prosthetic ankle feet. Also, for the next question about the springs that worded in a similar manner, subjects 3, 5, and 6 indicated no preference.

Table 10: Subject Individual Preference SACH Foot and Renegade® AT With vs. Without Weight

	SACH Foot	Renegade® AT
Without Weight	1,6,7,8,10	2,7,8,10
With Weight	2,3,4,5,9	1,3,4,5,6,9
No Preference	none	none

Table 11: Subject Individual Preference CAPA Foot Compliant vs. Stiff

	Small Radius	Large Radius
Compliant	2,8	2,8
Stiff	4,5,7,9,10	4,7,9,10
No Preference	3,6	3,5,6

The final question that the subject was asked was “Would you prefer more or less springs [on the CAPA foot]?” and the results shown in Table 11. More individuals indicated a preference for more springs as opposed to less. However, while both subjects 9 and 10 commented on the assistive effect of the CAPA foot during the trials, none of the subjects stated it as a reason for wanting more or less springs. The focus was on stability and support. Subjects 3 did not notice a difference in stiffness and subject 6 only noticed the difference while standing. Subjects 4 liked the greater support the stiff version provided. Subject 8 preferred the compliant versions because it was more natural and “bended like an actual foot.” Subject 9 said he preferred the stiff version because of the difference in lag time. Subject 10 liked the stiffer design because of “the feeling of the cushion when planting the foot,” but otherwise did not notice a difference. Subject 10 wore the experiment 2 versions of the CAPA foot with pretension.

At the end of the experiment subject 6 felt as if walking on the prosthetic simulator was easier at the end because he had practiced. In comparison, subject 9 felt more fatigued at the end of the experiment.

## CHAPTER 6: DISCUSSION

The most noticeable difference between the CAPA foot and an intact ankle-foot is that individuals wearing the prosthetic simulator with the CAPA foot spend significantly more time in heel strike plantar flexion than the intact ankle-foot. This can be observed by looking at the point in the gait cycle that the toe angles cross the x-axis in Figures 18. As a result of spending too much of the gait cycle in heel strike plantar flexion, individuals may have been forced to pick up their foot prematurely in order to keep up with the treadmill. The ankle angles would not have time to reach the dorsiflexion of an intact ankle, causing the CAPA foot to produce less push-off forces. Since trials with the SACH foot and the Renegade® AT show the same trend, the extended time in heel strike plantar flexion could be the result of the nature of walking with a prosthetic simulator as opposed to CAPA foot itself.

If the extended time in heel strike plantar flexion continues to occur when the ankle-foot is worn by an amputee, the CAPA foot design would need to be improved to address this problem. It may be more possible to address this with a small rocker radius as opposed to the large rocker radius. The CAPA-foot-large-radius has a rocker center of curvature in front of the ankle marker by necessity, possibly making it more difficult for the ankle-foot to proceed from plantar flexion into dorsiflexion. The experimental results in Figure 18 show that the average maximum dorsiflexion reached by the large radius versions are noticeably less than the small radius versions. As a result, in experiment 1, similar forces were produced by both the small radius and large radius in Figure 21 and 22 despite the large radius version having a shorter moment arm and larger effective rotational stiffness in Table 4. In experiment 2, the push-off forces of the small radius version are larger than the large radius version as shown in Figure 20. While four of five subjects in experiment 1 said they preferred the large radius version, when the dorsiflexion stiffness was increased in

experiment 2, only 2 of the 5 said they preferred the large radius version. It might be possible to achieve the stability of the CAPA-foot-large-radius with a CAPA-foot-small-radius with a greater stiffness. Another option is to change the curvature of the rocker component.

Premature lifting of the foot would also impact the individual's roll over shape by cutting the shape short in the x-direction in front of the ankle marker. This may describe the discrepancy between the length predicted during the design stage in Figure 12 and the experimental roll over shapes in Figures 23 and 24. The mathematical model was shown in Figure 25 to be capable of predicting the roll over shapes of the experimental trial with reasonably good accuracy, yet, the predicted roll over shape is much longer than the experimental shapes. The likely explanation is that the individual whose experimental data was used to predict the roll over shape during the design stage spent more time in dorsiflexion than the ten participants in the study. The capability of the mathematical model to predict the roll over shape of a different foot geometry is shown in Figure 26. Abnormalities in experimental data such as prematurely lifting the foot would translate to the calculated and experimental roll over shapes.

## **6.1 Versions of the CAPA Foot**

Throughout the entire study, eight different versions of the CAPA foot were tested. The CAPA feet used in experiment 1 with subjects 1-5 did not have dorsiflexion pretension and the CAPA feet used in experiment 2 with subjects 6-10 did have dorsiflexion pretension. For each experiment, compliant and stiff versions of a small-radius-long-moment-arm foot and a large-radius-short-moment-arm foot were tested.

The experiment 2 versions of the CAPA foot with pretension improved upon the experiment 1 versions of the CAPA foot by providing greater push-off forces as indicated in Figure 21 and 22. The greater forces produced by the CAPA foot translated to the ground reaction forces in Figure 20. Unlike the experiment 1 CAPA foot without pretension, the experiment 2 CAPA foot with pretension begins storing energy right at heel strike when the foot is in plantar flexion. The ground reaction forces of the CAPA foot with pretension have greater braking and push-off forces that are more similar to the intact ankle-foot.

The roll over shape radius of curvature and the length of the shape in front of the ankle marker improved as shown in Table 9. One major benefit of the pretension version is greater stability while standing. The pretension helps prevent the individual from rolling forward.

While the major increase in dorsiflexion stiffness through pretension increased the sagittal plane ground reaction forces, smaller increases in stiffness did not have a big effect on the ground reaction forces or the ankle angles. However, pretension and increases in stiffness improved the roll over shape by increasing the radius of curvature and the length of the shape in front of the ankle marker in Table 9.

The last comparison was the small-radius-long-moment-arm versus the large-radius-short-moment-arm. The CAPA-foot-large-radius bended less in dorsiflexion as shown in Figure 18. As a result, the forces produced by the CAPA-foot-small-radius and CAPA-foot-large-radius in Figure 21 were similar even though the CAPA-foot-large-radius had a larger rotational stiffness because of the shorter moment arm. The ground reaction forces for the CAPA-foot-small-radius were greater than the large radius version. However, participants in the study tended to prefer the large radius version over the small radius version.

## **6.2 Customizable**

One of the biggest differences between the CAPA foot and existing prostheses is the ability of the CAPA foot to be easily personalized for every individual, speed, and application. The application of 3D printing to make the components opens up a world of options that could meet the preference of every individual like weight, width, and component geometries. While traditional prostheses have been designed to be as light as possible, this thesis shows that not all individuals prefer a lighter prosthesis, usually referencing the way the prosthesis swings as the reason. These findings experimentally confirm the results of simulations performed by Tsai and Mansour [63]. All participants had an opinion with regard to the weight of the prosthesis, but the opinion varied, indicating weight customization may be a useful characteristic of an ankle-foot prosthesis. The springs can be easily replaced with the same foot to provide different stiffnesses



for dorsiflexion, plantar flexion, and different walking speeds and body weights. Section 3.3.3.1 elaborates on the effect of speed and body weight on stiffness.

The CAPA foot also has the mathematical model to support customization. Determining the angular stiffness of an ESAR foot requires experimental testing after the foot has been made [64], making personalization difficult and requiring the entire foot to be remade for a different angular stiffness. The CAPA foot design can be altered according to the desired roll over shape, an important characteristic of human gait. The same degree of personalization is not possible with existing passive designs.

### **6.3 Limitations**

The first limitation is the use of the prosthetic simulator. Aspects of the simulator such as the presence of the able-bodied subject's lower limb, an asymmetric knee height, and wiggle in the simulator could have affected the results. Because a simulator was used, information that would be important to the quality of the prosthesis such as socket forces were not gathered.

While we know that speed and body weight are considerations in the stiffness of a human ankle, the same stiffnesses were used for the entire experiment. All subjects had an intact foot size larger than all the ankle-foot prostheses used in this study. There are many commercial ESAR feet and the Renegade<sup>®</sup> AT may not be representative of all possible types.

The mathematical model has limitations as well. Assumptions were made that impact the accuracy of the model as shown in Figure 25. While the model is reasonably accurate at predicting general trends, it is poor at predicting individual points. It also requires some experimental data for the angular rotation of the shank and vertical forces.

## CHAPTER 7: CONCLUSIONS

Overall the CAPA foot performed well in comparison with the SACH foot and an exemplary ESAR foot. The ankle angles and push-off forces of the CAPA foot were more similar to an intact ankle-foot than either the SACH foot or the ESAR foot across both experiments, presenting a solution to the design problem explained in section 2.3. Nine out of ten able-bodied participants in the study preferred the CAPA foot over the existing prosthetics. The CAPA foot can be easily customized to the individual, unlike the existing prosthetics. However, individuals wearing the CAPA foot spent more time in heel strike plantar flexion than an able-bodied individual. This could have caused the individual to prematurely lift their leg and be the source of some of the discrepancies between the gait of the able-bodied individual and the gait of the individual wearing the CAPA foot with a prosthetic simulator. Since the same observations were made about the other ankle-foot prostheses used with the prosthetic simulator, this effect could be due the use of the simulator.

Additionally, it was found that the roll over shape of the individual wearing the CAPA foot could be experimentally predicted. The concept of roll over shape based design that originated with Hansen [6] has been hard to apply to the design of prostheses because of difficulties predicting the roll over shape. Mahmoodi et al. predicted the roll over shape of the SACH foot and ESAR foot using finite element analysis [65]. The concept has also been used to develop a control mechanism for a powered transfemoral prosthesis during stance phase [66]. This thesis demonstrates that the same concept of roll over shape based design can be applied to the CAPA foot in a manner that is simpler than finite element analysis or a powered transfemoral prosthesis. The changes in the calculated roll over shapes reflect that of the experimental roll over shapes.

For commercialization of the CAPA foot, more advanced additive manufacturing techniques can be explored to improve the strength of the components and optimize the weight. As opposed to painting rubber on the bottom, a slab of rubber or another more durable method could be used for adding traction. The shapes of the components themselves can be rounded and changed for visual appeal. A casing can be placed around the CAPA foot such that the underlying mechanism is preserved.

It is envisioned that each individual could have one CAPA foot that is made according to the roll over shape it will produce during gait. The springs on the CAPA foot can be replaced if desired for different speeds and applications. Practical considerations such as adding a shoe will need to be considered. Five subjects commented that the stability provided by the width of the CAPA foot was a major reason for preferring the CAPA foot over the existing prostheses. To fit the CAPA foot in a shoe, it may be necessary to either increase the width of the shoe or decrease the width of the CAPA foot. Neither option is ideal, but both are possible. Also, some shoes may limit the range of motion of the CAPA foot, and therefore, the ground reaction forces and the roll over shape. In this case, the stiffer springs can be used so that the CAPA foot still provides adequate forces and roll over shape arc length.

This work shows that the CAPA foot has potential to provide individuals with amputation an ankle-foot prosthesis that better mimics an able-bodied gait. However, future work with individuals with amputation as opposed to able-bodied individuals wearing a prosthetic simulator is necessary to refine the design, ensure the CAPA foot does not experience extended time in heel strike plantar flexion, and address practical considerations. Another study can be preformed looking at the CAPA foot during sloped walking. In addition, the fact that the CAPA foot can be quickly customized means that the effects of changing characteristics of ankle-foot prostheses such as the roll over shape can be easily studied.

For this study, the author designs and tests an ankle-foot prosthesis that is different from existing prostheses in design and functionality. By providing a linear relationship between ankle angle and force, the CAPA foot shows improvement from existing prosthetics that simultaneously better mimics the the ankle

angles and ground reaction forces of an able-bodied individual. Versions of the CAPA foot are explored to find that pretension and increased stiffness improve the design. A mathematical model was created to predict the roll over shape and was used to successfully demonstrate and validate the concept of roll over shape design. The assumption that a lighter prostheses is inherently better is challenged and it was found that a wider prostheses may increase stability. The CAPA foot shows commercial viability and could be used for research purposes to more easily compare different qualities of a prosthesis. The characteristics of the CAPA foot design that cause it to better mimic a able-bodied gait can be applied to other ankle-foot prosthesis

## REFERENCES

- [1] Kathryn Ziegler-Graham, Ellen J MacKenzie, Patti L Ephraim, Thomas G Travison, and Ron Brookmeyer. Estimating the prevalence of limb loss in the united states: 2005 to 2050. *Archives of physical medicine and rehabilitation*, 89(3):422–429, 2008.
- [2] Tad McGeer et al. Passive dynamic walking. *I. J. Robotic Res.*, 9(2):62–82, 1990.
- [3] Peter G Adamczyk, Steven H Collins, and Arthur D Kuo. The advantages of a rolling foot in human walking. *Journal of Experimental Biology*, 209(20):3953–3963, 2006.
- [4] February 2018. URL <https://www.footeducation.com/page/bones-of-foot-and-ankle>.
- [5] Van L Phillips. Composite prosthetic foot and leg, October 22 1985. US Patent 4,547,913.
- [6] AH Hansen, DS Childress, and EH Knox. Prosthetic foot roll over shapes with implications for alignment of transtibial prostheses. *Prosthetics and Orthotics International*, 24(3):205–215, 2000.
- [7] Hans Nägerl, D Kubein-Meesenburg, J Fanghänel, H Dathe, C Dumont, and MM Wachowski. The upper ankle joint: Curvature morphology of the articulating surfaces and physiological function. *Acta of bioengineering and biomechanics*, 18(3), 2016.
- [8] Millicent Schlafly, Tyagi Ramakrishnan, and Kyle Reed. 3D printed passive compliant and articulating prosthetic ankle foot. In *ASME 2017 International Mechanical Engineering Congress and Exposition*, pages V003T04A076–V003T04A076. American Society of Mechanical Engineers, 2017.
- [9] Judy Wagner, Susan Sienko, Terry Supan, and D Barth. Motion analysis of sach vs. flex-foot in moderately active below-knee amputees. *Clin Prosthet Orthot*, 11(1):55–62, 1987.
- [10] Jean-Marie Casillas, Véronique Dulieu, Martine Cohen, Inès Marcer, and Jean-Pierre Didier. Bioenergetic comparison of a new energy-storing foot and sach foot in traumatic below-knee vascular amputations. *Archives of physical medicine and rehabilitation*, 76(1):39–44, 1995.
- [11] Brian J Hafner, Joan E Sanders, Joseph M Czerniecki, and John Fergason. Transtibial energy-storage-and-return prosthetic devices: a review of energy concepts and a proposed nomenclature. *Journal of rehabilitation research and development*, 39(1):1, 2002.
- [12] Diego Torricelli, Jose Gonzalez, Maarten Weckx, René Jiménez-Fabián, Bram Vanderborght, Massimo Sartori, Strahinja Dosen, Dario Farina, Dirk Lefeber, and Jose L Pons. Human-like compliant locomotion: state of the art of robotic implementations. *Bioinspiration & biomimetics*, 11(5):051002, 2016.
- [13] Andrew H Hansen, Dudley S Childress, Steve C Miff, Steven A Gard, and Kent P Mesplay. The human ankle during walking: implications for design of biomimetic ankle prostheses. *Journal of biomechanics*, 37(10):1467–1474, 2004.

- [14] Rino Versluys, Anja Desomer, Gerlinde Lenaerts, Pieter Beyl, Michael Van Damme, Bram Vanderborght, Innes Vanderniepen, Georges Van der Perre, and Dirk Lefeber. From conventional prosthetic feet to bionic feet: a review study. In *Biomedical Robotics and Biomechatronics, 2008. BioRob 2008. 2nd IEEE RAS & EMBS International Conference on*, pages 49–54. IEEE, 2008.
- [15] Samuel K Au, Jeff Weber, and Hugh Herr. Powered ankle-foot prosthesis improves walking metabolic economy. *IEEE Transactions on Robotics*, 25(1):51–66, 2009.
- [16] Martin Grimmer, Matthew Holgate, Robert Holgate, Alexander Boehler, Jeffrey Ward, Kevin Hollander, Thomas Sugar, and André Seyfarth. A powered prosthetic ankle joint for walking and running. *Biomedical engineering online*, 15(3):141, 2016.
- [17] Samuel K Au and Hugh M Herr. Powered ankle-foot prosthesis. *IEEE Robotics & Automation Magazine*, 15(3), 2008.
- [18] Anthony Crimin, Anthony McGarry, Elena Jane Harris, and Stephan Emanuel Solomonidis. The effect that energy storage and return feet have on the propulsion of the body: a pilot study. *Proceedings of the Institution of Mechanical Engineers, Part H: Journal of Engineering in Medicine*, 228(9):908–915, 2014.
- [19] Jessica D Ventura, Glenn K Klute, and Richard R Neptune. The effects of prosthetic ankle dorsiflexion and energy return on below-knee amputee leg loading. *Clinical Biomechanics*, 26(3):298–303, 2011.
- [20] Courtney E Shell, Ava D Segal, Glenn K Klute, and Richard R Neptune. The effects of prosthetic foot stiffness on transtibial amputee walking mechanics and balance control during turning. *Clinical Biomechanics*, 49:56–63, 2017.
- [21] Peter Gabriel Adamczyk, Michelle Roland, and Michael E Hahn. Sensitivity of biomechanical outcomes to independent variations of hindfoot and forefoot stiffness in foot prostheses. *Human movement science*, 54:154–171, 2017.
- [22] David A Winter. *Biomechanics and motor control of human gait: normal, elderly and pathological*. 1991.
- [23] Claire L Brockett and Graham J Chapman. Biomechanics of the ankle. *Orthopaedics and trauma*, 30(3):232–238, 2016.
- [24] Marilyn Pink, Jacquelin Perry, Peggy A Houghlum, and Dennis J Devine. Lower extremity range of motion in the recreational sport runner. *The American journal of sports medicine*, 22(4):541–549, 1994.
- [25] Jack Crosbie, Toni Green, and Kathryn Refshauge. Effects of reduced ankle dorsiflexion following lateral ligament sprain on temporal and spatial gait parameters. *Gait & posture*, 9(3):167–172, 1999.
- [26] Erik P Lamers and Karl E Zelik. The importance of prosthetic ankle range-of-motion for ascending and descending slopes.

- [27] Deborah R Vickers, C Palk, AS McIntosh, and KT Beatty. Elderly unilateral transtibial amputee gait on an inclined walkway: a biomechanical analysis. *Gait & posture*, 27(3):518–529, 2008.
- [28] Kamran Shamaei, Massimo Cenciari, and Aaron M Dollar. On the mechanics of the ankle in the stance phase of the gait. In *Engineering in Medicine and Biology Society, EMBC, 2011 Annual International Conference of the IEEE*, pages 8135–8140. IEEE, 2011.
- [29] Kathryn M Olesnavage and Amos G Winter. Analysis of rollover shape and energy storage and return in cantilever beam-type prosthetic feet. In *ASME 2014 International Design Engineering Technical Conferences and Computers and Information in Engineering Conference*, pages V05AT08A018–V05AT08A018. American Society of Mechanical Engineers, 2014.
- [30] Joshua M Caputo and Steven H Collins. A universal ankle–foot prosthesis emulator for human locomotion experiments. *Journal of biomechanical engineering*, 136(3):035002, 2014.
- [31] Pierre Cherelle, Victor Grosu, Arnout Matthys, Bram Vanderborght, and Dirk Lefeber. Design and validation of the ankle mimicking prosthetic (amp-) foot 2.0. *IEEE Transactions on Neural Systems and Rehabilitation Engineering*, 22(1):138–148, 2014.
- [32] Pierre Cherelle, Victor Grosu, Manuel Cestari, Bram Vanderborght, and Dirk Lefeber. The amp-foot 3, new generation propulsive prosthetic feet with explosive motion characteristics: design and validation. *Biomedical engineering online*, 15(3):145, 2016.
- [33] Max K Shepherd and Elliott J Rouse. Design of a quasi-passive ankle–foot prosthesis with biomimetic, variable stiffness. In *Robotics and Automation (ICRA), 2017 IEEE International Conference on*, pages 6672–6678. IEEE, 2017.
- [34] Andrew H Hansen and Dudley S Childress. Investigations of roll-over shape: implications for design, alignment, and evaluation of ankle–foot prostheses and orthoses. *Disability and rehabilitation*, 32(26):2201–2209, 2010.
- [35] AH Hansen, MR Meier, M Sam, DS Childress, and ML Edwards. Alignment of trans-tibial prostheses based on roll-over shape principles. *Prosthetics and orthotics international*, 27(2):89–99, 2003.
- [36] Carolin Curtze, At L Hof, Helco G van Keeken, Jan PK Halbertsma, Klaas Postema, and Bert Otten. Comparative roll-over analysis of prosthetic feet. *Journal of biomechanics*, 42(11):1746–1753, 2009.
- [37] Eduardo Barocio, Karla Bustamante, Roger V Gonzalez, and Joel C Huegel. Comparison via roll-over shape of the kinematic performance of two low-cost foot prostheses. In *Biomedical Robotics and Biomechatronics (2014 5th IEEE RAS & EMBS International Conference on*, pages 1028–1032. IEEE, 2014.
- [38] Andrew Hansen and Felix Starker. Prosthetic foot principles and their influence on gait. *Handbook of Human Motion*, pages 1–15, 2017.
- [39] James T Webber and David A Raichlen. The role of plantigrady and heel-strike in the mechanics and energetics of human walking with implications for the evolution of the human foot. *Journal of experimental biology*, 219(23):3729–3737, 2016.

- [40] Thomas Schmalz, Siegmund Blumentritt, and Rolf Jarasch. Energy expenditure and biomechanical characteristics of lower limb amputee gait: The influence of prosthetic alignment and different prosthetic components. *Gait & posture*, 16(3):255–263, 2002.
- [41] Tyagi Ramakrishnan, Millicent Schlafly, and Kyle B Reed. Effect of asymmetric knee height on gait asymmetry for unilateral transfemoral amputees. *International Journal of Current Advanced Research*, 6(10):6896, 2017.
- [42] Michael Mitchell, Peter J Kyberd, and Edmund Biden. A study of the rollover shape in unimpaired persons. *JPO: Journal of Prosthetics and Orthotics*, 25(3):138–142, 2013.
- [43] Andrew Hansen. Effects of alignment on the roll-over shapes of prosthetic feet. *Prosthetics and orthotics international*, 32(4):390–402, 2008.
- [44] Andrew H Hansen, Margrit R Meier, Pinata H Sessoms, and Dudley S Childress. The effects of prosthetic foot roll-over shape arc length on the gait of trans-tibial prosthesis users. *Prosthetics and Orthotics International*, 30(3):286–299, 2006.
- [45] Andrew H Hansen, Michel Sam, and Dudley S Childress. The effective foot length ratio: a potential tool for characterization and evaluation of prosthetic feet. *JPO: Journal of Prosthetics and Orthotics*, 16(2):41–45, 2004.
- [46] Michel Sam, Andrew H Hansen, and Dudley S Childress. Characterisation of prosthetic feet used in low-income countries. *Prosthetics and orthotics international*, 28(2):132–140, 2004.
- [47] Michel Sam, Dudley Childress, Andrew Hansen, Margrit Meier, Sophie Lambla, Edward Grahn, and Joshua Rolock. The 'shape&roll' prosthetic foot: I. design and development of appropriate technology for low-income countries. *Medicine, Conflict & Survival*, 20(4):294–306, 2004.
- [48] Andrew H Hansen and Charles C Wang. Effective rocker shapes used by able-bodied persons for walking and fore-aft swaying: Implications for design of ankle-foot prostheses. *Gait & posture*, 32(2):181–184, 2010.
- [49] Arthur D Kuo, J Maxwell Donelan, and Andy Ruina. Energetic consequences of walking like an inverted pendulum: step-to-step transitions. *Exercise and sport sciences reviews*, 33(2):88–97, 2005.
- [50] A Lundberg, OK Svensson, G Nemeth, and G Selvik. The axis of rotation of the ankle joint. *Bone & Joint Journal*, 71(1):94–99, 1989.
- [51] C Lee Ventola. Medical applications for 3D printing: current and projected uses. *Pharmacy and Therapeutics*, 39(10):704, 2014.
- [52] Masahiro Mori, Karl F MacDorman, and Norri Kageki. The uncanny valley [from the field]. *IEEE Robotics & Automation Magazine*, 19(2):98–100, 2012.
- [53] Ismet Handžić and Kyle B Reed. Perception of gait patterns that deviate from normal and symmetric biped locomotion. *Frontiers in psychology*, 6:199, 2015.



- [54] Jessica D Ventura, Glenn K Klute, and Richard R Neptune. The effect of prosthetic ankle energy storage and return properties on muscle activity in below-knee amputee walking. *Gait & posture*, 33(2):220–226, 2011.
- [55] Elliott J Rouse, Robert D Gregg, Levi J Hargrove, and Jonathon W Sensinger. The difference between stiffness and quasi-stiffness in the context of biomechanical modeling. *IEEE Transactions on Biomedical Engineering*, 60(2):562–568, 2013.
- [56] Elliott J Rouse, Levi J Hargrove, Eric J Perreault, and Todd A Kuiken. Estimation of human ankle impedance during walking using the perturber robot. In *Biomedical Robotics and Biomechatronics (BioRob), 2012 4th IEEE RAS & EMBS International Conference on*, pages 373–378. IEEE, 2012.
- [57] Edward D Lemaire, David Nielen, and Marie Andrée Paquin. Gait evaluation of a transfemoral prosthetic simulator. *Archives of physical medicine and rehabilitation*, 81(6):840–843, 2000.
- [58] Tyagi Ramakrishnan. *Asymmetric unilateral transfemoral prosthetic simulator*. University of South Florida, 2014.
- [59] Helco G van Keeken, Aline H Vrieling, At L Hof, Klaas Postema, and Bert Otten. Stabilizing moments of force on a prosthetic knee during stance in the first steps after gait initiation. *Medical Engineering and Physics*, 34(6):733–739, 2012.
- [60] Natalie Vanicek, David J Sanderson, Romeo Chua, Dave Kenyon, and J Timothy Inglis. Kinematic adaptations to a novel walking task with a prosthetic simulator. *JPO: Journal of Prosthetics and Orthotics*, 19(1):29–35, 2007.
- [61] Helco G van Keeken, Aline H Vrieling, At L Hof, Klaas Postema, and Bert Otten. Principles of obstacle avoidance with a transfemoral prosthetic limb. *Medical Engineering and Physics*, 34(8):1109–1116, 2012.
- [62] Haris Muratagic, Tyagi Ramakrishnan, and Kyle B Reed. Combined effects of leg length discrepancy and the addition of distal mass on gait asymmetry. *Gait & posture*, 58:487–492, 2017.
- [63] C-S Tsai and JM Mansour. Swing phase simulation and design of above knee prostheses. *Journal of Biomechanical Engineering*, 108(1):65–72, 1986.
- [64] Peter G Adamczyk, Michelle Roland, and Michael E Hahn. Novel method to evaluate angular stiffness of prosthetic feet from linear compression tests. *Journal of biomechanical engineering*, 135(10):104502, 2013.
- [65] P Mahmoodi, S Aristodemou, RS Ransing, N Owen, and MI Friswell. Prosthetic foot design optimisation based on roll-over shape and ground reaction force characteristics. *Proceedings of the Institution of Mechanical Engineers, Part C: Journal of Mechanical Engineering Science*, 231(17):3093–3103, 2017.
- [66] Robert D Gregg, Tommaso Lenzi, Nicholas P Fey, Levi J Hargrove, and Jonathon W Sensinger. Experimental effective shape control of a powered transfemoral prosthesis. In *Rehabilitation robotics (ICORR), 2013 IEEE international conference on*, pages 1–7. IEEE, 2013.

- [67] Tyagi Ramakrishnan, Millicent Schlafly, and K Reed. Biomimetic transfemoral knee with gear mesh locking mechanism. *International Journal of Engineering Research & Innovation*, 2017.
- [68] Christina-Anne Lahiff, Millicent Schlafly, and Kyle Reed. Effects on balance when interfering with proprioception at the knee. In *ASME 2017 International Mechanical Engineering Congress and Exposition*, pages V003T04A095–V003T04A095. American Society of Mechanical Engineers, 2017.
- [69] Tyagi Ramakrishnan, Millicent Schlafly, and Kyle B Reed. Evaluation of 3D printed anatomically scalable transfemoral prosthetic knee. In *Rehabilitation Robotics (ICORR), 2017 International Conference on*, pages 1160–1164. IEEE, 2017.

## APPENDIX A: COPYRIGHT PERMISSIONS

Figure 8 and portions Chapter 2: Background and section 3.2 of this thesis was published in ASME's International Mechanical Engineering Congress and Exposition (IMECE). Copyright permission is given in the email below.

From: **Beth Darchi** [DarchiB@asme.org](mailto:DarchiB@asme.org)  
Subject: RE: Permission for inclusion in thesis  
Date: February 6, 2018 at 4:05 PM  
To: Millicent Schlafly [mschlafly@mail.usf.edu](mailto:mschlafly@mail.usf.edu)



Dear Prof. Schlafly,

It is our pleasure to grant you permission to use **all or any part of** the ASME paper "3D Printed Passive Compliant and Articulating Prosthetic Ankle Foot," by Millicent Schlafly; Tyagi Ramakrishnan; Kyle Reed, Paper Number IMECE2017-71568, cited in your letter for inclusion in a master's thesis entitled Design and Testing of a Passive Prosthetic Ankle foot Optimized to Mimic an Able-bodied Gait to be published by University of South Florida.

Permission is granted for the specific use as stated herein and does not permit further use of the materials without proper authorization. Proper attribution must be made to the author(s) of the materials. **Please note:** if any or all of the figures and/or Tables are of another source, permission should be granted from that outside source or include the reference of the original source. ASME does not grant permission for outside source material that may be referenced in the ASME works.

As is customary, we request that you ensure full acknowledgment of this material, the author(s), source and ASME as original publisher. Acknowledgment must be retained on all pages where figure is printed and distributed.

Many thanks for your interest in ASME publications.

Sincerely,

**Beth Darchi**  
Publishing Administrator  
ASME  
2 Park Avenue  
New York, NY 10016-5990  
[darchib@asme.org](mailto:darchib@asme.org)

## APPENDIX B: TOE ANGLES

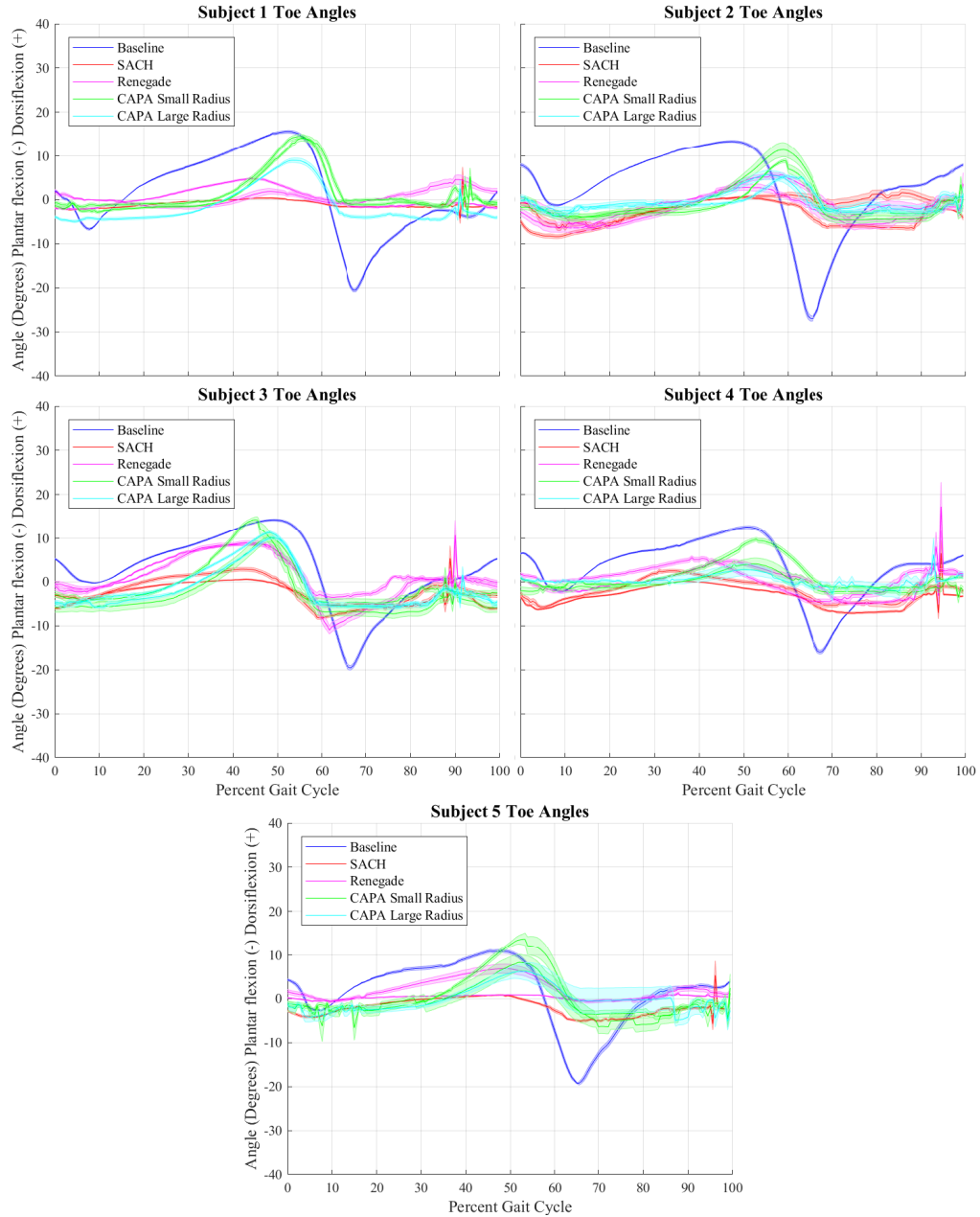


Figure B.1: Experiment 1 Toe Angles Subjects 1-5. The shaded error bars represent one standard error between steps for each subject. Subject 1 SACH foot with weight and CAPA-foot-large-radius-stiff; subject 4 CAPA-foot-large-radius-compliant; and subject 5 SACH foot with weight and CAPA-foot-large-radius-stiff were removed because of difficulties post-processing the data.

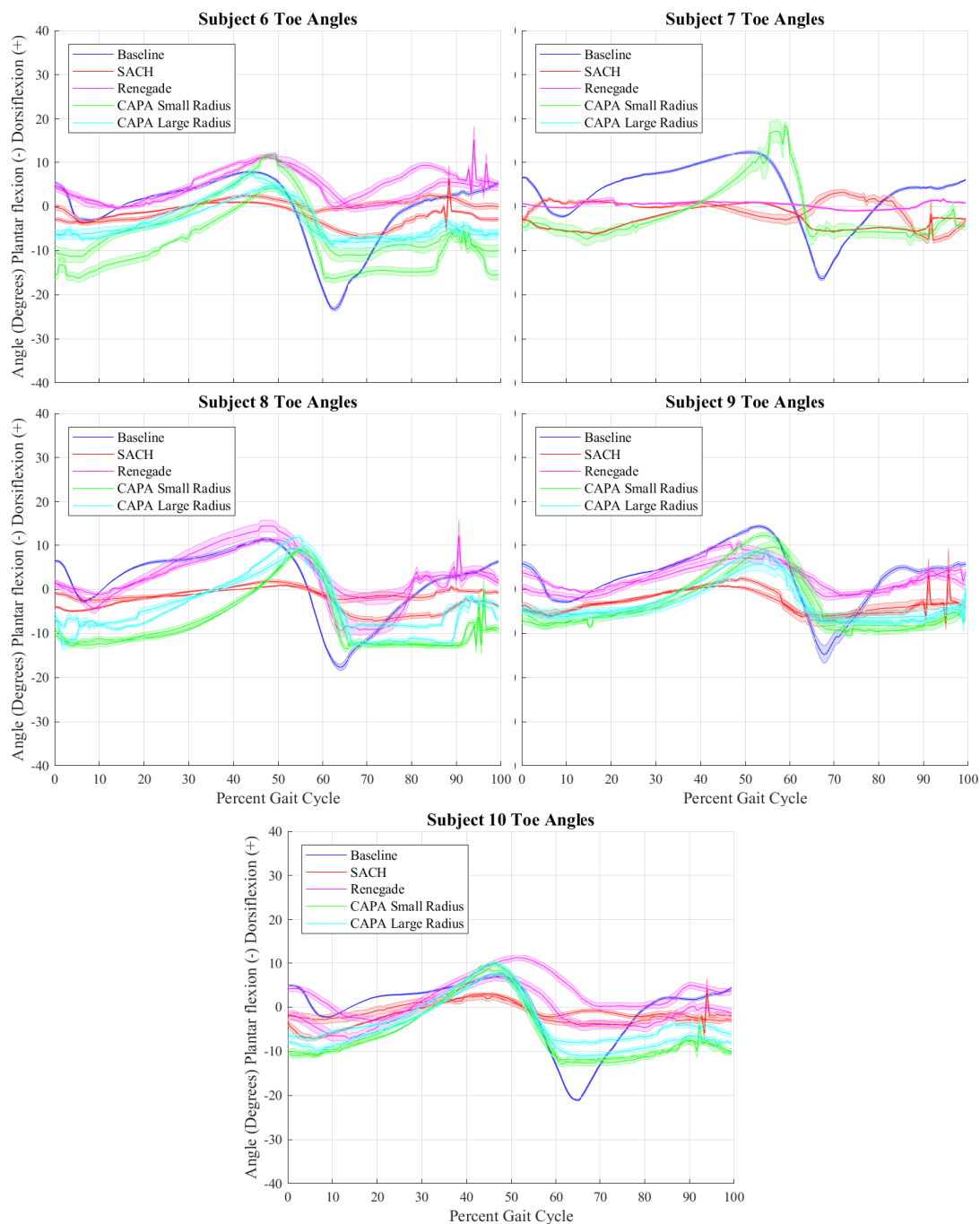


Figure B.2: Experiment 2 Toe Angles Subjects 6-10. The shaded error bars represent one standard error between steps for each subject. Subject 7 Renegade with weight, CAPA-foot-small-radius-stiff, and CAPA-foot-large-radius were removed because of difficulties post-processing the data.

## APPENDIX C: ANKLE ANGLES

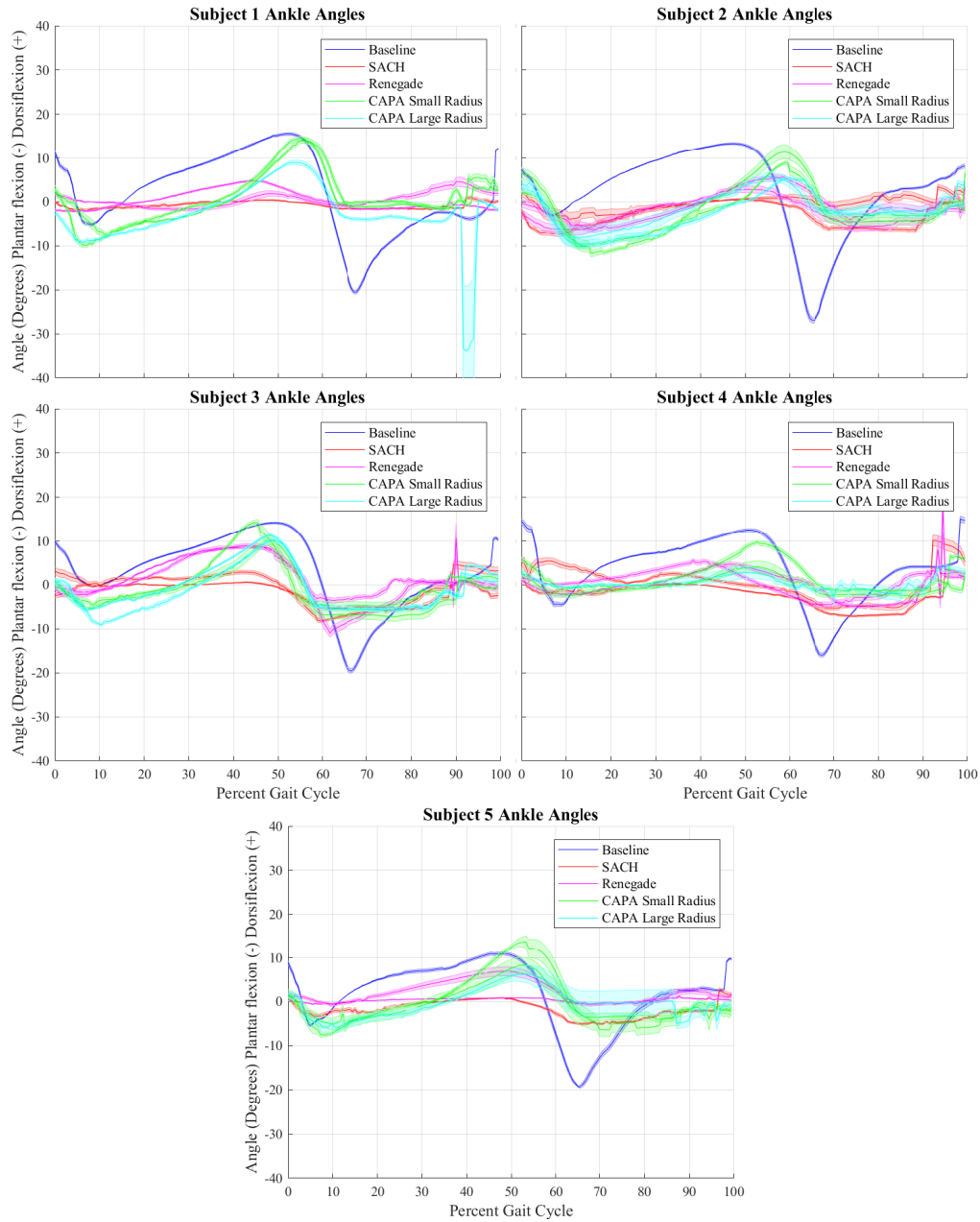


Figure C.1: Experiment 1 Ankle Angles Subjects 1-5. The shaded error bars represent one standard error between steps for each subject. Subject 1 SACH foot with weight and CAPA-foot-large-radius-stiff; subject 4 CAPA-foot-large-radius-compliant; and subject 5 SACH foot with weight and CAPA-foot-large-radius-stiff were removed because of difficulties post-processing the data.

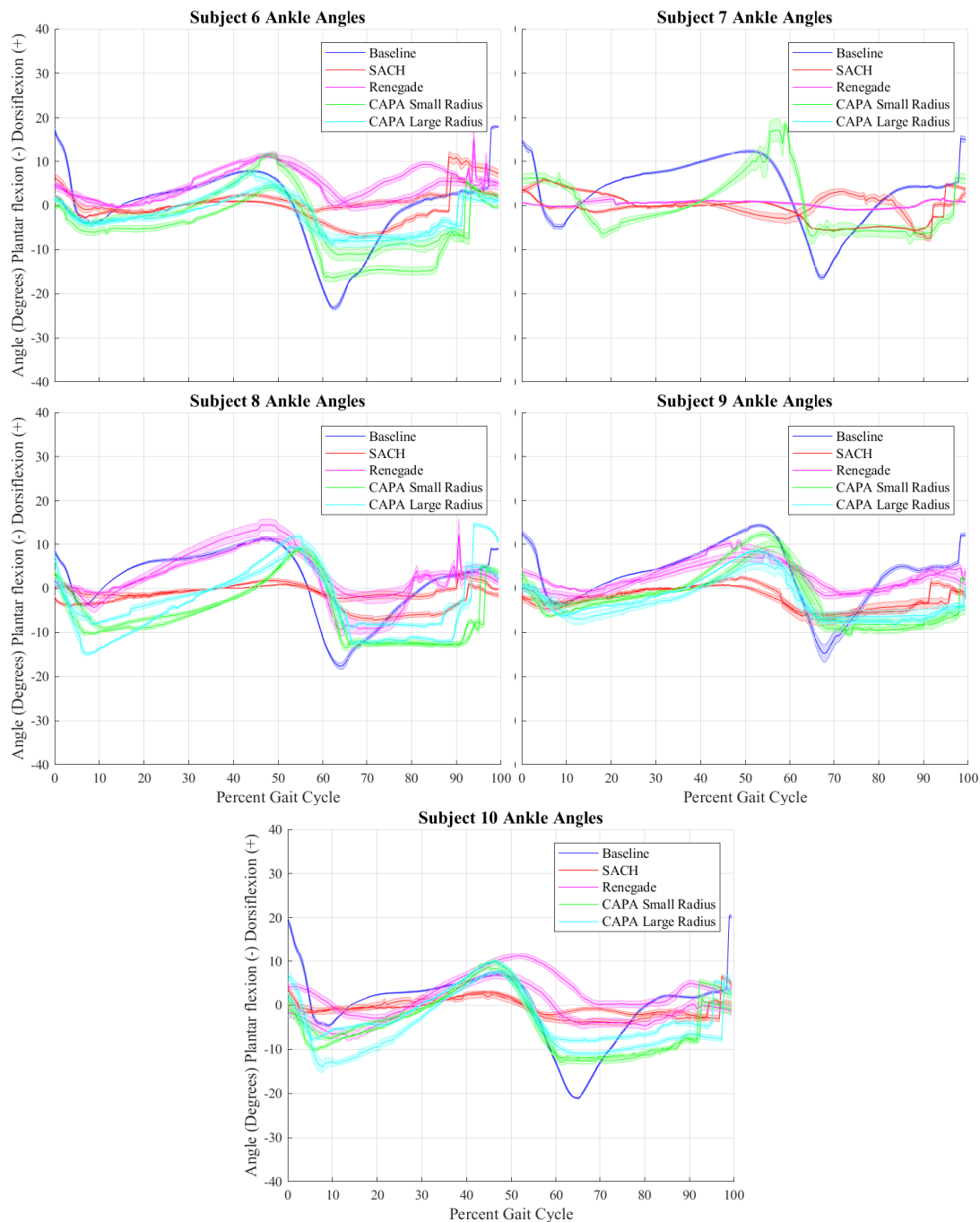


Figure C.2: Experiment 2 Ankle Angles Subjects 6-10. The shaded error bars represent one standard error between steps for each subject. Subject 7 Renegade with weight, CAPA-foot-small-radius-stiff, and CAPA-foot-large-radius, and subject 10 SACH foot without weight were removed because of difficulties post-processing the data.

## APPENDIX D: SHANK ANGLES

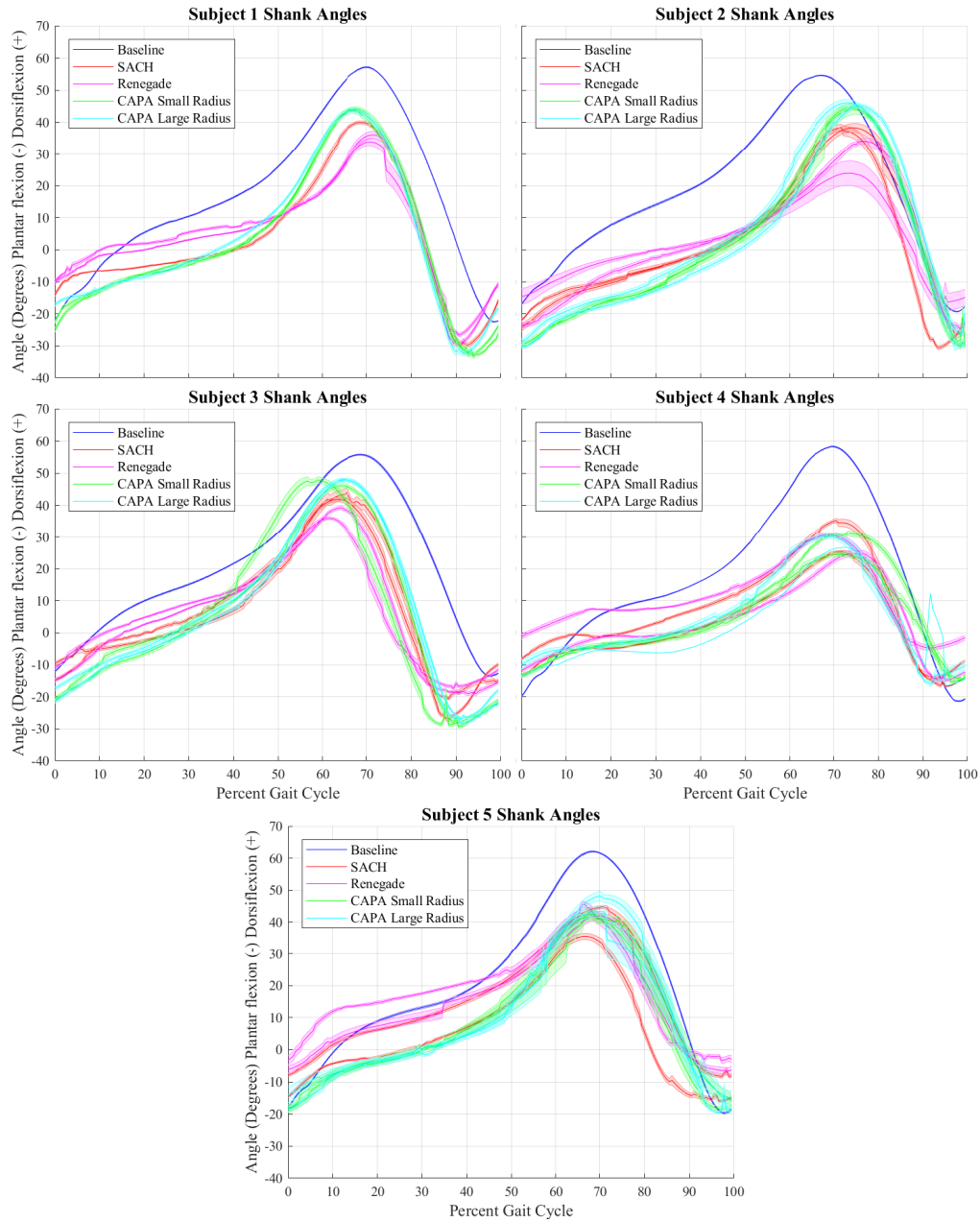


Figure D.1: Experiment 1 Shank Angles Subjects 1-5. The shaded error bars represent one standard error between steps for each subject. Subject 1 SACH foot with weight and CAPA-foot-large-radius-stiff were removed because of difficulties post-processing the data.



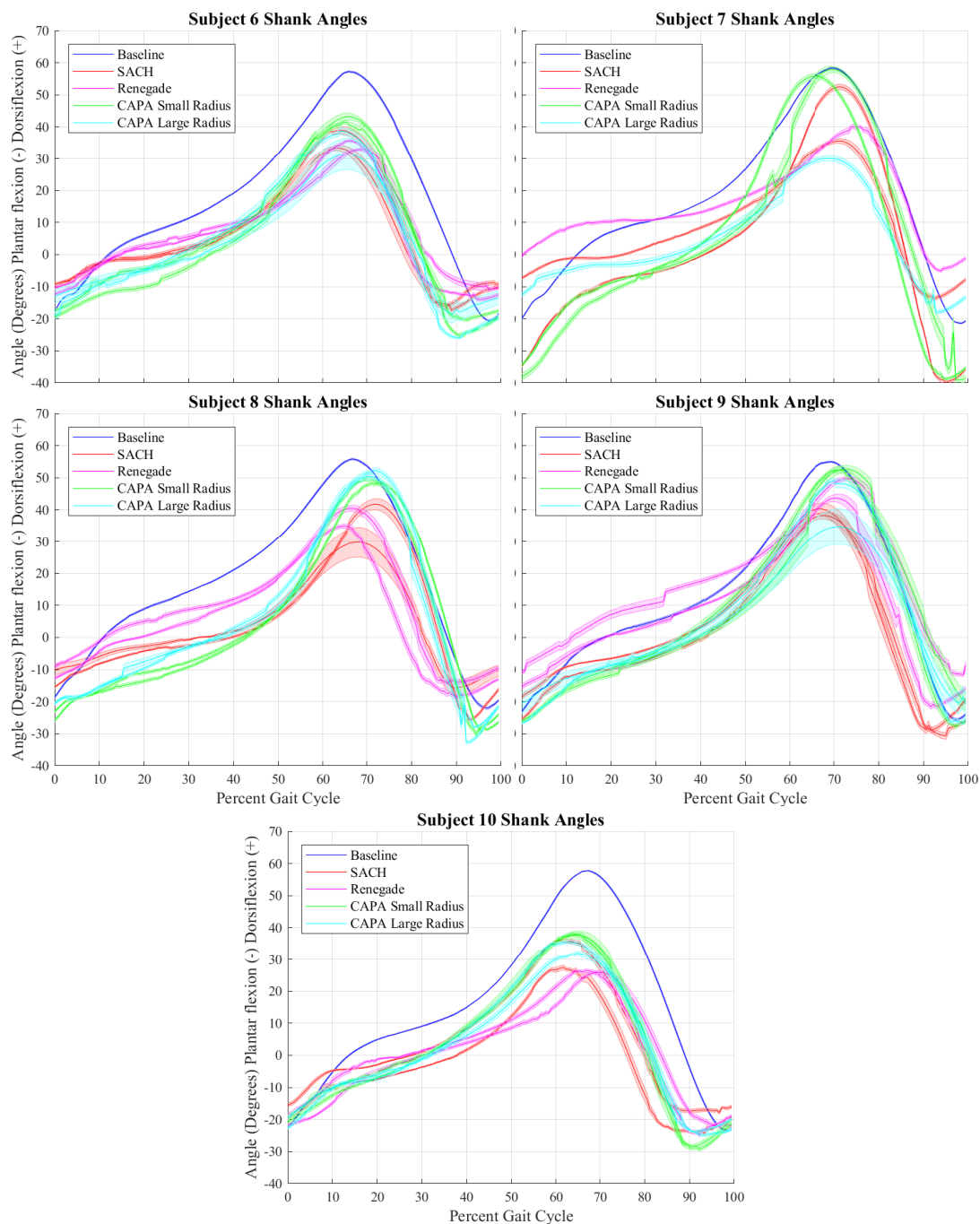


Figure D.2: Experiment 2 Shank Angles Subjects 6-10. The shaded error bars represent one standard error between steps for each subject. Subject 7 Renegade with weight and CAPA-foot-small-radius-stiff were removed because of difficulties post-processing the data.

## APPENDIX E: VERTICAL GROUND REACTION FORCES

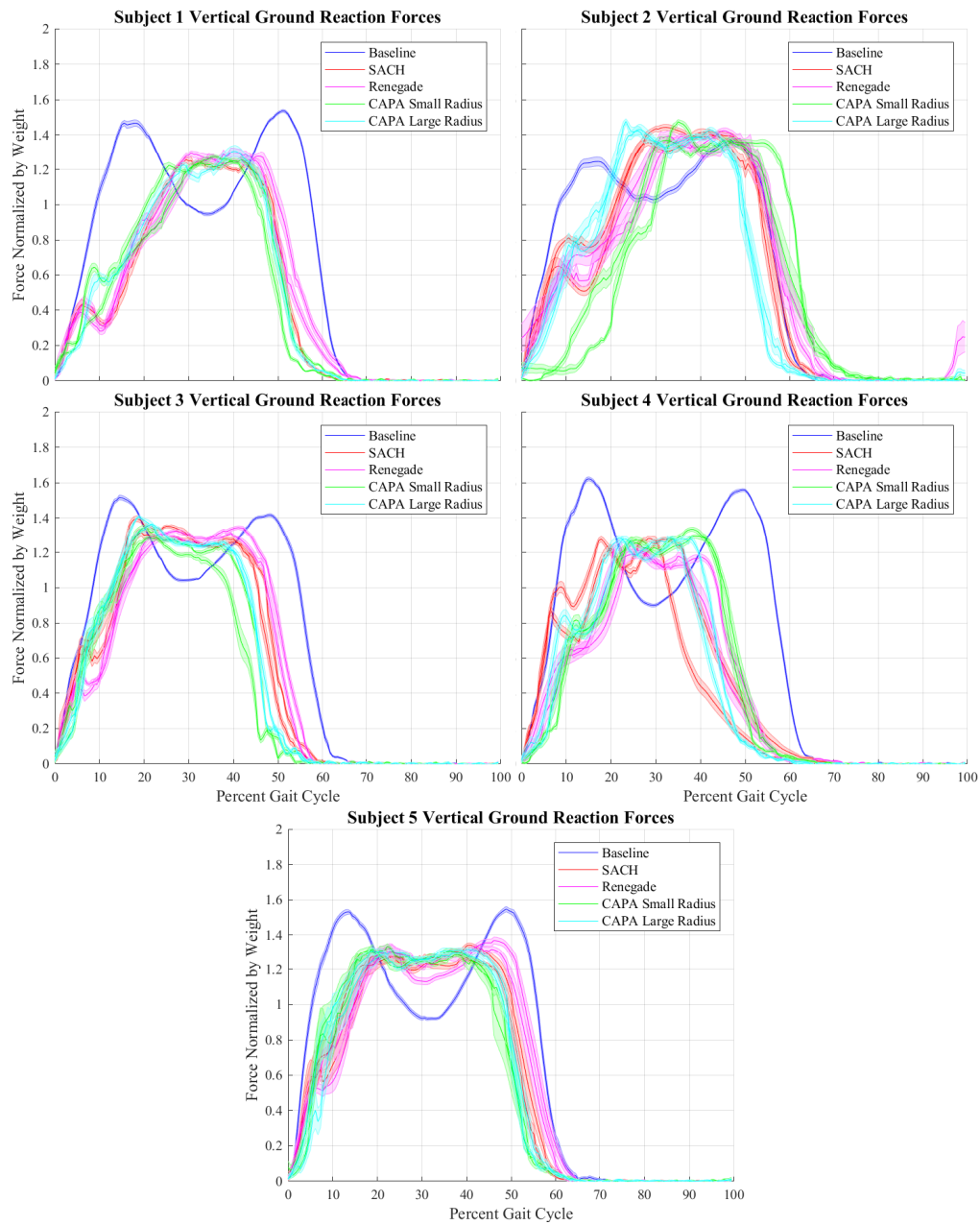


Figure E.1: Experiment 1 Vertical Ground Reaction Forces Subjects 1-5. The shaded error bars represent one standard error between steps for each subject. Subject 1 SACH foot with weight and CAPA-foot-large-radius-stiff were removed because of difficulties post-processing the data.

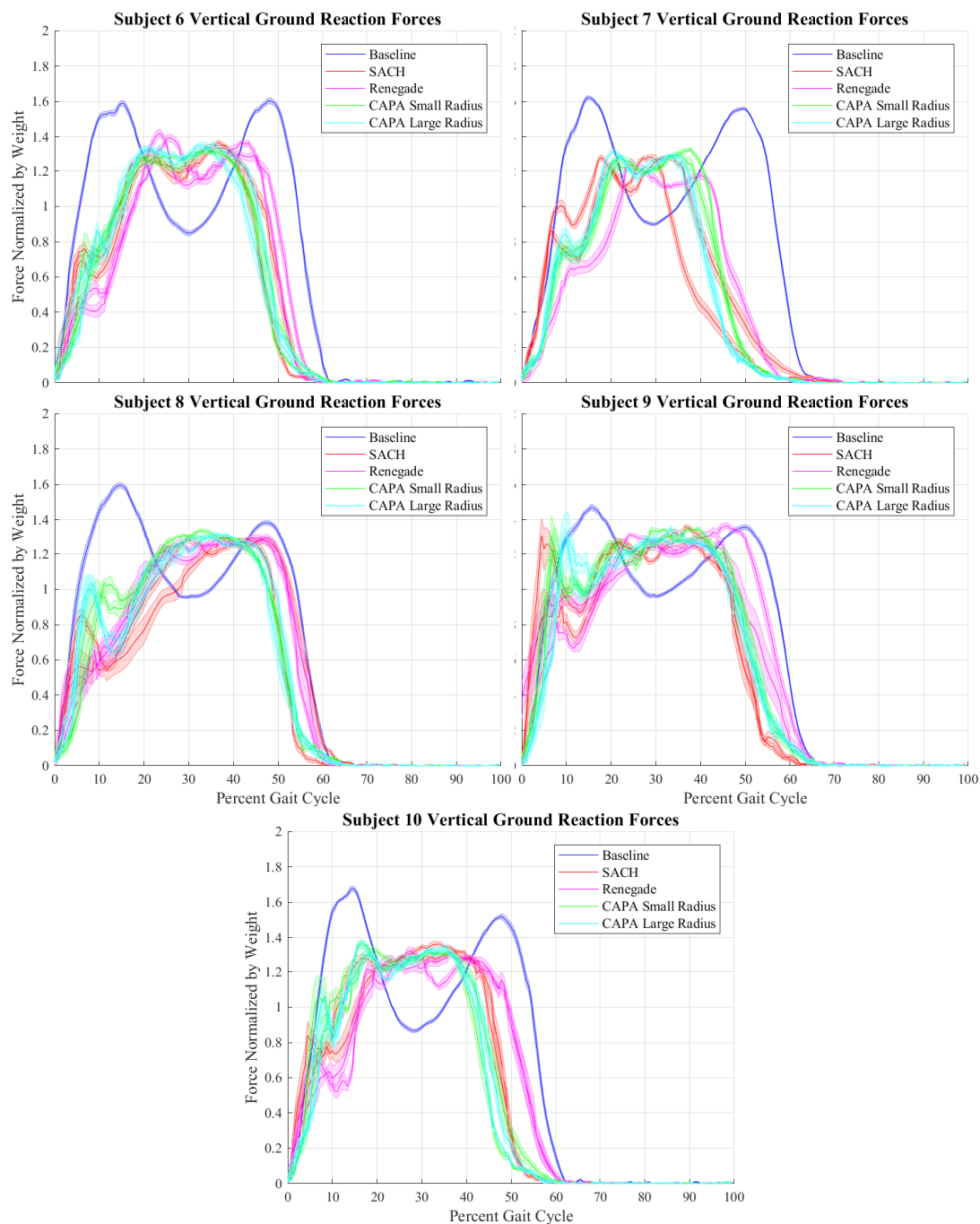


Figure E.2: Experiment 2 Vertical Ground Reaction Forces Subjects 6-10. The shaded error bars represent one standard error between steps for each subject. Subject 7 Renegade with weight was removed because of difficulties post-processing the data.

## APPENDIX F: SAGITTAL PLANE GROUND REACTION FORCES

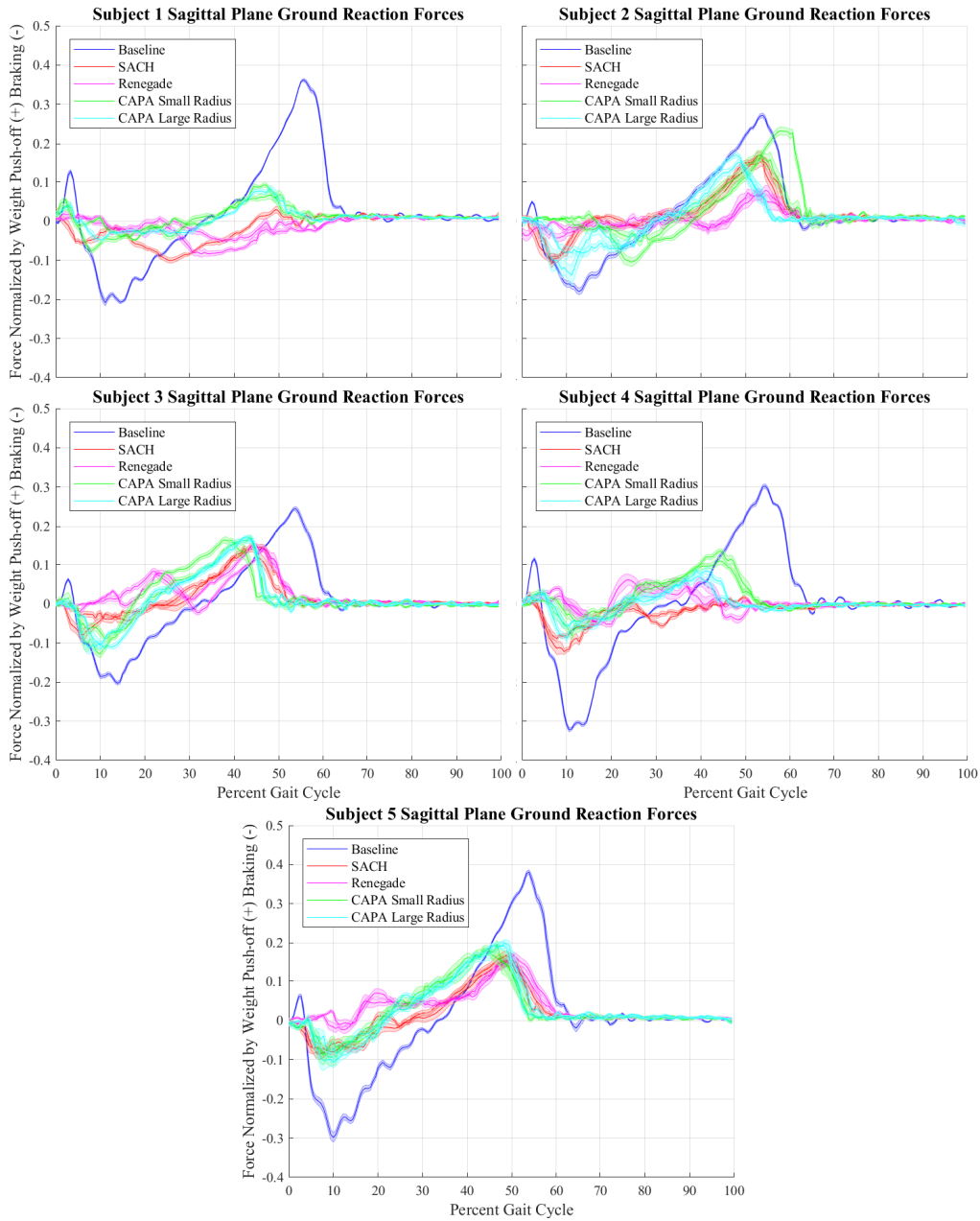


Figure F.1: Experiment 1 Sagittal Plane Ground Reaction Forces Subjects 1-5. The shaded error bars represent one standard error between steps for each subject. Subject 1 SACH foot with weight and CAPA-foot-large-radius-stiff were removed because of difficulties post-processing the data.

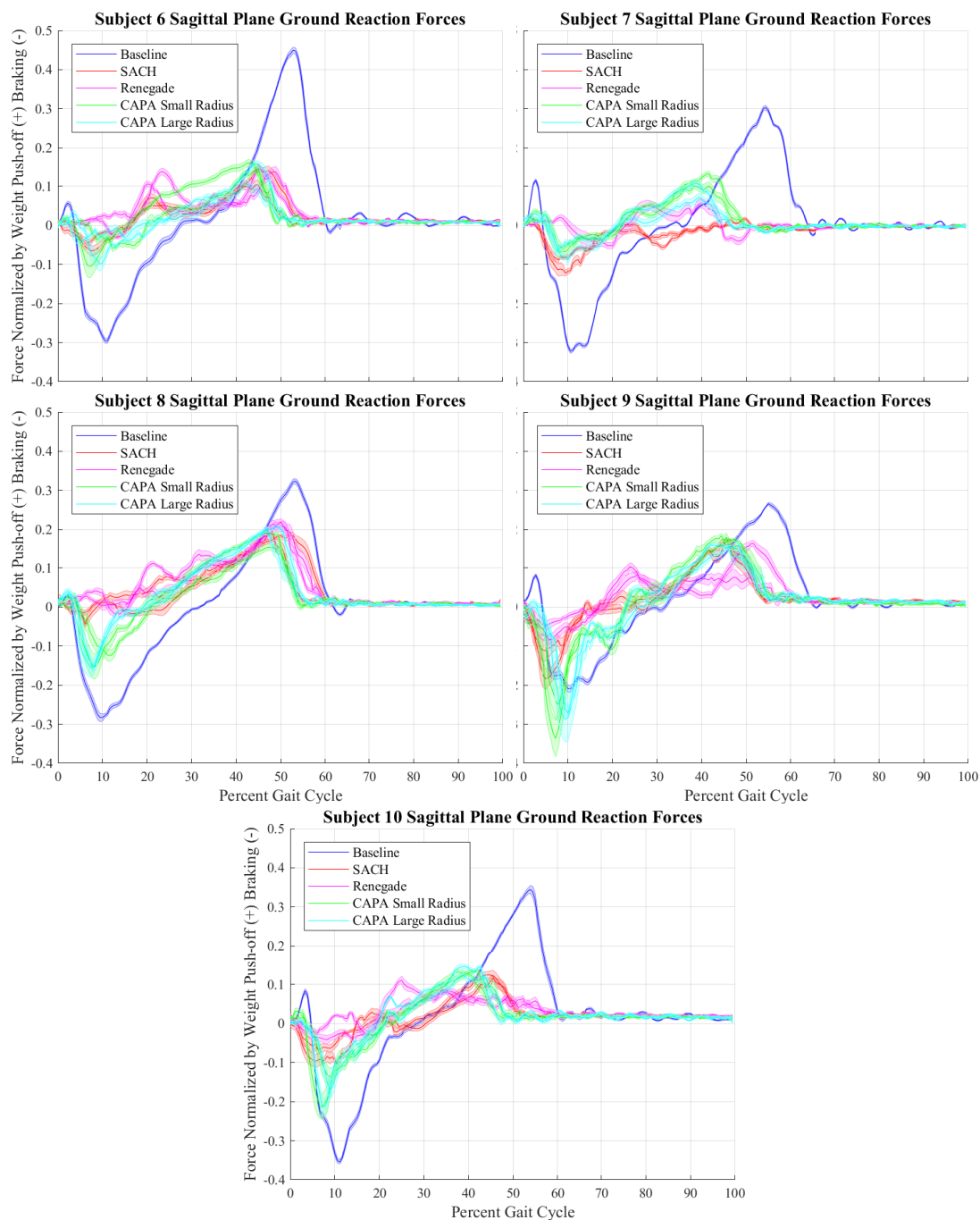


Figure F.2: Experiment 2 Sagittal Plane Ground Reaction Forces Subjects 6-10. The shaded error bars represent one standard error between steps for each subject. Subject 7 Renegade with weight was removed because of difficulties post-processing the data.

## APPENDIX G: VERTICAL GROUND REACTION FORCES PRODUCED BY CAPA FOOT

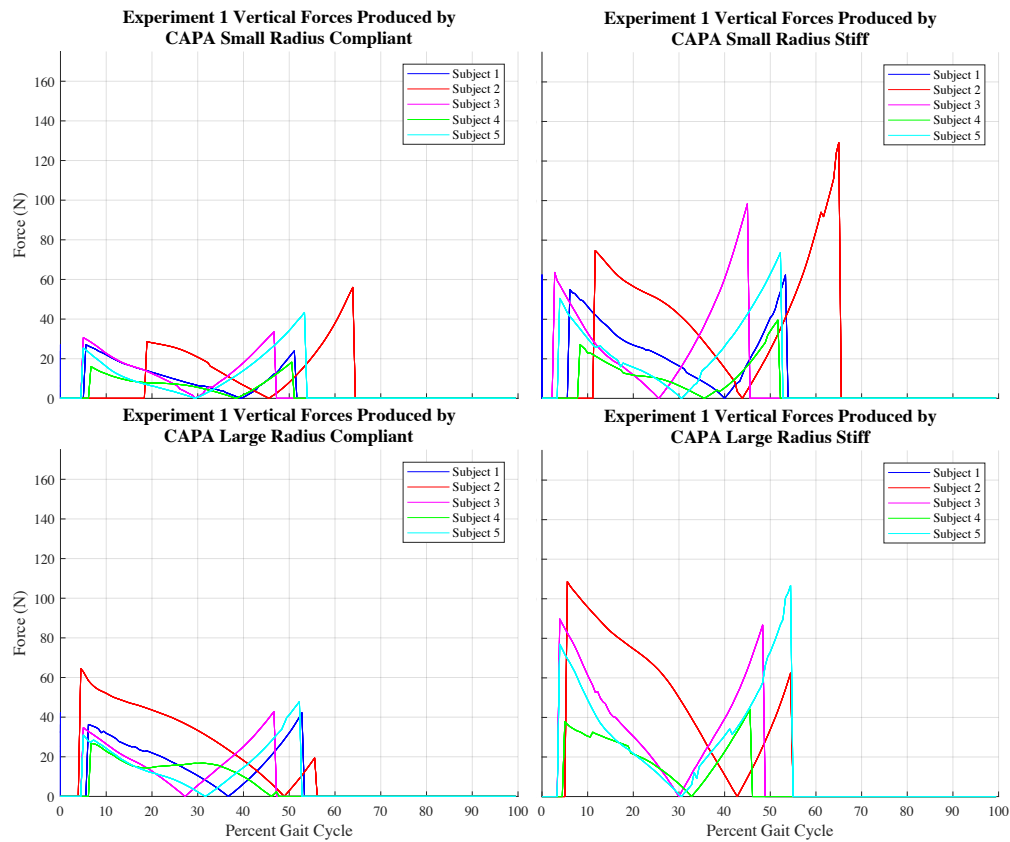


Figure G.1: Vertical component of ground reaction forces produced by each CAPA foot during experiment 1. Because the model is only valid during stance phase, the model is cut off when the vertical forces are less than 25% body weight. Subject 1 SACH foot with weight and CAPA-foot-large-radius-stiff were removed because of difficulties post-processing the data.

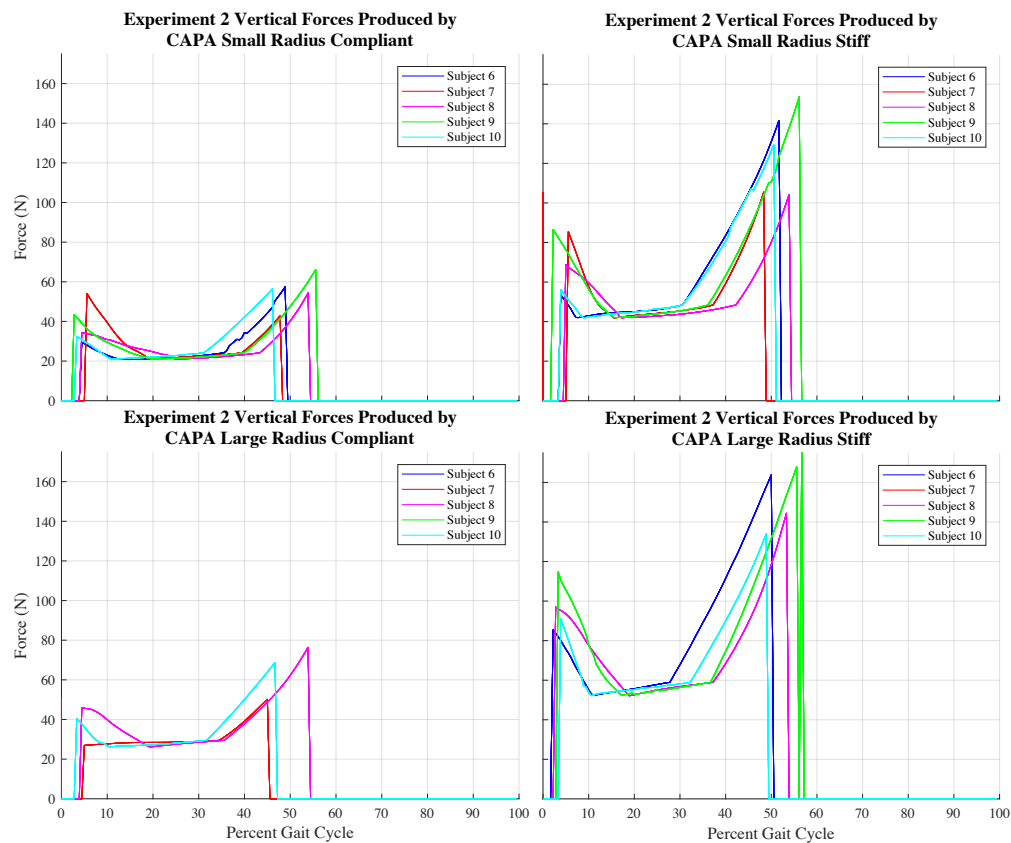


Figure G.2: Vertical component of ground reaction forces produced by each CAPA foot during experiment 2. Because the model is only valid during stance phase, the model is cut off when the vertical forces are less than 25% body weight. subject 6 CAPA-foot-small-radius-stiff; subject 7 Renegade with weight and CAPA-foot-small-radius-stiff; and subject 9 CAPA-foot-small-radius-stiff were removed because of difficulties post-processing the data.

## APPENDIX H: INDIVIDUAL SUBJECT DIFFICULTY LEVEL RATING

Table H.1: Experiment 1 Individual Subject Difficulty Level Ratings

	Subject 1	Subject 2	Subject 3	Subject 4	Subject 5
SACH foot	4.5	2	2	3	4
SACH foot with weight	4	2.5	2	2	3
Renegade® AT	4	3	4	2.5	3
Renegade® AT with weight	3	2.5	4	3	2
CAPA Small Radius Compliant	2.75	2	1	2	3
CAPA Small Radius Stiff	3	2	3	2.5	2.75
CAPA Large Radius Compliant	3	3	1	2.5	1.3
CAPA Large Radius Stiff	2.75	2	1	2	1.4

Table H.2: Experiment 2 Individual Subject Difficulty Level Ratings

	Subject 6	Subject 7	Subject 8	Subject 9	Subject 10
SACH foot	2	2	3	3.5	4
SACH foot with weight	1	2	4	4	4
Renegade® AT	3	4	5	4	4
Renegade® AT with weight	2	3	4	4	5
CAPA Small Radius Compliant	2	2	2	2	4
CAPA Small Radius Stiff	2	2	1	3	3.5
CAPA Large Radius Compliant	3	2	3	4	3
CAPA Large Radius Stiff	3	2	2	3	2.5



## APPENDIX I: STEP TIME

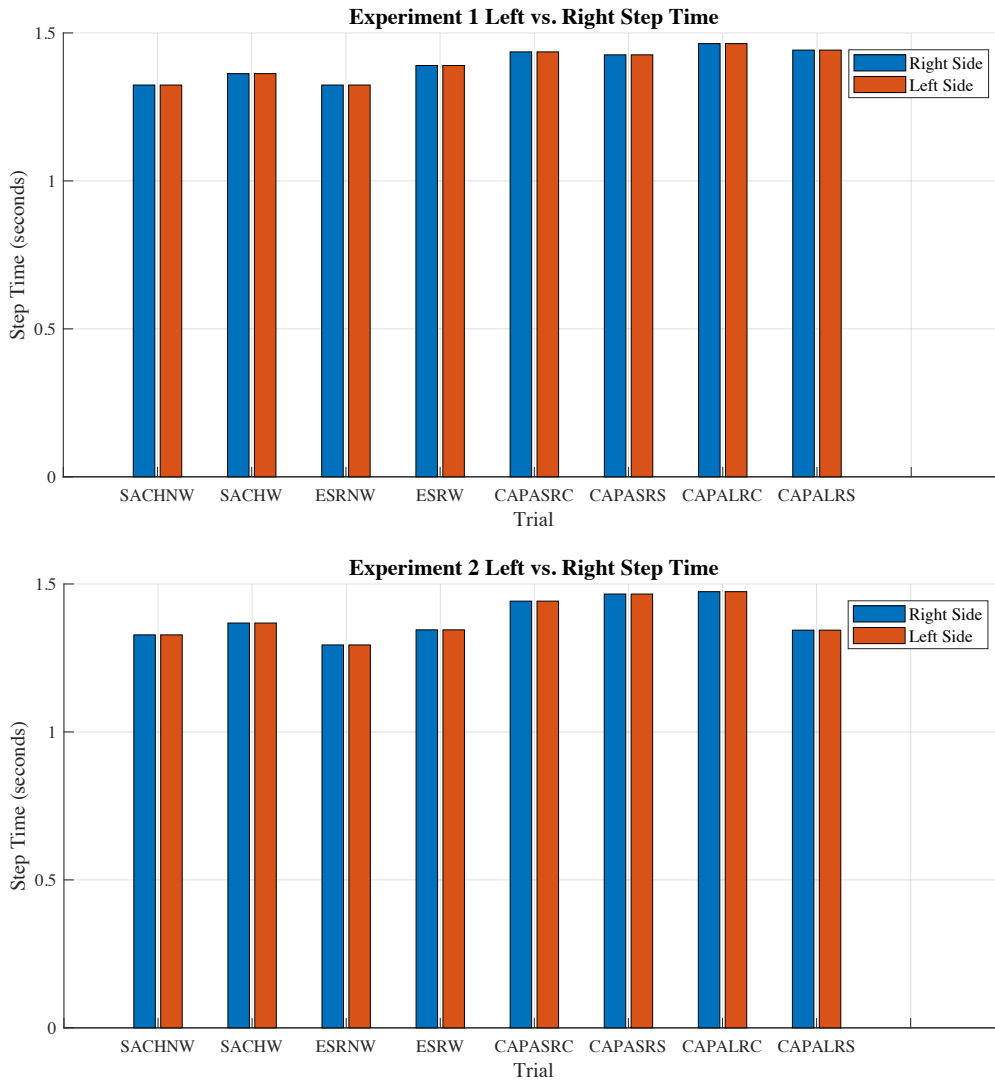


Figure I.1: Average mode step time between subjects for trials with an ankle-foot prosthesis. The mode average mode step time for the right is shown in blue and the left in orange. The bars represent SACH Foot No Weight (SACHNW), SACH Foot With Weight (SACHW), Renegade<sup>®</sup> AT No Weight (ESRNW), Renegade<sup>®</sup> AT With Weight (ESRW), CAPA-foot-small-radius-compliant (CAPASRC), CAPA-foot-small-radius-stiff (CAPASRS), CAPA-foot-large-radius-compliant (CAPALRC), and CAPA-foot-large-radius-stiff (CAPALRS)